IMPORTANT RESEARCH IN THE FIELD OF CHEMISTRY IN A GLOBALIZING WORLD
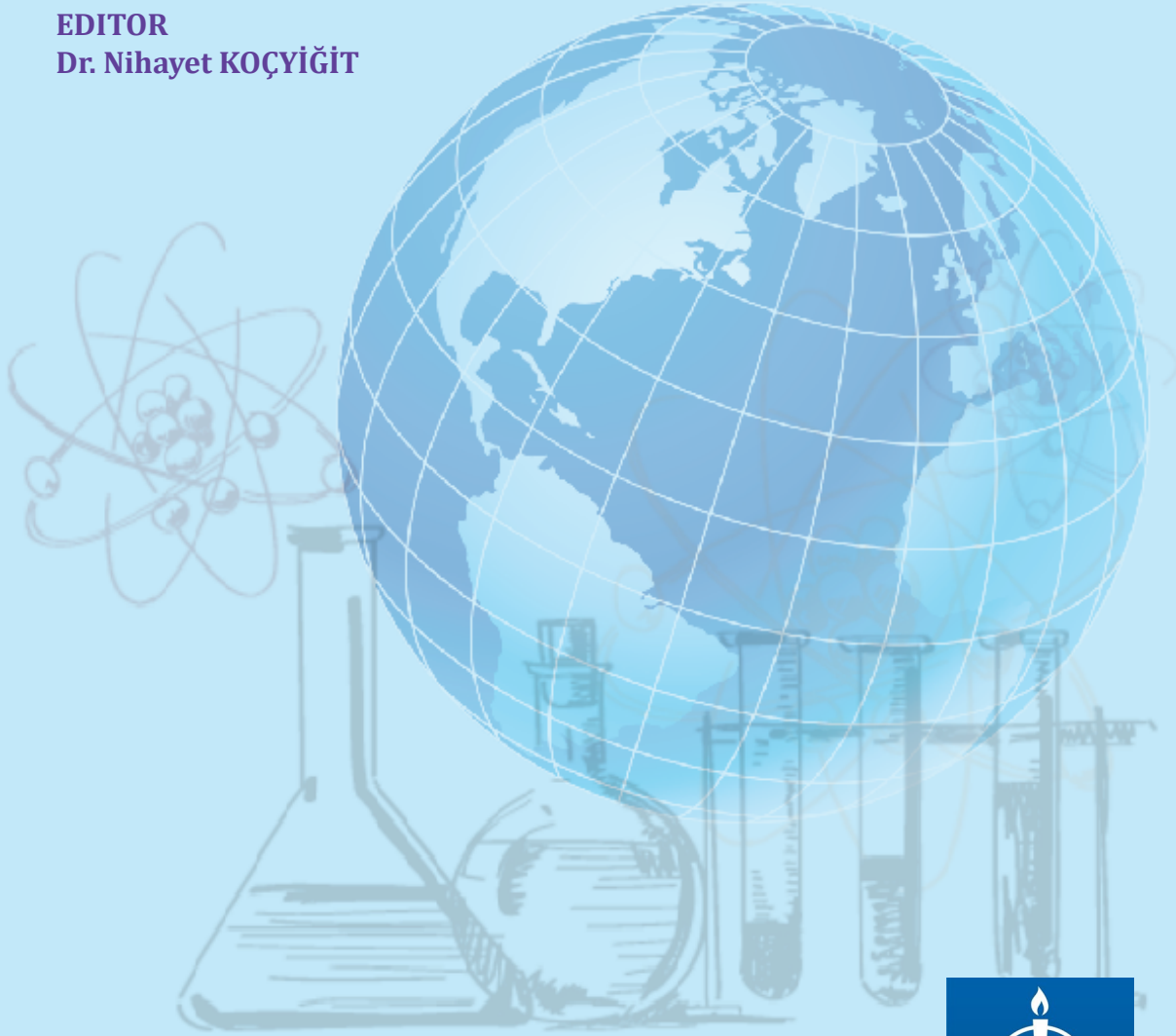
EDITOR
Dr. Nihayet KOÇYİĞİT

IMPORTANT RESEARCH IN THE FIELD OF CHEMISTRY IN A GLOBALIZING WORLD

EDITOR

Dr. Nihayet KOÇYİĞİT

AUTHORS

Prof. Dr. Mehtap EMİRDAG-EANES

Prof. Dr. Murat ATEŞ

Assoc. Prof. Dr. Mehmet Fırat BARAN

Assist. Prof. Dr. Hacer DOLAS
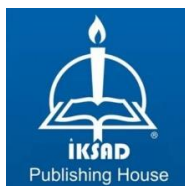
Assist. Prof. Dr. Nilgün ONURSAL

Dr. Barış KURT

Dr. Mehmet Can DAL

Dr. Murat EVCİL

Dr. Nihayet KOÇYİGİT

Mertcan TOPUZ

Sinem KAYA

It is responsibility of the author to abide by the publishing ethics rules.

CONTENTS

PREFACE

In the globalizing world, science and technology continue to advance and develop rapidly. The main reason for this is based on different basic sciences such as physics, chemistry and biology.

Chemistry, one of these basic sciences, investigates the structure, properties, combinations, interactions and reactions of matter and explains them with atoms, various atomic theories, chemical compounds, chemical reactions, states of matter, intermolecular and molecular forces, chemical bonds and reaction kinetics. Thus, it enables us to understand nature, life and the functioning of the world by using observation and experiment methods.

The history of the science of chemistry dates back to the ancient Egyptian period. In the 2000s BC, the Egyptians produced cosmetic powders using chemical methods, and in the years BC (1792-1750), the Babylonians defined metals such as gold, silver, mercury, lead, iron and copper and gave symbols to these metals. In BC (624-546), Tales investigated the principles of matter and suggested that water was the basic substance of the universe, and in BC (490-430), Empedocles claimed that the universe consisted of four basic elements: fire, air, water and earth.

In the late 17th century AD, German scientist Johann Joachim Becher developed the Phlogiston theory of combustion, but it was refuted by Lavoisier. Between 1785 and 1787, French physicist Coulomb discovered Coulomb's law, and in 1803, British scientist John Dalton put forward the atomic theory.

In the 19th century AD, the era of modern chemistry began. During this period, William Crookes made advances in atomic theory and

discovered the cathode ray, Eugene Goldstein proved the existence of the proton, Thomson developed his own atomic model, Mendelyev discovered the periodic table, Marie Curie discovered radioactivity and later Polonium and Radium. Ernest Rutherford discovered the alpha particle, beta particle and gamma radioactive ray.

With the contributions of many scientists, the science of chemistry has developed and survived until today. Today, studies on chemistry are rapidly increasing and developing. This contributes to the rapid development of science and technology.

In this book, today's leading chemistry-related research topics are included and references are made to previous studies on these topics. The book was published by Iksad publishing house and is thought to be a useful resource for researchers.

Dr. Nihayet KOÇYİĞİT[1]

---

[1] Batman Üniversitesi Kimya Bölümü

CHAPTER 1

AEROGELS: CHARACTERISTICS, CLASSIFICATION, STRUCTURE, PROPERTIES, PREPARATION, TYPES AND APPLICATIONS

Dr. Nihayet KOÇYİGİT[1]

---

[1] Batman University, Chemistry Department,Batman Turkiye.
nihayet.kocyigit@batman.edu.tr, Orcid ID:0000-0002-3472-1127

1. INTRODUCTION

Aerogels are lightweight, nanoporous, and nanostructured materials with diverse chemical compositions and a huge potential for applications in a broad spectrum of fields. Although the densities of solids and liquids (or gases and plasma) are very similar, liquids and gases differ by 3–4 orders of magnitude. The aerogel could fill the gap between the liquid and gas state. A material having three-dimensional open networks produced by coherent NPs or polymer molecules is called aerogel. A novel state of matter as well as a unique functional material could be identified with the aerogel in light of recent developments. Like the solid state, aerogel maintains a fixed volume and shape. However, the density of aerogel can shift significantly, from 1000 kg/m^3 (solid density) to roughly 1 kg/m^3 (lower than the density of air) (Du et al., 2013).

IUPAC (International Union of Pure and Applied Chemistry) selected aerogels among the top ten developing technologies in chemistry for 2022. Solid colloidal or polymeric networks that have had their entire volume expanded by a gas are known as aerogels (Vareda et al., 2018). Aerogels actually contain more empty space than anything else (>80% v/v). Aerogel exhibits a variety of unique properties including ultralow refractive index, ultralow thermal conductivity, ultralow sonic velocity, ultralow modulus, ultralow dielectric constant, ultralow sound speed, high specific surface area, and ultrawide adjustable ranges of the density and the refractive index due to not only high porosity like other foams but also dual structural natures of microscopic (nanoscale skeleton) and macroscopic (condensed state

matter) features. According to IUPAC, an aerogel is a gel made up of a microporous solid in which a gas is dispersed (Du et al., 2013).

The most well-known variety of aerogel, silica aerogels, were originally prepared by Kistler in 1931. Because it replaced the liquid component of the wet gel with air without affecting the solid microstructure, its inventor gave it the term "aerogel" (air + gel). The Monsanto Chemical Corporation was the first to commercialise these original proprietary silica aerogels (Kistler, 1941). Subsequently, in 1966, Peri reported on a new technique that used alkoxides as aerogel precursors (1966). Despite the intriguing qualities that this material displayed, it appears that the aerogel did not attract widespread interest prior to 1970. Nowadays, aerogels are a vast family of materials that include carbons, metals, ceramics, inorganic oxides, chalcogenides, metals, and organic polymers, both natural and manmade (Ratke & Gurikov, 2021). There are actually no chemical substances that cannot be produced in an aerogel form (Du et al., 2013). Any desired form of aerogel can be formed, most commonly as monoliths, but also as blankets, fibres, films, millimeter-sized beads, or small powders. The majority of aerogels are mesoporous substances with pore diameters between 2 and 50 nm. The solid network is made up of primary particles that clump together to generate fractal porous secondary particles, which eventually clump together to form a "pearl-necklace" structure (Georgiou et al., 2023).

Aerogels are made from gels in which the pore liquid is replaced by air with some matrix shrinkage, according to Kistler's original definition. Yet, because supercritical drying is often the sole condition that has a minimum impact on the porous structure, aerogels have

traditionally been thought of as materials that are generated under this state. Different methods of drying gels have been used for a while, but using them required that the gel undergo significant changes as it dried. Modern drying techniques now allow for the drying of monolithic gels with a much more minimal influence on the porous matrix (Vareda et al., 2018).

Aerogels have frequently been documented in two-dimensional (2D) thin-film, monolithic bulk, and monolithic three-dimensional (3D) geometries. Due to their brittle network architecture, lack of flexibility, and lack of extensibility, their commercialization has been severely constrained. Aerogel fibres are a novel type of aerogel that has recently come into existence. The performance of traditional aerogels may significantly improve when they are converted into fibres (sub-micron or nanofibers). As a result, these aerogel fibres can demonstrate enhanced extensibility, favourable flexibility, and improved mechanical performance. They will thus be a better match for applications that need them to be stretchable and have high mechanical flexibility. Aerogel fibres can be widely used in other industry sectors where load-bearing is essential, in addition to their high thermal insulation capability (Tafreshi et al., 2022).

2. CHARACTERISTICS AND CLASSIFICATION OF AEROGELS

The following two characteristics should be present in an aerogel state matter: 1) Structure characteristic: Gel-like structure, typically with nanoscale coherent skeletons and pores; hierarchical and fractal microstructure (primary structure coexists and is connected to larger-

scale structure); ability to form macroscopic monolith; randomly crosslinking network, typically made up of non-crystalline matter. 2) Property characteristic: Unique bulk properties that set them apart from solids, gases, or regular foam include extremely low thermal conductivity, extremely low modulus, extremely low refractive index, extremely low sound speed, extremely high specific surface area, extremely wide adjustable ranges of density, and extremely high porosity (especially for silica aerogel) (Du et al., 2013).

The most logical way to categorise aerogel is to separate them based on their composition. Single-component aerogels and aerogel composites are two categories into which the aerogel could be categorised. 1) Single-component aerogel is made up of oxide aerogel (silica and non-silica), organic aerogel (resin- and cellulose-based), carbon aerogel (carbonised plastic, CNT, and graphene), chalcogenide aerogel, and other types of aerogel (single element, carbide, etc.). 2) Aerogel composites comprise micro- and nano-aerogel composites, gradient aerogel, and multi-composition aerogel (Du et al., 2013).

The aerogel that has been studied and used the most extensively is oxide-based. It is a class that is extremely common and contains almost all species of aerogels that are primarily made of metal-oxygen bonds. The oxide-based aerogel can be made in a variety of ways, but three are the most adaptable. The traditional sol-gel (TS) approach is the first technique. The most traditional and popular way to produce different aerogels is still this one currently. Organic aerogel, which is made up of resin- and cellulous-based aerogel, is normally considered of as a highly porous kind of amorphous graphite-based foam. A high carbon-content template (RF aerogel) is pyrolyzed at a high temperature (often 800–

1200 °C), ambient pressure, and inert gas in order to produce carbonised RF (CRF) aerogel. One of the newest types of carbon aerogels is graphene-based. The graphene aerogel was synthesized by ultrasonic-induced gelation, drying, and thermal reduction from a graphene oxide solution. Carbon nanotube (CNT) aerogel is another intriguing type of carbon aerogel. A carbothermal conversion could be used to produce the metal-based and carbide-base aerogels (Du et al., 2013).

3. PREPARATION OF AEROGELS

The aerogel's properties, which depend on its microstructure, provide the basis for the application design. Realizing microstructure control during preparation is crucial, for this reason. Three essential steps are typically involved in the aerogel preparation process: i) Solution-sol transition: In the precursor solution, nanoscale sol particles can form on their own or with the assistance of catalysts through condensation and hydrolysis processes. (ii) Sol-gel transition (gelation): Using the coherent network, the sol particles are crosslinked and hierarchically organised into a wet gel. (iii) Gel-aerogel transition (drying): the solvent inside the wet gel is replayed by the air without serious microstructure damage. The microstructure of the aerogel and its properties and uses could be determined by all three stages. The varied and well-established drying techniques include freezing drying, natural drying, solvent-replaced ambient drying, surface-modified ambient drying, high temperature supercritical fluid drying (SCFD), low temperature SCFD, and more. As long as a wet gel forms, there would be, in a sense, a viable drying route to an aerogel (a key point in preparing the aerogel). The drying procedure is therefore the main focus rather than the solution-sol-

gel transitions (sol-gel method). The fundamental concept is the same, synthesizing aerogels with various compositions or structures requires quite varied preparation methods (Du et al., 2013).

3.1. Supercritical Drying

Supercritical drying uses the liquid-gas transition that happens beyond the substance's critical point in order to dry the gel while maintaining the highly porous network of an aerogel. By adopting this liquid-gas transition that avoids crossing the liquid-gas phase boundary, the surface tension that would form within the pores owing to the evaporation of a liquid is reduced, hence preventing the collapse of the pores (Gurav et al., 2010). The liquid solvent is heated and pressed until it reaches its critical point, at which time the liquid and gas phases blend together. Past this point, the supercritical fluid is transformed into the gaseous phase following an isothermal de-pressurization. Without crossing the liquid-gas phase border, this mechanism causes a phase transition. This technique has been shown to be excellent at maintaining the solid network's highly porous structure without appreciable shrinkage or cracking (Barrios et al., 2019).

3.2. Freeze-Drying

The process of freeze-drying, often referred to as freeze-casting or ice-templating, provides an alternative to supercritical drying's high temperature and high pressure requirements. Additionally, by regulating the formation of ice crystals during freezing, freeze-drying provides greater control over the development of the solid structure (Wang et al., 2018). This approach involves freezing a colloidal dispersion of the aerogel precursors, with the liquid component freezing into various

morphologies based on the concentration of the precursors, the kind of liquid, the freezing temperature, and the freezing container (Jimenez-Saelices et al., 2017). The solid precursor molecules are pushed into the gaps between the forming crystals when this liquid freezes. Following complete freezing, the liquid is transformed into a gas by the process of lyophilization, which substantially reduces capillary forces, as was seen with supercritical drying (Deville, 2018). Although being categorised as "cryogels," aerogels produced by freeze-drying frequently exhibit some shrinkage and cracking in addition to forming a non-homogenous aerogel structure. This frequently results in the use of freeze-drying to produce aerogel powders or as a framework for composite aerogels (Barrios et al., 2019).

3.3. 3D Printing

Aerogel production is undergoing a revolution since of three-dimensional printing (3DP), which makes it possible to quickly and accurately leading to a successful 3D porous structures with improved reliability (Zhang et al., 2018). In general, 3DP is a form of additive manufacturing technique that produces 3D items by building them layer by layer (Zhu et al., 2017). Using a variety of materials like polymers, ceramics, and metals, this approach enables the fabrication of highly customised and complicated structures for numerous industrial sectors in noticeably shorter amounts of time (Tang et al., 2018). The 3DP of aerogels is regarded as a hybrid fabrication technique to produce very light 3D structures, employing new depositional strategies for the construction of the 3D gel constructs while utilising the conventional drying methods of supercritical drying and freeze-drying. According to

the sol-gel transitions that occur during the printing process, 3DP of aerogel techniques are divided into different categories. These categories are: 1) direct ink writing (DIW), in which a gel is produced before printing; 2) stereolithography (SLA), in which the sol-gel transition takes place during printing; and 3) inkjet printing (IJP), in which the sol-gel transition occur after printing. SLA is a method for producing 3D structures out of photocurable materials. Photopolymerization is a process whereby polymer layers harden when exposed to particular laser wavelengths. IJP is a non-contact, droplet-based material deposition method that could be altered to deposit photocurable materials for high-resolution patterning. In the development of the 3D constructions, DIW is an extrusion-based printing technology that uses the layer-by-layer deposition of continuous ink filaments. The 3D printing of aerogels has restrictions just like conventional methods of aerogel synthesis. For instance, only photocurable materials must be used with SLA, but a far wider range of materials are available with DIW and IJP (Ambrosi & Pumera, 2016). The most used 3DP methodology for aerogels is DIW, which does not offer quick gelation. IJP is a special method renowned for its uniqueness, ease of use, and ability to produce highly customised 3D aerogels (Barrios et al., 2019).

4. MAINSTREAM AEROGELS

4.1. SiO_2 Aerogels

Silica aerogels contain 95% air and the remaining is comprised of silica crystal (SiO_2). They are made of tiny particles with a diameter of less than 10 nm and pores with a size of less than 50 nm, and they have an open porous structure. Due to these characteristics, silica aerogels

have relatively high BET surface areas (500–1200 m^2/g) and a very low density of 0.03-0.35 g/cm^3. Moreover, they have a low dielectric constant of 1.1, a speed of sound of 100 m/s, a thermal conductivity coefficient of less than 0.02 W/(mK), and a refractive index of between 1.00 and 1.08. (Aegerter et al., 2011). Due to its outstanding qualities, silica aerogels are used in a wide range of sectors, including sensors, catalytic converters, thermal and acoustic insulators, carriers of active ingredients, and absorbents of gases, liquids, or energy (Slosarczyk et al., 2022).

Nevertheless, they require numerous, energy-intensive production processes and have limited mechanical characteristics. Aerogels made of silica are often weak, have poor mechanical qualities, require a lengthy manufacturing process, and have limited uses. Increased connection in the aerogel backbone is essential for enhancing the mechanical characteristics of such a material. The aerogel can be customised with various functional capabilities by tweaking the material composition and processing conditions of components. The most crucial element in the development of aerogel products with certain morphologies (particulate, fiber-like, or non-particulate) and their resulting properties is the interaction between the materials-processing-structure-properties in different sorts of aerogels. This method of developing precursor systems yields the multipurpose, next-generation silica-based aerogel materials (Karamikamkar et al., 2020). Aerogel and fibres can be combined to improve mechanical and insulating qualities as well as reduce dust release and make practical application easier. With sol-gel methods, the aerogel can be produced in between fibres by impregnating them in a silica precursor sol; however, the sol can also be spun into aerogel fibres. In other methods, pre-formed silica aerogel is blended with polymer or

solvent matrices or slurries to generate aerogel-filled composite fibres, aerogel-filled blankets, and aerogel-filled material coated fibres. Textile packaging loaded with aerogel particles have also been suggested (Mazrouei-Sebdani et al., 2022).

4.2. Hydrophobic Silica Aerogels

Aerogels made of silica and composite materials are hydrophobic, allowing them to find use in a wide range of industries. These materials have attracted the interest of researchers from all over the world due to their extraordinary structural, morphological, and physiochemical features such high porosity, surface area, chemical stability, and selectivity. Furthermore, the hydrophobic conduct of these aerogels has made it possible for them to absorb materials, such as organic contaminants, without causing the pore and network structure to collapse. Exploiting these materials for environmental and biological applications is therefore becoming more popular due to their remarkable characteristics and high adsorption potential (Akhter et al., 2023). Fabrication techniques is based on forming the wet sol gel and drying the wet gel. Applications are environmental clean-up and protection, biological applications and superhydrophobic surfaces. Hydrophobic silica aerogels have qualities that make them desirable materials for use in a variety of applications, from transparent insulating systems to drug delivery platforms. These aerogel materials were manufactured utilizing a variety of methods, including surface modification of the matrix after gelation and the addition of silica precursors containing non-polar substituents to the sol-gel matrix (Anderson & Carroll, 2011).

4.3. Superhydrophobic and Flexible Aerogels

Superhydrophobic and flexible aerogels synthesis is based on sol-gel synthesis and supercritical drying. Specific characteristics are water-surface interactions (water droplet sliding and liquid marbles - superhydrophobic aerogel coated water droplets), mechanical and elastic properties (elasticity and mechanical damping), hydrocarbon sorption behavior (with capacity of uptake, desorption and reuse). Aerogels with reduced fragility and increased hydrophobicity have significant potential to expand their use as lightweight structural, insulating or shock absorbing materials especially in aeronautics, microelectronics, and sensing applications. Very hydrophobic aerogels may also be used in applications for cleaning up oil spills. Flexible superhydrophobic silica aerogels have high mechanical flexibility and typical water contact angles >150°. Such materials can be produced from methyl-trialkoxysilane precursors using a two-step sol-gel method. Extraordinary hydrophobicity has been attained with water contact angles up to 175 degrees, according to measurements. In a superhydrophobic aerogel, a water droplet size of 2.7 mm was determined to be critical. The velocity of the water droplet on such a superhydrophobic surface has been observed to be 1.44 m/s for 55° inclination, which is close to the free fall velocity (~1.5 m/s) (Rao et al., 2011). Oil recovery and oily water disposal in practical applications urgently required the production of superhydrophobic and long-lasting oil-absorbing materials due to the huge discharge of industrial oily wastewater and the frequent occurrence of oil spills at sea in recent years (Liu et al., 2018).

4.4. Sodium Silicate Based Aerogels via Ambient Pressure Drying

The first step in the preparation of silica aerogels is a sol–gel process producing a gel. The gel is then dried using either ambient pressure drying (APD) or supercritical drying (SCD). For making silica aerogels traditionally, alkoxide precursors like tetraethoxysilane (TEOS) or tetramethoxysilane (TMOS) are used, which requires more energy and is more expensive. This decision limits the commercialization of aerogels in some ways. A few research has demonstrated the APD's considerable promise as a substitute approach that uses sodium silicate (Na_2SiO_3) as a wholly inorganic precursor. Such aerogels' characteristics are extremely comparable to those attained through more traditional means (Rao et al., 2011).

Multiwalled carbon nanotubes (MWCNTs) were successfully incorporated into silica aerogels made using the sol-gel process. Pure silica aerogels produced by ambient pressure drying with sodium silicate precursor are too fragile to be utilised frequently. The mechanical characteristics of silica aerogels were enhanced by the use of MWCNTs as reinforcements. The results demonstrate that adding modest amounts of MWCNTs to the gels improves their dimensional stability (Bangi et al., 2012).

The synthesis of sodium silicate-based aerogels utilising a two-step sol-gel technique was motivated by the desire to increase the optical transmission of these materials by ambient pressure drying (Bangi et al., 2013).

4.5. ZrO$_2$ Aerogels

Zirconia aerogels are porous nanomaterials that are well suited for a variety of uses because they have large specific surface areas and low thermal conductivities. Zirconia aerogels have a wide range of uses in thermal management systems, many of which are advantageous for aerospace and aviation systems. The numerous unique synthesis methods and processing conditions of zirconia aerogels, however, can make it challenging to optimise these materials, thereby impeding further development. Zirconium precursor, rare earth stabiliser, solvent system, gelation agent, and surfactant templating agent are independent variables in the synthesis process alone. Up to 32 different synthetic pathways would be feasible if each synthetic variable had only two distinct alternatives; with three options, each synthetic variable might have 243 different synthetic pathways. Processing conditions, such as drying method, temperature, solvent, and sintering temperature, as well as numerous methods used to characterise aerogels, must be taken into account in addition to the gel synthesis (Walker et al., 2021).

The two well-known techniques of "alkoxide hydrolysis" and "epoxide addition" have been established to produce ZrO$_2$ aerogels in the literature. The first one uses the controlled hydrolysis of organic zirconium alkoxide, whereas the latter one uses propylene epoxide and inorganic zirconium salts as reagents (Wang et al., 2018). Applications of zirconia aerogels are catalysis, ceramics, solid oxide fuel cells.

4.6.TiO₂ Aerogels-Like Materials Prepared under Ambient Pressure

Principle is templating with polymer and surfactant by the mixing method or by the immersion method and preparation of aerogels-like materials (dried-gels and annealed gels). Highly porous titania is attractive because of various applications such as photocatalysts. The sol-gel process combined with templating can be used to generate mesoporous titania gels. Wet gels' integrated surfactant micelles or polymer aggregates stop shrinkage during ambient pressure drying. Depending on the preparation circumstances, such as the species of templating materials, the specific surface area, porosity, and pore size are much larger than those of xerogels but not significantly larger than those of aerogels. A proper pore structure for a certain application can enhance the performance of porous titania, for instance, the photocatalytic activity (Hirashima, 2011).

Because of its potent oxidising power, low cost, lack of toxicity, ready availability, activity over a wide pH range, and long-term stability, TiO_2 is preferred among the various semiconducting materials for use as a photocatalyst in the photo oxidation reactions of alkenes, allyl alcohol, and other organic contaminants in both air and water, including the complete destruction of 4-CP. TiO_2's efficiency as a catalyst in the photo oxidation reaction is strongly influenced by the material's surface area and particle size (Ingale et al., 2012). TiO_2 aerogels are appealing for their uses in solar energy conversion, photocatalysis, pigments, electrical devices, etc. because of their ultra low density, high homogeneity, and high surface area. Aerogel ambient pressure drying has been extensively researched, mostly for SiO_2 aerogel, in order to commercialise less

expensive aerogel. Unfortunately, there are currently few reports of the synthesis of TiO_2 aerogels using ambient pressure drying methods (Chen et al., 2015).

4.7. Monoliths and Fibrous Cellulose Aerogels

A new era of technologies is predicted by the silica aerogel monoliths (SAMs), which have three-dimensional (3D) porous structures and distinct physical and chemical properties. Because to these materials' poor mechanical characteristics in large-scale manufacturing, the crucial obstacle still exists. To avoid this problem and investigate SAMs' applicability in other areas, several methods have been used to improve the mechanical properties of SAMs. SAMs have also been used in numerous applications, like as electronic devices, catalysis, thermal and acoustic insulation, and more (Lin et al., 2021).

4.8. Cellulosic and Polyurethane Aerogels

Hydrogel composites can be prepared from cellulose-based materials and other gel materials, thus combining the advantages of both kinds of material. The hydrogel's network structure can be preserved by the aerogel, a porous substance formed after the water was removed. Aerogel and hydrogel have many possible applications. The viability of repeated usage is constrained by the cellulose hydrogel's poor mechanical strength and weight loss brought on by water absorption and dehydration (Huang et al., 2022). Because to the high hydrophilicity of cellulose, a lot of water can be stored in the holes within the network structure. It may be possible to repeatedly hydrate and absorb water using the cellulose aerogel generated by dehydrating cellulose hydrogel (Li et al., 2018). As a flexible material, cellulose aerogels have advantages like

high surface area, good chemical and thermal stability, a porous structure that can be adjusted, widespread availability, and low cost (Wang et al., 2020).

Due to their affordability and insulating power, polyurethane foams are frequently used as thermal insulators in walls and roofs. Nonetheless, there is potential for improvement in their thermal insulating performance, which ranges from 20 to 30 mW/(m K)27. In order to meet the expanding needs in this industry, polyurethane aerogels must meet reduced thermal conductivity standards while maintaining the good qualities of this polymeric matrix and its affordability (Merillas et al., 2021). When polyurethane / polyisocyanurate-based transparent aerogels are used, it may be possible to combine a transparent material with very low thermal conductivity with a practical, cost-effective solution based on a well-known polymer matrix in the construction industry (Merillas et al., 2022).

4.9. Resorcinol-Formaldehyde Aerogels (RF aerogels)

The most well-known organic aerogel is resorcinol-formaldehyde (RF), which is made by polycondensing resorcinol and formaldehyde in a sol-gel method (Motahari et al., 2016). Both base- and acid-catalyzed gelation processes are used to prepare them. Due to its distinct characteristics, this aerogel exhibits greater mechanical properties than silica aerogel and has numerous applications. The molar ratios of resorcinol to catalyst (R/C), resorcinol to formaldehyde (R/F), and resorcinol to solution (R/S) are among the RF aerogel's synthesis parameters. The mechanical properties can be improved by a decrease in R/C and an increase in R/F and R/S. (Aghabararpour et al., 2018).

Typically, an organic solvent is employed to exchange reaction byproducts such water and unreacted monomers before the resultant gel is dried under supercritical conditions (Schwan & Ratke, 2013). RF aerogels are studied intensely for their potential uses in thermal insulation, catalysis, and as precursors of electrically conducting carbon aerogels with applications in filtration, energy storage, and the green energy initiative (Mulik & Sotiriou-Leventis, 2011). With a sol-gel method and supercritical drying, novel super-flexible RF aerogels were developed. These soft aerogels can deform reversibly by up to 25%. These sponge-like aerogels are distinguished from traditional RF-aerogels made specifically by ambient drying by their low density of 0.06 g cm3 and low Young's modulus of roughly 116 kPa. A very diluted sol-solution is used for the synthesis, which necessitates great preparation accuracy. Little particle formation and relatively large pores allow pore walls to stretch without breaking and facilitate new microstructural conditions (Schwan et al., 2016).

4.10. Polymer-Crosslinked Aerogels

They are produced by crosslinking polymers to 3D nanoparticle networks that have already been established (crosslinking through postgelation introduced monomers; improving the processability of polymer-crosslinked aerogels by crosslinking in one pot and crosslinking in the gas phase). Aerogels that have undergone polymer crosslinking have a conformal polymer coating that covalently binds the skeletal nanoparticles of regular aerogels. The bulk density remains low, but the specific compressive strength of the resulting materials is higher than

those of mild steel and aluminum, while the ability to store energy may surpass that of armor-grade ceramics (Leventis & Lu, 2011).

The silica skeleton's nanoparticles are crosslinked during the polymerization of a di-isocyanate with the amine-modified surface of a mesoporous silica network generated from a sol-gel, strengthening the network's otherwise weak structure. Aerogels with controllable macroscopic properties are produced by methodically altering the processing variables impacting density, which is done by altering the nanoscale morphology. Aerogels that have been crosslinked with the least amount of silica possible are flexible and have up to a 40-fold improvement in strength compared to the similar non-crosslinked framework (Capadona et al., 2006).

4.11. Resorcinol-Formaldehyde/Metal Oxide Aerogels

Types are native RF-MOx aerogels, xerogels, and X-RF-MOx aerogels. High surface-to-volume ratios and high compactness are both essential elements for an effective response between nanoparticles. For this, a simple one-pot method may be used to produce an array of interpenetrating networks of resorcinol-formaldehyde (RF) and metal oxide (MOx, M: Fe, Co, Ni, Sn, Cu, Cr, Ti, Hf, Y, Dy) nanoparticles. The acidity of the gelling solutions of hydrated metal ions can be used to catalyse the gelation of RF. The drying process determines how compact the nanoparticles are in the dry composites: supercritical fluid (SCF) CO_2 drying produces aerogels with open skeletal frameworks, whereas ambient pressure drying produces significantly more compact xerogels. Pyrolysis at higher temperatures triggers carbothermal reactions that result in pure metal monolithic nanostructures (up to 800 °C; examples

of M: Fe, Co, Ni, Sn, Cu) or carbides (up to 1400 °C; cases of M: Cr, Ti, Hf). This depends on the chemical identity of the metal ion. The intrinsic compactness of xerogels or the induced skeletal compactness in X-aerogels determines the rate of those changes regardless of the precise chemical processes involved. The influence of compactness on the activation of the carbothermal processes has substantial implications for process-design engineering, in addition to the significance of the RF-MOx interpenetrating networks in the design of novel materials (mesoporous and macroporous monolithic metals and carbides) (Leventis et al., 2010).

4.12. Polymer-Reinforced Aerogels

Types are hexyl-linked polymer-reinforced silica aerogels (di-isocyanate-reinforced aerogels, styrene-reinforced aerogels, epoxy-reinforced aerogels from ethanol solvent); alkyl trialkoxysilane-based reinforced aerogels.

Mechanically stronger aerogels are necessary if silica aerogels are to have a wide range of uses. Several methods have been investigated to enhance the mechanical properties of silica aerogels (Maleki et al., 2014), including conformal coating of the silica backbone through cross-linking their surface with polymers (Duan et al., 2013), structural reinforcement using flexible silica precursors in the silica gel backbone, and dispersing various fibre networks in the initial sol of the silica aerogel (Meador et al., 2008). In theory, integrating organic chemicals into the inorganic portion of silica aerogels to produce hybrid silica aerogels is the most efficient way to increase the flexibility or elastic recovery in silica aerogels. This can be accomplished by first adding the

relevant functional groups to the silica network's surface and then growing the polymer from the changed surface. The secondary silica nanoparticles can be coated with a conformal polymer using this technique, which increases the connection between the particles and strengthens the aerogel (Randall et al., 2011). Up till now, silica aerogels have been reinforced with a variety of polymeric systems, including epoxide, polyurea, polyurethane, poly (methyl methacrylate), polyacrylonitrile, and polystyrene (Boday et al., 2010).

4.13. Graphene Aerogels

Many exceptional and distinctive characteristics of graphene include its great electrical properties, high mechanical strength, flexibility, thermal conductivity, stability, and effective energy absorption capacity (Cao et al., 2018). Graphene aerogels (GAs) display lightweight, ultra-strength, and ultra-tough features because they combine the special properties of two-dimensional graphene with the structural characteristics of microscale porous materials. GAs are a class of potential carbon-based metamaterials suited for abrasive conditions in the aerospace, defence, and energy industries. However, there are still certain difficulties in applying graphene aerogel (GA) materials, which necessitates a thorough comprehension of the mechanical characteristics of GAs and the related mechanisms of enhancement (Qi et al., 2023). The assembly of two-dimensional graphene sheets to form GAs with three-dimensional (3D) porous structures can be a good strategy. This particular form of material exhibits ultra-low density, high porosity, high specific surface area, compressibility, super-elasticity, and high stability, inheriting the exceptional features of graphene and the distinctive porous

structure of aerogels (Zhang et al., 2018). GAs have a bright future due to these qualities in applications such sensors, capacitors, electromagnetic shields, microwave absorption, oil adsorbents, and insulation materials (Qi et al., 2023). To diversify the mechanical properties of GAs, researchers have experimented with freeze casting (Wang et al., 2018), chemical vapour deposition (CVD) (Jiang et al., 2016), hydrothermal methods (Huang et al., 2017), 3D printing techniques (Yuan et al., 2021), and other assembly techniques (Wu et al., 2022).

The general strategy of GAs preparation is to use graphene oxide (GO) flakes as precursors to form a 3D network structure connected by multiple intermolecular forces, such as π-π bonds, van der Waals (vdW) force, and cross-link (Chandrasekaran et al., 2018). Presently, there are three categories of GA preparation methods: 3D printing, template-free assembly, and template-assisted assembly processes. Due to the ease of usage and low cost of the synthesis process, the template-free technique is frequently utilised in practise. By lowering graphene oxide or adding crosslinks, template-free techniques' fundamental synthesis mechanism is to increase the attraction or decrease the repulsion between adjacent graphene sheets. The naturally structured stacking nature of graphene allows the graphene sheets to later be put together into porous 3D structures. The hydrothermal reduction method (Hu et al., 2017), the chemical reduction method (Pang et al., 2020), and the cross-linking method are the more popular template-free assembly techniques (Zhao et al., 2019). The most popular technique for manufacturing graphene aerogels is the sol-gel processing of graphene oxide (GO) dispersions. Nonetheless, there have been barriers to the widespread use of graphene

aerogels, including the heterogeneity in graphene aerogel characteristics and the lack of knowledge of GO dispersions (Hu et al., 2017).

5. APPLICATIONS

Aerogels can be used in a variety of fields, such as thermal, space applications, acoustic insulation, energy storage, gas and humidity adsorption, dielectrics, sensors, catalysis, actuators, biomedicine, food industry, environmental remediation (Georgiou et al., 2023), chemistry, optics, heat, electricity, high-efficiency thermal insulation materials for buildings, chemical catalysts and carriers (Fu et al., 2022).

5.1. Energy

Common types are 1) inorganic aerogel materials as nanostructured energetic composites; 2) aerogel and sol-gel composites nanostructured pyrophoric materials; 3) organic aerogel materials as nanostructured energetic composites.

Among the most cutting-edge energy storage technologies are batteries and supercapacitors. Batteries and supercapacitors, which rank among the most technologically sophisticated and expensive energy storage options currently on the market, are two examples of energy storage technologies that can be used to store energy. Although it is possible to store energy using these technologies, doing so is not recommended due to the high cost of these solutions. Graphene aerogels were able to attain great energy storage performance due to their distinctive structural and morphological characteristics. Depending on composition, the supercapacitor materials based on graphene aerogel exhibit various features. As cathodes for various types of batteries,

graphene aerogel composites with Boron/Sulfur, TiO2/Sulfur, Cobalt, and Iron phosphide Phosphide/Nitrogen were utilised (Thakur, 2022).

Flexibility, light weight, high power density, and environmental friendliness are just a few of the distinctive and promising benefits that flexible quasi-solid-state supercapacitors (FSSCs) exhibit. Hydrogels are produced by chemically and/or physically connecting monomers and/or polymers together, and they have already established themselves as a promising platform for the quick production of FSSCs. The development of lignocellulose-based hydrogels and aerogels with distinctive physicochemical properties (such as high flexibility, good mechanical strength, and rapid charge transport) presents emerging opportunities for FSSCs because lignocellulose materials are environmentally friendly and sustainable, abundant, and inexpensive (Gu et al., 2021).

5.2. Superinsulation

Applications are thermal insulation for buildings; thermal conductivity for heat transport; off-shore oil and gas; aeronautics and aerospace applications; high temperature; cryogenic applications; refrigeration systems, outdoor clothing, and shoes.

Low thermal conductivity, renewability, cost-effectiveness, use of environmentally acceptable resources, etc. are some of the key factors that determine the quality of a thermally insulating material. In this context, cellulose aerogel made from biomass can be a desirable material because it can meet these requirements in comparison to other traditional insulating materials. Many outstanding physical and chemical properties, such as a large surface area and low heat conductivity, are present in cellulose aerogels. These factors make them a useful thermal insulating

material for the building industry that can help save energy. It's interesting to note that cellulose has the benefit of containing various hydroxyl groups, which can be easily modified by fillers such as inorganic materials through non-covalent interactions, improving their mechanical and thermal stability for improved thermal insulator performance (Sen et al., 2022).

Carbon aerogels are nanostructured carbons formed by supercritical drying and high-temperature carbonization from resorcinol and formaldehyde precursors. Due to their nanosized pores and particle morphologies, carbon aerogels have very low thermal conductivity, making them attractive candidates for high-temperature insulation applications. It is widely known that a variety of factors affect and contribute to the thermal conductivity of carbon aerogels. Additionally, the applications of pristine carbon aerogels are constrained by their poor mechanical qualities; as a result, it is important to fortify the carbon aerogels and enhance their mechanical properties. Aerogels made of reinforced carbon were introduced (Hu et al., 2019).

5.3. Chemistry and Physics

Some types and their applications of these classes are: Optical sensors based on silica aerogel platforms; silica aerogel platforms as conductimetric sensors; carbon-based aerogel composites as conductimetric sensors; titania aerogels as sensor platforms; clay aerogels for sensing applications; hydrophobic silica aerogel blocks; aerogel cherenkov counter; nuclear glass ceramics; biomedical and pharmaceutical aerogels (aerogels used for cardiovascular implantable devices; aerogels as tissue engineering substrates; aerogels as drug

delivery systems; silica aerogels as host matrix for drugs -drug carriers-; organic aerogels as drug delivery systems).

5.4. Space and Airborne

Some types and their applications of these classes are: Hypervelocity particle capture; thermal insulation; cryogenic fluid containment; airborne ultrasonic transducer.

Aerogel and related composites are a new class of thermal insulation materials with extraordinarily low effective thermal conductivity. Aerogels' nanoporous structure prevents gas molecules from moving around, and the size effect on the nano-skeleton system limits the transfer of heat from solids. To comprehend and forecast heat exchanges, a lot of modelling and research has been conducted (Fu et al., 2022). The silica aerogel's pores are primarily in the nanoporous range (2–50 nm), which is smaller than the free mean path of the vibration of air molecules at ambient temperature, which is around 97 nm. This considerably reduces the air's ability to transport heat via the pores (Cahill et al., 2014). As a result, silica aerogel has a substantially lower thermal conductivity than traditional thermal insulation materials, measuring between 12 and 20 mW/(mK) at ambient temperature. Although silica aerogel composite exhibits ideal thermal insulation performance, its practical applicability is severely constrained by its extreme brittleness and poor strength. In order to improve the mechanical properties of silica aerogel, fibres are typically added to minimise brittleness and increase strength (Fu et al., 2022).

High porosity and a loose foam structure characterise aerogel. Particle size and pore diameter of the silica aerogel solid skeleton are

both less than 50 nm. Primary and secondary particles make up the silica aerogel's solid framework. Dense amorphous secondary particles (1-2 nm) generated by condensation polymerization of a silicon source are aggregated into spherical primary particles, which are 10 nm in size. Primary particles are linked together by a 3-D skeleton structure like a pearl necklace. The silica aerogel has a significant number of gaps between the nanoparticles, which contributes to its low density (100-200 kg/m3) and high porosity (90-99%) (Fu et al., 2022).

5.5. Metal Industry

Some types and their applications of these classes are: Mold preparation for castings; molds and cores; resorcinol-formaldehyde aerogels as binders; aeroSand, RF aerogel-sand mixtures; thermal decomposition; gas permeability; carbon aerogels as binder materials; aerogels as nanoadditives for foundry sands; aerogels in solidification and casting.

Electrocatalysts frequently employ nanomaterials because of their high usage efficiency and quantum size effect. The intrinsic activity of each catalytic site can be improved, as well as the number of active sites, to increase the activity of nanoelectrocatalysts. By increasing the amount of exposed active sites per unit mass, the catalyst's structure can be strengthened. Aerogels have the properties of a large specific surface area, exposing many active sites, and offering structural stability due to the self-supporting nature of aerogels. This is made possible by the high porosity and three-dimensional network structure. Consequently, the synergetic effect generated by alloy elements can be used to further

improve the single-site activity by modifying the compositions of aerogels (Zhang & Zhao, 2020).

5.6. Food

Food-grade aerogels are an emerging material that are developed to generate functional food components (delivery vehicle for bioactive compounds, nutraceuticals, etc. and sensing material for the detection of pesticides, spoilage, etc.). Functional chemicals can be infused into food-grade aerogels, which has application in the food industry. In applications based on food packaging, food-grade aerogels have enormous potential as a moisture absorber, bioactive compound releaser, transporting material, preserver, etc. Additionally, it enhances the bioavailability of the compounds it is filled with, safeguards them from harmful environments, and can be used as a target-based delivery vehicle. Moreover, food-grade aerogels are naturally biodegradable. Due to their remarkable qualities, food-grade aerogels (based on polysaccharide, protein, and mucilage) are meeting the demand for food application (high porosity, high specific surface area, and very low density) (Dhua et al., 2022).

5.7. Environmental Remediation

Aerogels have drawn a lot of interest as an adsorption medium that eliminates a variety of pollutants that are harmful to the environment and human health in a number of high performance applications. Aerogels' efficacy in environmental sanitation is positive, but there are significant drawbacks, including a difficult drying process, a mechanically weak structure, and high processing costs. These drawbacks have been identified in various research (Jatoi et al., 2021).

Hexavalent uranium can be sorbed with exceptional efficiency using aerogel-based adsorbents. The uranyl cation and surface active moieties combine to produce inner-sphere complexes, which are the basis for adsorption. It has been effective to regenerate and recover uranium through acidification and complexation utilising carbonate or chelating ligands (such as EDTA). Aerogel-based adsorbents have been successfully used to remove uranium from waste fluids and industrial processes, leading experts to believe that these substances would make excellent adsorbents for water treatment and uranium recovery technologies. However, the examined materials' poor hexavalent uranium selectivity points to the need for new aerogel materials with surface derivatization using chelating chemicals (such as salophen and iminodiacetate) that have a high affinity for uranyl moieties (Georgiou et al., 2023).

An efficient method to produce strongly oxidative species for the removal of refractory organic contaminants in water is by Fenton-like reactions. Several research efforts have been put towards developing heterogeneous catalysts for Fenton-like reactions over the past few decades in an effort to solve problems with homogeneous Fenton systems, such as limited pH appropriateness, sluggish reduction of Fe^{3+} to Fe^{2+}, and iron sludge generation. With its distinctive -conjugated structure and features, graphene aerogel (GA) has found widespread use in a variety of applications, including as a substrate for the development of composite catalysts utilised in a variety of reactions (Wang et al., 2021).

REFERENCES

Aegerter, M. A., Leventis, N., & Koebel, M. M. (Eds.). (2011). Aerogels handbook. *Springer Science & Business Media.*

Aghabararpour, M., Mohsenpour, M., Motahari, S., & Abolghasemi, A. (2018). Mechanical properties of isocyanate crosslinked resorcinol formaldehyde aerogels. *Journal of Non-Crystalline Solids*, 481, 548-555.

Akhter, F., Jamali, A. R., Abbasi, M. N., Mallah, M. A., Rao, A. A., Wahocho, S. A., ... & Chandio, Z. A. (2023). A comprehensive review of hydrophobic silica and composite aerogels: synthesis, properties and recent progress towards environmental remediation and biomedical applications. *Environmental Science and Pollution Research,* 30(5), 11226-11245.

Ambrosi, A., & Pumera, M. (2016). 3D-printing technologies for electrochemical applications. *Chemical Society Reviews,* 45(10), 2740-2755.

Anderson, A. M., & Carroll, M. K. (2011). Hydrophobic silica aerogels: review of synthesis, properties and applications. *Aerogels handbook,* 47-77.

Bangi, U. K., Jung, I. K., Park, C. S., Baek, S., & Park, H. H. (2013). Optically transparent silica aerogels based on sodium silicate by a two step sol–gel process and ambient pressure drying. *Solid State Sciences,* 18, 50-57.

Bangi, U. K., Kavale, M. S., Baek, S., & Park, H. H. (2012). Synthesis of MWCNTs doped sodium silicate based aerogels by ambient pressure drying. *Journal of Sol-gel Science and Technology,* 62, 201-207.

Barrios, E., Fox, D., Li Sip, Y. Y., Catarata, R., Calderon, J. E., Azim, N., ... & Zhai, L. (2019). Nanomaterials in advanced, high-performance aerogel composites: A review. *Polymers,* 11(4), 726.

Boday, D. J., Keng, P. Y., Muriithi, B., Pyun, J., & Loy, D. A. (2010). Mechanically reinforced silica aerogel nanocomposites via surface initiated atom transfer radical polymerizations. *Journal of Materials Chemistry,* 20(33), 6863-6865.

Cahill, D. G., Braun, P. V., Chen, G., Clarke, D. R., Fan, S., Goodson, K. E., ... & Shi, L. (2014). Nanoscale thermal transport. II. 2003–2012. *Applied Physics Reviews,* 1(1), 011305.

Cao, Q., Geng, X., Wang, H., Wang, P., Liu, A., Lan, Y., & Peng, Q. (2018). A review of current development of graphene mechanics. *Crystals,* 8(9), 357.

Capadona, L. A., Meador, M. A. B., Alunni, A., Fabrizio, E. F., Vassilaras, P., & Leventis, N. (2006). Flexible, low-density polymer crosslinked silica aerogels. *Polymer,* 47(16), 5754-5761.

Chandrasekaran, S., Yao, B., Liu, T., Xiao, W., Song, Y., Qian, F., ... & Worsley, M. A. (2018). Direct ink writing of organic and carbon aerogels. *Materials Horizons*, 5(6), 1166-1175.

Chen, J., Zhang, B., Wei, M. Q., Men, J., & Miao, G. W. (2015). The optimum of preparation and characterization of aerogels like hydrophobic titania by ambient pressure drying. *In Advanced Materials Research* (Vol. 1120, pp. 264-274). Trans Tech Publications Ltd.

Deville, S. (2018). The lure of ice-templating: Recent trends and opportunities for porous materials. *Scripta Materialia,* 147, 119-124.

Dhua, S., Gupta, A. K., & Mishra, P. (2022). Aerogel: Functional Emerging Material for Potential Application in Food: A Review. *Food and Bioprocess Technology,* 15(11), 2396-2421.

Dizon, J. R. C., Espera Jr, A. H., Chen, Q., & Advincula, R. C. (2018). Mechanical characterization of 3D-printed polymers. *Additive Manufacturing,* 20, 44-67.

Du, A., Zhou, B., Zhang, Z., & Shen, J. (2013). A special material or a new state of matter: a review and reconsideration of the aerogel. *Materials,* 6(3), 941-968.

Duan, Y., Jana, S. C., Lama, B., & Espe, M. P. (2013). Reinforcement of silica aerogels using silane-end-capped polyurethanes. *Langmuir,* 29(20), 6156-6165.

Farahani, R. D., Dubé, M., & Therriault, D. (2016). Three-dimensional printing of multifunctional nanocomposites: manufacturing techniques and applications. *Advanced Materials,* 28(28), 5794-5821.

Fu, Z., Corker, J., Papathanasiou, T., Wang, Y., Zhou, Y., Madyan, O. A., ... & Fan, M. (2022). Critical review on the thermal conductivity modelling of silica aerogel composites. *Journal of Building Engineering,* 57, 104814.

Georgiou, E., Raptopoulos, G., Anastopoulos, I., Giannakoudakis, D. A., Arkas, M., Paraskevopoulou, P., & Pashalidis, I. (2023). Uranium Removal from Aqueous Solutions by Aerogel-Based Adsorbents—A Critical Review. *Nanomaterials,* 13(2), 363.

Gu, P., Liu, W., Hou, Q., & Ni, Y. (2021). Lignocellulose-derived hydrogel/aerogel-based flexible quasi-solid-state supercapacitors with high-performance: A review. *Journal of Materials Chemistry A,* 9(25), 14233-14264.

Gurav, J. L., Jung, I. K., Park, H. H., Kang, E. S., & Nadargi, D. Y. (2010). Silica aerogel: synthesis and applications. *Journal of Nanomaterials,* 2010, 1-11.

Hirashima, H. (2011). Preparation of TiO 2 aerogels-like materials under ambient pressure. *Aerogels Handbook,* 145-153.

Hu, K., Szkopek, T., & Cerruti, M. (2017). Tuning the aggregation of graphene oxide dispersions to synthesize elastic, low density graphene aerogels. *Journal of Materials Chemistry A,* 5(44), 23123-23130.

Hu, L., He, R., Lei, H., & Fang, D. (2019). Carbon aerogel for insulation applications: a review. *International Journal of Thermophysics,* 40, 1-25.

Huang, J., Liu, H., Chen, S., & Ding, C. (2017). Graphene aerogel prepared through double hydrothermal reduction as high-performance oil adsorbent. *Materials Science and Engineering: B,* 226, 141-150.

Huang, L. J., Lee, W. J., & Chen, Y. C. (2022). Bio-based hydrogel and aerogel composites prepared by combining cellulose solutions and waterborne polyurethane. *Polymers,* 14(1), 204.

Ingale, S. V., Sastry, P. U., Wagh, P. B., Tripathi, A. K., Rao, R., Tewari, R., ... & Gupta, S. C. (2012). Synthesis and micro structural investigations of titania–silica nano composite aerogels. *Materials Chemistry and Physics,* 135(2-3), 497-502.

Jatoi, A. S., Hashmi, Z., Mazari, S. A., Abro, R., & Sabzoi, N. (2021). Recent developments and progress of aerogel assisted environmental remediation: A review. *Journal of Porous Materials*, 28, 1919-1933.

Jimenez-Saelices, C., Seantier, B., Cathala, B., & Grohens, Y. (2017). Effect of freeze-drying parameters on the microstructure and thermal insulating properties of nanofibrillated cellulose aerogels. *Journal of Sol-Gel Science and Technology,* 84, 475-485.

Karamikamkar, S., Naguib, H. E., & Park, C. B. (2020). Advances in precursor system for silica-based aerogel production toward improved mechanical properties, customized morphology, and multifunctionality: A review. *Advances in Colloid and Interface Science,* 276, 102101.

Kistler, S. S. (1931). Coherent expanded aerogels and jellies. *Nature,* 127(3211), 741-741.

Kistler, S. S. (1941). U.S. Patent No. 2,249,767. *W*ashington, DC: U.S. Patent and Trademark Office.

Leventis, N., Chandrasekaran, N., Sadekar, A. G., Mulik, S., & Sotiriou-Leventis, C. (2010). The effect of compactness on the carbothermal conversion of interpenetrating metal oxide/resorcinol-formaldehyde nanoparticle networks to porous metals and carbides. *Journal of Materials Chemistry,* 20(35), 7456-7471.

Leventis, N., & Lu, H. (2011). Polymer-crosslinked aerogels. *Aerogels Handbook,* 251-285.

Li, Z., Shao, L., Hu, W., Zheng, T., Lu, L., Cao, Y., & Chen, Y. (2018). Excellent reusable chitosan/cellulose aerogel as an oil and organic solvent absorbent. *Carbohydrate Polymers,* 191, 183-190.

Lin, J., Li, G., Liu, W., Qiu, R., Wei, H., Zong, K., & Cai, X. (2021). A review of recent progress on the silica aerogel monoliths: Synthesis, reinforcement, and applications. *Journal of Materials Science,* 56, 10812-10833.

Liu, Y., Peng, Y., Zhang, T., Qiu, F., & Yuan, D. (2018). Superhydrophobic, ultralight and flexible biomass carbon aerogels derived from sisal fibers for highly efficient oil–water separation. *Cellulose,* 25, 3067-3078.

Maleki, H., Durães, L., & Portugal, A. (2014). Synthesis of lightweight polymer-reinforced silica aerogels with improved mechanical and thermal insulation properties for space applications. *Microporous and Mesoporous Materials,* 197, 116-129.

Mazrouei-Sebdani, Z., Naeimirad, M., Peterek, S., Begum, H., Galmarini, S., Pursche, F., ... & Malfait, W. J. (2022). Multiple assembly strategies for silica aerogel-fiber combinations–a review. *Materials & Design,* 111228.

Meador, M. A. B., Vivod, S. L., McCorkle, L., Quade, D., Sullivan, R. M., Ghosn, L. J., ... & Capadona, L. A. (2008). Reinforcing polymer cross-linked aerogels with carbon nanofibers. *Journal of Materials Chemistry,* 18(16), 1843-1852.

Merillas, B., Martin-de Leon, J., Villafane, F., & Rodriguez-Perez, M. A. (2021). Transparent polyisocyanurate-polyurethane-based

aerogels: key aspects on the synthesis and their porous structures. *ACS Applied Polymer Materials,* 3(9), 4607-4615.

Merillas, B., Martín-de León, J., Villafañe, F., & Rodríguez-Pérez, M. Á. (2022). Optical Properties of Polyisocyanurate–Polyurethane Aerogels: Study of the Scattering Mechanisms. *Nanomaterials,* 12(9), 1522.

Motahari, S., Nodeh, M., & Maghsoudi, K. (2016). Absorption of heavy metals using resorcinol formaldehyde aerogel modified with amine groups. *Desalination and Water Treatment,* 57(36), 16886-16897.

Mulik, S., & Sotiriou-Leventis, C. (2011). Resorcinol–formaldehyde aerogels. *Aerogels handbook,* 215-234.

Nadargi, D. Y., Latthe, S. S., Hirashima, H., & Rao, A. V. (2009). Studies on rheological properties of methyltriethoxysilane (MTES) based flexible superhydrophobic silica aerogels. *Microporous and Mesoporous Materials,* 117(3), 617-626.

Pang, K., Song, X., Xu, Z., Liu, X., Liu, Y., Zhong, L., ... & Gao, C. (2020). Hydroplastic foaming of graphene aerogels and artificially intelligent tactile sensors. *Science Advances,* 6(46), eabd4045.

Qi, P., Zhu, H., Borodich, F., & Peng, Q. (2023). A review of the mechanical properties of Graphene Aerogel materials: experimental measurements and computer simulations. *Materials,* 16(5), 1800.

Rao, A. V., Pajonk, G. M., Bangi, U. K., Rao, A. P., & Koebel, M. M. (2011). Sodium silicate based aerogels via ambient pressure drying. *Aerogels Handbook,* 103-124.

Rao, A. V., Pajonk, G. M., Nadargi, D. Y., & Koebel, M. M. (2011). Superhydrophobic and flexible Aerogels. *Aerogels handbook,* 79-101.

Randall, J. P., Meador, M. A. B., & Jana, S. C. (2011). Tailoring mechanical properties of aerogels for aerospace applications. ACS Applied Materials & Interfaces, 3(3), 613-626.

Ratke, L., & Gurikov, P. (2021). The chemistry and physics of aerogels: Synthesis, processing, and properties. Cambridge University Press.Peri, J. (1966). Infrared study of OH and NH_2 groups on the surface of a dry silica aerogel. *The Journal of Physical Chemistry*, 70(9), 2937-2945.

Schwan, M., & Ratke, L. (2013). Flexibilisation of resorcinol–formaldehyde aerogels. *Journal of Materials Chemistry A,* 1(43), 13462-13468.

Schwan, M., Tannert, R., & Ratke, L. (2016). New soft and spongy resorcinol–formaldehyde aerogels. *The Journal of Supercritical Fluids,* 107, 201-208.

Sen, S., Singh, A., Bera, C., Roy, S., & Kailasam, K. (2022). Recent developments in biomass derived cellulose aerogel materials for thermal insulation application: *A review. Cellulose*, 29(9), 4805-4833.

Slosarczyk, A., Vashchuk, A., & Klapiszewski, Ł. (2022). Research Development in Silica Aerogel Incorporated Cementitious Composites—A Review. *Polymers,* 14(7), 1456.

Tafreshi, O. A., Mosanenzadeh, S. G., Karamikamkar, S., Saadatnia, Z., Park, C. B., & Naguib, H. E. (2022). A review on multifunctional

aerogel fibers: processing, fabrication, functionalization, and applications. *Materials Today Chemistry,* 23, 100736.

Tang, X., Zhu, C., Cheng, D., Zhou, H., Liu, X., Xie, P., ... & Fan, T. (2018). Architectured leaf-inspired Ni0. 33Co0. 66S2/graphene aerogels via 3D printing for high-performance energy storage. *Advanced Functional Materials,* 28(51), 1805057.

Thakur, A. (2022). Graphene aerogel based energy storage materials–A review. *Materials Today: Proceedings.*

Vareda, J. P., Lamy-Mendes, A., & Durães, L. (2018). A reconsideration on the definition of the term aerogel based on current drying trends. *Microporous and Mesoporous Materials*, 258, 211-216.

Wang, Y., Chen, L., Cheng, H., Wang, B., Feng, X., Mao, Z., & Sui, X. (2020). Mechanically flexible, waterproof, breathable cellulose/polypyrrole/polyurethane composite aerogels as wearable heaters for personal thermal management. *Chemical Engineering Journal,* 402, 126222.

Wang, C., Chen, X., Wang, B., Huang, M., Wang, B., Jiang, Y., & Ruoff, R. S. (2018). Freeze-casting produces a graphene oxide aerogel with a radial and centrosymmetric structure. *ACS Nano,* 12(6), 5816-5825.

Wang, X., Li, C., Shi, Z., Zhi, M., & Hong, Z. (2018). The investigation of an organic acid assisted sol–gel method for preparing monolithic zirconia aerogels. *RSC advances,* 8(15), 8011-8020.

Wang, L., Zhang, Y., & Qian, J. (2021). Graphene aerogel-based catalysts in Fenton-like reactions for water decontamination: a short review. *Chemical Engineering Journal Advances*, 8, 100171.

Walker, R. C., Potochniak, A. E., Hyer, A. P., & Ferri, J. K. (2021). Zirconia aerogels for thermal management: Review of synthesis, processing, and properties information architecture. *Advances in Colloid and Interface Science,* 295, 102464.

Yuan, S., Fan, W., Wang, D., Zhang, L., Miao, Y. E., Lai, F., & Liu, T. (2021). 3D printed carbon aerogel microlattices for customizable supercapacitors with high areal capacitance. *Journal of Materials Chemistry A,* 9(1), 423-432.

Zhang, Q., Zhang, F., Xu, X., Zhou, C., & Lin, D. (2018). Three-dimensional printing hollow polymer template-mediated graphene lattices with tailorable architectures and multifunctional properties. *ACS Nano,* 12(2), 1096-1106.

Zhang, R., & Zhao, Y. (2020). Preparation and electrocatalysis application of pure metallic aerogel: A review. *Catalysts,* 10(12), 1376.

Zhao, K., Zhang, T., Chang, H., Yang, Y., Xiao, P., Zhang, H., ... & Chen, Y. (2019). Super-elasticity of three-dimensionally cross-linked graphene materials all the way to deep cryogenic temperatures. *Science Advances,* 5(4), eaav2589.

Zhu, C., Liu, T., Qian, F., Chen, W., Chandrasekaran, S., Yao, B., ... & Li, Y. (2017). 3D printed functional nanomaterials for electrochemical energy storage. *Nano Today,* 15, 107-120.

CHAPTER 2

3D PRINTING (ADDITIVE MANUFACTURING) OF SINGLE AND COMPOSITE POLYMERS: AN OVERVIEW

Dr. Nihayet KOÇYİĞİT[1]

---

[1] Batman University, Chemistry Department, Batman, Turkiye.
nihayet.kocyigit@batman.edu.tr,   Orcid ID:0000-0002-3472-1127

1. INTRODUCTION

The method of layer-by-layer adding and linking materials to produce objects is known as additive manufacturing. Through the use of this technical procedure, three-dimensional materials can be manufactured directly from CAD models (Guo & Leu, 2013). The main industries where additive manufacturing is employed are industrial/business machinery, consumer goods, and the automobile industry (Jiang et al., 2017). Despite this, there are industries where the use of additive manufacturing techniques is growing, including the medical sector (via the printing of living tissue), the energy and aerospace sectors (Valvez et al., 2021).

Major polymers printed by the currently available commercial additive manufacturing techniques are: 1) ABS (acrylonitrile butadiene styrene), 2) PLA (polylactic acid), 3) PA (polyamide), 4) PET (Polyethylene terephthalate), 5) TPE (thermoplastic elastomers), 6) PC (polycarbonate), 7) PEI (polyethyleneimine), 8) PP (polypropylene), 9) ASA (acrylonitrile styrene acrylate), 10) PEEK (polyaryletheretherketone), 11) PPS (polyphenylene sulfide), 12) Acrylic, 13) PMMA (poly(methyl methacrylate)), 14) Oxycetane, 15) HDPE (high-density polyethylene), 16) Rubber, 17) Silicone, 18) Epoxy (Low et al., 2017).

3D printing has emerged as a feasible method for the fabrication of engineering components. Due to its benefits, which include little post-processing, easy manufacturing, reduced material waste, and energy efficiency, 3D printing is suitable for application in industry. A rapidly developing technology, 3D printing for the production of polymer composites outperforms conventional polymer composite fabrication

methods in terms of part complexity, production time, and prototype flexibility (Mishra & Jagadesh, 2022). Composites printed by the currently available commercial additive manufacturing techniques are: 1) ABS-Carbon, 2) ABS-PP, 3) ABS-PBT, 4) ABS-Acrylic, 5) ABS-PC, 6) PLA-Carbon, 7) PLA-wood, 8) PA-Carbon, 9) PA-Glass, 10) PA-Metal, 11) PET-Carbon (Low et al., 2017).

Higher-dimensional accuracy and shorter time to construct prototypes have become the reason to use 3D printed techniques in modern industries. There are several types of 3D printed techniques that have been commonly used in modern industry such as selective laser sintering (SLS), stereolithography (SLA), fused deposition modelling (FDM), direct metal laser sintering (DMLS) and laminated object manufacturing (LOM) (Halim et al., 2021); fabrication with fused filament (FFF), inkjet printing (IJP), powderbed fusion (PBD), dynamic optical projection stereolithography (DOPsL), micro-stereolithography (MSL), direct-write assembly (DW), conformal 3DP (C-3DP), solvent-cast 3DP (SC-3DP), two-photon polymerization (TPP), and UV-3DP (Farahani et al., 2016; Tian et al., 2016). The most commonly used 3D printed technique in the industry is "fused deposition modelling" because of its ability to construct a complex structure in a shorter time and lower cost (Halim et al., 2021).

Additive manufacturing is capable of easily building complex, real custom objects layer by layer (Ligon et al., 2017). A computer-aided design (CAD) model serves as the basis for the entire process before being transformed into the stereolithography format (STL). A specific piece of software is used to pre-process the received 3D file, defining process parameters like the orientation of the 3D part within the build

volume and the slicing settings. After that, the data is transferred to the 3D printer, which performs layer-by-layer construction (Thiam et al., 2022).

It has been widely used in applications such as electrical and electronics (Johnson et al., 2020), medical (Ceretti et al., 2017), rapid tooling (Singh et al., 2018), aircraft industries (Halim et al., 2021) and automotive sector (Sheoran & Kumar, 2020). Traditional fused deposition modelling systems only used to fabricate parts with thermoplastics. Current fused deposition modelling systems can produce parts in a wide range of engineering and industrial thermoplastics such as acrylonitrile butadiene styrene (ABS), polylactic acid (PLA), etc (Halim et al., 2021).

The fundamental idea behind the fused deposition modelling (FDM) technology is that it can extrude a broad variety of different materials, including carbon, metals, and ceramics, and then deposit them layer by layer through a nozzle of feedstock filament. The filament winder, driving wheels, filament feedstock, extrusion heads, nozzle, and building platform are all components of the fused deposition modelling system, which is utilised to deposit the extruded materials used in 3D printing layer by layer. Depending on the intended use, the 3D printing filament feedstock can be a single polymer, a blend of polymers, or a composite material made of a base polymer plus filler components. Metals, ceramics, and carbon are examples of filler materials. The new composites materials from a combination of base polymers and filler materials in feedstock filament can be developed and used in the fused deposition modelling process with suitable size and properties. Fused deposition modelling technique has been used in improving mechanical

properties (Kotsilkova et al., 2019), improving electrical conductivity (Dorigato et al., 2017), improving thermal properties (Ebrahimi & Ju, 2018), improve process ability (Yang et al., 2019), and fabricate complex parts (Sang et al., 2019).

2. TYPES OF 3D PRINTED POLYMERS

The classification of 3D printed polymers can be divided into a single polymer, poly-polymer, and composite. Materials used for single polymer 3D printing are a single polymer. In contrast, poly-polymer 3D printed materials are the materials that blend two or more polymers together. Single polymer composites, polymer blends, hybrid fillers, and base-filler hybrids are all included in the classification of composites. By combining two or more polymers and adding filler material, polymer blends composite can be produced (Halim et al., 2021).

2.1. 3D Printing Single Polymers and Poly-Polymers

Using an ultraviolet (UV) laser beam, stereolithography (SLA) solidifies a photosensitive liquid resin layer by layer (Zhou et al., 2020). The build platform is initially positioned in the tank with the photopolymer resin, one layer height away from the build window (Fig. 1). On the basis of the cross-section of the 3D model, the laser beam travels along a specified path. The construction platform is then elevated to reveal a fresh layer of liquid polymer after the first layer has set. The object's cross section is traced by the laser once more, and this time it immediately adheres to the hardened portion. A digital light-processing (DLP) projector can replace the UV laser to achieve resin hardening, enabling a cost reduction system and faster processing. However, this results in reduced XY resolution (Thiam et al., 2022).
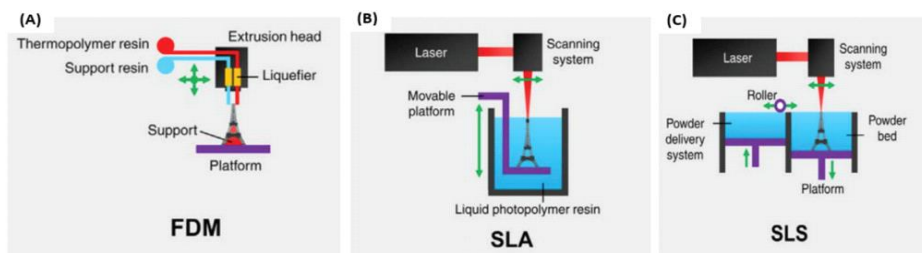
Fig. 1. Schematic illustrations of 3D printing technologies. (A) FDM printing. (B) SLA printing. (C) SLS printing. (Low et al., 2017; Thiam et al., 2022).

SLS relies on a powerful laser beam to fuse powder at very precise points of the 3D file (Ligon et al., 2017). A new layer of fine powder is then spread before fusing the laser onto the previous layer (Thiam et al., 2022).

Polymer membranes are central to the proper operation of several processes used in a wide range of applications. These membranes are manufactured using techniques like electrospinning, phase inversion, stretching, track etching, and sintering. Utilising additive manufacturing, which makes it simpler to produce customised membranes, is a cutting-edge and competitive method in the production of membranes (Thiam et al., 2022).

Water treatment, electrodialysis, batteries, the food and pharmaceutical sectors, and many other fields utilise membrane technology, notably polymer membranes (Dong et al., 2021). A polymer membrane is a physical barrier separating two habitats that has been specifically designed to allow some species to pass through. It is ideal for membranes to have good selectivity, stability, and affordability in all applications. Choosing a membrane relies on the application. According to Low et al. (2017), membranes can be microporous, asymmetric

composite thin-film, dense, or ion-exchange. A typical filter's ability to reject large particles (those larger than 10 m) while permitting the smallest particles to pass is remarkably similar to the function of a microporous membrane. For a dense membrane, permeants are transported by diffusion under the driving force of pressure, concentration, or electric potential gradient. A thin-film composite asymmetric membrane (TFC) has a thick, thin selective layer and is microporous. Ion exchange membranes contain fixed ions that are either positively or negatively charged and can be either dense or microporous in their polymer matrix. Their working theory is based on the passage of ions with the opposite charge to those of the fixed ions in the membrane structure and the exclusion of ions with the same charge (Thiam et al., 2022).

Examples of 3D-printed membranes are 1) PET(PMMA-gPDMS) prepared by method FDM combined with Electrospinning, 2) PLA/PDA-gPSBMA prepared by method Nonsolvent induced phase separation (NIPS), 3) (PDMS)/SiO2 prepared by method FDM using ink, 4) ABS–PES prepared by method MultiJet 3D Printing, 5) PLA/polystyrène (PS) prepared by method FDM, 6) polysulfone (PSU) prepared by method SLS, 7) PSU/Fe3O4 prepared by method Electrospinning, 8) PA6 prepared by method Electrospinning, 9) PVDF prepared by method 3D printing near-field electrospinning (NFES), 10) PVDF prepared by method Melt spinning and stretching (Thiam et al., 2022).

Hybrid membranes are ones with a unique phase that controls the membrane's selectivity and permeability integrated inside a second phase that provides structural support and integrity, allowing a continuous transport channel to be established across the separating layer. These

hybrid membranes are different from mixed-matrix membranes, which disseminate a second phase at a low concentration in the selective layer of a thin film composite membrane to offer, for instance, a minimal increase in permeability or some anti-fouling resistance. Though not yet scalable, so-called vertically-aligned carbon nanotube membranes are a good illustration of a hybrid membrane in which the polymer matrix hiding the tubes does not actively contribute to the separation process and the nanotubes themselves provide both the permeating pathway and selectivity by size exclusion (Mattia et al., 2014). The positioning of the transport channels in both the support and the separating layers, the adhesion between the various phases and with the support, and fabrication techniques that are scalable and cost-effective compared to current technology are just a few of the difficulties that remain in the preparation of hybrid membranes. Here, additive manufacturing (AM) has the potential to significantly change the way membranes are made by enabling the printing of the entire membrane as a single monolithic piece with the use of several materials and intricate configurations that can all be precisely specified. By incorporating microporous materials into the printing materials, this strategy may also be able to get around the resolution limitations now associated with additive manufacturing. The product therefore would consist of currently achievable micrometer-size features but with microporosity of the porous components. Specifically, AM can provide a tailored scaffold-like membrane made up by polymer and porous nanomaterials (Low et al., 2017).

2.2. 3D Printing Polymer Composites

Additive Manufacturing technology has a significant impact on the modern world because of its ability to fabricate highly complex computerized geometrics. Pure 3D-printed polymer parts have limited potential applications due to inherently inferior mechanical and anisotropic properties. For more utilization and versatility, the addition of fillers has enhanced their functionalities. 3D printing has innovative advantages including low cost, customized geometry, minimal wastage, and ease of material change. Development of 3D printing techniques of matrix composite materials improve properties and their applications in the fields of automotive, aerospace, biomedical, and electronics. AM techniques are mainly fused deposition modeling (FDM), selective laser sintering (SLS), Powder-liquid 3D printing (PLP), stereolithography (SLA), digital light processing (DLP), and robocasting. Process methodologies and behavior of different filler additives, reinforcement fibers, nanoparticles, and ceramic polymer composites are important. Major issues of difficulty include printing parameters, homogeneous desperation of fillers, nozzle clogging due to filler aggregation, void formation, augmented curing time, and anisotropic attributes (Saroia et al., 2020).

Without the use of specialised equipment, jigs, or tools, 3D printing (3DP) has made it possible to produce complex geometries in their final form. The printing of composite materials is a new field of study, with just one commercially available printer type and a small number of others under development, in contrast to the 3DP of polymers, which has attracted considerable attention over the past two decades. The process of 3DP can also be difficult because it typically involves trial

and error to determine the proper combination of elements (material, printer, process settings, and post-processing) to achieve the desired result (Sanei & Popescu, 2020).

It is called polymer blends when a system combines or blends two polymers to improve specific properties to the composite while maintaining others. The examples of polymer blends in FDM 3D printing are polyetherimide (PEI)/ polycarbonate (PC), polylactic acid (PLA)/polyhydroxyalkanoate (PHA), polycaprolactone (PCL)/ hydrolyzed collagen (HC), and polyethylene terephthalate (PET)/ polypropylene (PP) (Halim et al., 2021).

Diferent original equipment manufacturers of composite printing are: Markforged, Anisoprint, Desktop Metal, Fortify, Continuous composites, Impossible Objects, Arevo. The printing technology used by these companies are FDM, FDM combined with AFP, Continuous fber 3D printing with FDM, Digital light processing, Composite-Based Additive Manufacturing (CBAM), FDM with Multi-axis Robotics. The applications conducted by these are functional prototyping, tooling, jigs, fxtures, various end-use parts, parts with diferent composites material, composite tooling, lightweight components, lightweight industrial parts (Mishra & Jagadesh, 2022)

ASTM standarts for composite 3D printing using FDM are: ISO 527/ ASTM–D638 (Tensile test for polymer), ASTM–D3039 (Tensile test for polymer composite), ASTM–D790 (Flexural test), ASTM–D695 (Compression test), ASTM–D256 (Izod impact test), ASTM–D6110 (Charpy impact test), ASTM–D785 (Rockwell hardness test), ASTM–D2240 (Shore hardness test), ASTM–E384 (Micro indentation test),

ASTM–D7791 (Fatigue testing under uniaxial loading), ASTM–D7774 (Fatigue testing under fexural loading) (Dizon et al., 2018).

2.3. 3D Printing of Polymer Nanocomposites

Building multifunctional objects with good electrical and thermal conductivity, mechanical strength, and stiffness at relatively low cost using 3D printing of polymer nanocomposites with a relatively low amount of layered silicate fillers or conductive nanofillers, such as carbon nanotubes, graphene, and metal particles is possible (Francis & Jain 2016). Electrical percolation, which controls electrical conductivity in conductive polymer nanocomposites, necessitates a minimum filler content (volume fraction) in order to transform an insulating polymer matrix into a conductive composite (Alig et al., 2007). This minimum volume fraction of nanofillers, referred as percolation threshold, strongly depends on factors like, shape and size distribution of the nanofillers (Gnanasekaran et al., 2014), processing methods such as dispersion and agglomeration of nanofillers (Gnanasekaran et al., 2016), and attractive interactions (Vigolo et al., 2005). Several studies have been reported on 3D printing of conductive polymer nanocomposites, based on conventionally used 3D printing polymers like acrylonitrile butadiene styrene (ABS) and poly lactic acid (PLA) (Rymansaib et al., 2016). However, the development of new conductive polymer nanocomposite materials for a desktop 3D printer is highly desirable to achieve better printability, mechanical properties and electrical conductivity (Gnanasekaran et al., 2017).

Carbon nanotubes (CNT) are a good choice to incorporate 3DP polymers due to their excellent mechanical, electrical, and thermal

properties. The structural deficiencies in Multiwall Carbon Nanotubes (MWCNTs) enable for strong interactions with polymers as well as cross-linking and functionalization (Ventura et al., 2010). For improved CNT-based filaments, a homogenous dispersion of CNTs in polymeric solutions is necessary. Studies has focused on figuring out the concentration of CNTs that would surpass the percolation threshold while maintaining the parameters for 3D printing because the well-known issue of CNTs aggregation can be detrimental to FDM, potentially causing blockages at the nozzle and flux instability while printing. Continuous CNT yarn filaments can be employed as an inherently multifunctional feedstock for 3DP, since it becomes possible to use a single material to impart multiple functionalitiesin components and take advantage of the tailor-ability offered by FFF over other conventional fabrication techniques (Gardner et al., 2016).

The engineering substance graphene (Gr) is extremely expensive and has exceptional mechanical, metallurgical, thermal, and electrical properties. Some studies reported the production of low-cost Gr-reinforced polymer matrix-based feedstock filament for FDM applications. Due to its intriguing properties, including low resistivity, excellent thermal conductivity, optical transparency, and high electron mobility, graphene has grown in popularity as a material that will revolutionise electronics. Fortunately, Gr has safely passed the peak of overestimated expectations and is now settling on some novel applications. Gr demonstrates a number of unique characteristics, including as flexibility and conductivity. Gr-infused 3DP filaments have the potential to improve the manufacturing of highly conductive composites. These carbon nanostructured additives are used in 3DP

filaments for a variety of purposes, such as sensors, trackpads, electromagnetic shielding, and RF shielding (Horst & Junior, 2021). Due to the combination of structural interconnectivities and Gr's exceptional properties, 3D-Gr-based architectures like Gr-based hydrogels, aerogels, foams, and sponges have received a lot of attention. These structures offer fascinating structures with low density, large surface areas, high porosity, stable mechanical properties, fast mass, and optimal electron transport. Being carefully explored for a variety of applications, including as batteries, sensors, catalysts, and capacitors (Yang et al., 2015). The design and development of Gr-based polymer nanocomposites, characterised by a regulated arrangement of the graphene-based nanosheets into spatially segregated 3D architectures, has attracted a lot of attention during the past ten years. From a technological standpoint, the development of a continuous filler network by containing the nanosheets within a restricted volume of the polymeric matrix is very appealing. The realisation of segregated 3D-Gr-based structures does, in fact, enable correct tailoring of the overall performances of the resulting polymer nanocomposites, offering appreciable enhancements in terms of structural and functional properties. The manufacturing 3D-Gr monolith with high mechanical and electrical performance has become an urgent issue in view of their potential applications in energy and electronics fields. Due to the structure rigidity and poor liquid-phase processing capability of graphene sheets, it is challenging to fabricate 3D-Gr monolith with high mechanical performance, including strength, toughness and resiliency (Horst & Junior, 2021).

Although thermoplastic polymers are frequently used in 3D printing, the demand for polymer composites with higher performance is rising due to their poor mechanical properties. The focus has shifted to the development and characterisation of diverse nanocomposites due to the advantageous features provided by nanocomposites. The potential for additive manufacturing to enhance polymeric composites' characteristics is enormous. Additionally, the 3D printing technology is adaptable enough to reduce the time needed for manufacturing goods. But careful research must be done to determine how different process factors affect the mechanical characteristics (Kichloo et al., 2021).

2.4. 3D printing Fiber Reinforced Polymer Composites

Utilising a layer-by-layer deposition of materials, 3D printing is advantageous for producing parts because it requires fewer steps in the manufacturing process, offers tremendous flexibility for prototyping, especially of complicated parts, and generates little waste. The weak inter-layer bonding and rough surface of 3D printed objects, however, have always raised questions about their mechanical characteristics. Continuous fibre reinforcements are used for the polymer matrix in 3D printed continuous fibre reinforced polymer composites (CFRPCs), which greatly enhance the mechanical properties of printed objects. Due to its exceptional particular mechanical qualities, CFRPCs are frequently utilised in the automotive, medical, and aerospace industries, among other sectors. Compared with other 3D printing technologies, fused deposition modeling (FDM) has the advantages of low cost and simple operation to fabricate CFRPCs (Zhang et al., 2021).

Currently, the most used additive technique for producing parts for fiber-reinforced polymers is fused deposition modelling (FDM). The paradigm spans from functioning elements that need excellent mechanical performances to prototypes. Many aspects of composite 3DP still need to be defined, examined further, and studied in greater detail because this discipline is still in its infancy. Efforts dedicated to 3DP of composite materials can be classified based on the choice of material, the fiber/matrix impregnation method and the hardware used. Similar to traditional composites, 3D-printed composites' mechanical behaviour depends on the constituents' characteristics, the morphology of the reinforcement, the adhesion of the constituents to one another, the volume fraction of the reinforcement, and the manufacturing method. For the case of 3DP, the manufacturing process can be controlled with the choice of print parameters. Factors influencing mechanical performances of 3DP specimen are 1) Material (matrix type, humidity, reinforcement, producer, batch), 2) 3D Printer (Nozzle/s diameter, temperature, envelope, platform/bed temperature, equipment/machine calibration), 3) Process parameters (layer thickness, infill pattern, infill density, raster width, raster angle, building orientation, air gaps, extrusion temperature, flow rate, deposition speed, fiber volume fraction, number of shells/perimeters, fiber orientation), 4) Environment (temperature, humidity), 5) Post processing (heat treatment, pressure) (Sanei & Popescu, 2020).

3. SELECTED APPLICATIONS

The goal of blending polymers is to make the composite easier to process. While a hybrid filler composite is produced by combining a

polymer and two or more fillers, a single polymer composite employs just one type of polymer and one type of filler. Hybrid composite purposes are to enhance the properties (crystallinity, thermal, electrical, and mechanical properties) while maintaining the others to the composite materials. A base-filler hybrid composite is one that has been produced by fusing two or more polymers with two or more fillers. Researchers prefer composites to single polymers or poly-polymers because they give materials varying properties depending on the polymer and filler employed in the composite (Tambrallimath et al., 2019). Since 2011, there has been an increase in research into 3D printed polymer composite materials due to the rapid development of nanotechnology and microelectronic devices, which call for new materials for a variety of applications. MXene is an example of a new material described in 2011 that has developed into a supermaterial with excellent thermal and electrical conductivity, chemical stability, and high mechanical properties. It is anticipated that this new material will prompt a significant increase in polymer composite research in material engineering that can be compared to graphene. Additionally, graphene exhibits exceptional thermal characteristics and has considerable promise for use in electronic devices and energy storage technologies (Halim et al., 2021).

Various industries such as aerospace, biomedical, apparel, dentistry, electronics, automotive, and oceanography are researching additive manufacturing technique to produce parts (Safai et al., 2019).

In recent years, tissue engineering scaffolds have turned into the preferred option for the clinical treatment of pathological and traumatic bone defects. Due to their shared extraordinary benefits, such as high

biocompatibility, good biodegradability, and excellent osteogenesis, silicate-based bioactive glasses (SBGs) and biodegradable medical synthetic polymers (BMSPs) have received a lot of attention in this field. In addition to simulating the mechanical characteristics and microstructure of natural bone, three-dimensional (3D) printed SBG/BMSP scaffolds can also collapse in place after use and ultimately be replaced by regenerated bone tissue in vivo. SBG/BMSP composites offer excellent promise for regenerating and repairing bone tissue (Li et al., 2022).

The association of 3D-printed polymers and incorporation with antimicrobial agents is reported to be effective against different microorganisms. High capacity of incorporating antimicrobial agents into printed polymers as potential dental materials and biomaterials against several microorganisms, including *Staphylococcus aureus*, *Streptococcus mutans*, *Candida scotti*, *Staphylococcus epidermidis*, *Escherichia coli*, and *Candida albicans* was demonstrated in many studies. Studies showed a good interaction between the technologies, which allowed the combination of polymers and antimicrobials, demonstrating efficacy against several species, in addition to the chemical, mechanical, and biological properties presenting good results (de Campos et al., 2022).

Some of the parts printed by polymer composite 3D printing processes include small drones, the wing of an unmanned aerial vehicle, and components of a gas turbine engine. In the case of drone structure, the major achievement was reducing the structural weight without compromising the required structural properties (Mishra & Jagadesh, 2022).
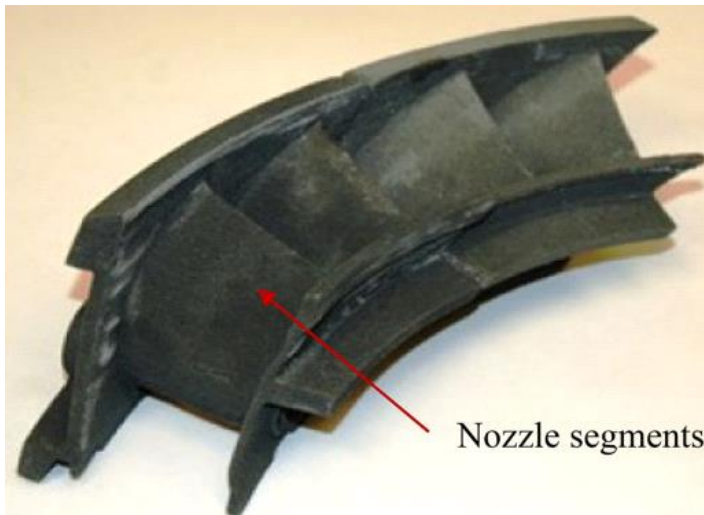
Fig. 2. Applications in aerospace : 3D ceramic composite printing of nozzle segments (Grady et al., 2015).

3D printing of automotive components is now mostly replacing the parts manufactured by conventional manufacturing methods due to lesser manufacturing time and making complex parts easy to fabricate (Mishra & Jagadesh, 2022).

Due to its novel production process and top-notch product quality, 3D printing of energetic materials (EMs) has attracted interest. A fused deposition modelling (FDM) 3D printer was used by Zong et al., (2022) to produce TNT/HMX-based explosive grains (about 20 mm20 mm) that were made up of 60% superfine HMX and 40% TNT to investigate the potential of 3D printing technology in melt-cast explosives. The test results revealed that the printed grains' density was 98.6% of the theoretical value, and their compressive and tensile strengths were 87.5% and 66.7%, respectively, higher than those of the cast grains, demonstrating the printed grains' superior mechanical properties. The

idea and platform for 3D-printed melt-cast explosives with complex structures and great performance were intended to be provided by this effort.

4. ADDITIVE MANUFACTURING MEMBRANE AS SUBSTRATE

The printed membrane can also be used as a novel substrate for functional materials such as 1) metals, 2) metal oxides (e.g. ZnO, TiO2), ceramics (e.g. SiO2, Al2O3), 3) porous materials (metal-organic framework (MOF), zeolite, covalent organic framework (COF), porous organic polymers, zeolitic imidazolate framework (ZIF), and porous molecular solids), 4) carbon-based material (graphene oxide (GO), graphene, and carbon nanotubes (CNT)) and 5) other polymers including hydrogels (Breuer & Sundararaj, 2004; Allen et al., 2010; Kabiri et al., 2011; Slater & Cooper, 2015)

Potential techniques for transferring functional materials on the printed substrate are: 1) atomic layer deposition (ALD), 2) chemical vapor deposition (CVD), 3) LIGA method process (German acronym for Lithography, Galvanization and Abformung (molding)), 4) dip-coating, 5) spin-coating, 6) direct growth (on a chemically-modified substrate), 7) contra-diffusion, 8) vacuum filtration followed by secondary growth, 9) hydrothermal growth, 10) electrospinning, 11) electrodeposition, 12) vacuum deposition, 13) interfacial polymerization, 14) layer-by-layer assembly (Low et al., 2017).

Some companies active in this sector are: Allied photopolymers, 3DXTech, EnvisionTEC, Bolson Materials, Stratasys, Filoalfa, Form Futura, OO-Kuma, 3D Systems, Kevvox, Orbi-Tech, DSM Somos,

Taulman 3D, Proto Pasta, ColorFabb, BnK, ALM, Arzauno, Hunan Farsoon, Mark Forged, Exceltec, EOS, TreeD, CRP Technology, MadeSolid, Arevo, DR3D Filament, DWS, Voxeljet, Diamond Plastics, D-Mec, FFF World, CMET, Asiga, Graphene 3D Lab, Functionalize, Lithoz, ExOne, Sandvik, Concept Laser, Optomec, SLM Solutions, Fabrisonic, Renishaw, Arcam, Cookson Gold and LPW Technology (Low et al., 2017).

REFERENCES

Alig, I., Skipa, T., Engel, M., Lellinger, D., Pegel, S., & Pötschke, P. (2007). Electrical conductivity recovery in carbon nanotube–polymer composites after transient shear. *Physica Status Solidi (b),* 244(11), 4223-4226.

Allen, M. J., Tung, V. C., & Kaner, R. B. (2010). Honeycomb carbon: a review of graphene. *Chemical Reviews,* 110(1), 132-145.

Breuer, O., & Sundararaj, U. (2004). Big returns from small fibers: a review of polymer/carbon nanotube composites. *Polymer Composites,* 25(6), 630-645.

Ceretti, E., Ginestra, P., Neto, P. I., Fiorentino, A., & Da Silva, J. V. L. (2017). Multi-layered scaffolds production via fused deposition modeling (FDM) using an open source 3D printer: Process parameters optimization for dimensional accuracy and design reproducibility. *Procedia Cirp,* 65, 13-18.

de Campos, M. R., Botelho, A. L., & dos Reis, A. C. (2022). Antimicrobial incorporation on 3D-printed polymers used as potential dental materials and biomaterials: A systematic review of the state of the art. *Polymer Bulletin,* 1-28.

Dizon, J. R. C., Espera Jr, A. H., Chen, Q., & Advincula, R. C. (2018). Mechanical characterization of 3D-printed polymers. *Additive Manufacturing,* 20, 44-67.

Dong, X., Lu, D., Harris, T. A., & Escobar, I. C. (2021). Polymers and solvents used in membrane fabrication: a review focusing on sustainable membrane development. *Membranes,* 11(5), 309.

Dorigato, A., Moretti, V., Dul, S., Unterberger, S. H., & Pegoretti, A. (2017). Electrically conductive nanocomposites for fused deposition modelling. *Synthetic Metals*, 226, 7-14.

Ebrahimi, N. D., & Ju, Y. S. (2018). Thermal conductivity of sintered copper samples prepared using 3D printing-compatible polymer composite filaments. *Additive Manufacturing,* 24, 479-485.

Farahani, R. D., Dubé, M., & Therriault, D. (2016). Three-dimensional printing of multifunctional nanocomposites: manufacturing techniques and applications. *Advanced Materials,* 28(28), 5794-5821.

Francis, V., & Jain, P. K. (2016). Experimental investigations on fused deposition modelling of polymer-layered silicate nanocomposite. Virtual and Physical Prototyping, 11(2), 109-121.

Gardner, J. M., Sauti, G., Kim, J. W., Cano, R. J., Wincheski, R. A., Stelter, C. J., ... & Siochi, E. J. (2016). 3-D printing of multifunctional carbon nanotube yarn reinforced components. *Additive Manufacturing,* 12, 38-44.

Gnanasekaran, K., de With, G., & Friedrich, H. (2014). On packing, connectivity, and conductivity in mesoscale networks of polydisperse multiwalled carbon nanotubes. *The Journal of Physical Chemistry C*, 118(51), 29796-29803.

Gnanasekaran, K., de With, G., & Friedrich, H. (2016). Quantitative analysis of connectivity and conductivity in mesoscale multiwalled carbon nanotube networks in polymer composites. *The Journal of Physical Chemistry C,* 120(48), 27618-27627.

Gnanasekaran, K., Heijmans, T., Van Bennekom, S., Woldhuis, H., Wijnia, S., De With, G., & Friedrich, H. (2017). 3D printing of

CNT-and graphene-based conductive polymer nanocomposites by fused deposition modeling. *Applied Materials Today*, 9, 21-28.

Grady, J. E., Haller, W. J., Poinsatte, P. E., Halbig, M. C., Schnulo, S. L., Singh, M., ... & Mehl, J. (2015). A fully non-metallic gas turbine engine enabled by additive manufacturing part I: system analysis, component identification, additive manufacturing, and testing of polymer composites (No. GRC-E-DAA-TN22162).

Guo, N., & Leu, M. C. (2013). Additive manufacturing: technology, applications and research needs. Frontiers of mechanical engineering, 8, 215-243.Valvez, S., Reis, P. N., Susmel, L., & Berto, F. (2021). Fused filament fabrication-4D-printed shape memory polymers: a review. *Polymers,* 13(5), 701.

Halim, N. A., Mogan, J., Sandanamsamy, L., Harun, W. S. W., Kadirgama, K., Ramasamy, D., & Tarlochan, F. (2021). A review on 3D printed polymer-based composite for thermal applications. In IOP Conference Series: Materials Science and Engineering (Vol. 1078, No. 1, p. 012029). IOP Publishing.

Horst, D. J., & Junior, P. P. A. (2021). 3D-Printed Conductive Filaments Based on Carbon Nanostructures Embedded in A Polymer Matrix: A Review. *Research Anthology on Synthesis, Characterization, and Applications of Nanomaterials,* 1725-1742.

Jiang, R., Kleer, R., & Piller, F. T. (2017). Predicting the future of additive manufacturing: A Delphi study on economic and societal implications of 3D printing for 2030. *Technological Forecasting and Social Change,* 117, 84-97.

Johnson, P. R., Copeland, P. M., Ayodele, A. O., Tarekegn, E. N., Bromley, S. J., Harrell, W. R., ... & Marler, J. P. (2020). In-vacuum performance of a 3D-printed ion deflector. *Vacuum, 172,* 109061.

Kabiri, K., Omidian, H., Zohuriaan-Mehr, M. J., & Doroudiani, S. (2011). Superabsorbent hydrogel composites and nanocomposites: a review. *Polymer composites, 32*(2), 277-289.

Kichloo, A. F., Aziz, R., Haq, M. I. U., & Raina, A. (2021). Mechanical and physical behaviour of 3D printed polymer nanocomposites-a review. *International Journal of Industrial and Systems Engineering, 38*(4), 484-502.

Kotsilkova, R., Petrova-Doycheva, I., Menseidov, D., Ivanov, E., Paddubskaya, A., & Kuzhir, P. (2019). Exploring thermal annealing and graphene-carbon nanotube additives to enhance crystallinity, thermal, electrical and tensile properties of aged poly (lactic) acid-based filament for 3D printing. *Composites Science and Technology, 181,* 107712.

Li, F., Chen, X., & Liu, P. (2022). A Review on Three-Dimensional Printed Silicate-Based Bioactive Glass/Biodegradable Medical Synthetic Polymer Composite Scaffolds. *Tissue Engineering Part B: Reviews.*

Ligon, S. C., Liska, R., Stampfl, J., Gurr, M., & Mülhaupt, R. (2017). Polymers for 3D printing and customized additive manufacturing. *Chemical Reviews, 117*(15), 10212-10290.

Low, Z. X., Chua, Y. T., Ray, B. M., Mattia, D., Metcalfe, I. S., & Patterson, D. A. (2017). Perspective on 3D printing of separation membranes and comparison to related unconventional fabrication techniques. *Journal of Membrane Science, 523,* 596-613.

Mattia, D., Lee, K. P., & Calabrò, F. (2014). Water permeation in carbon nanotube membranes. *Current Opinion in Chemical Engineering,* 4, 32-37.

Mishra, P. K., & Jagadesh, T. (2022). Applications and Challenges of 3D Printed Polymer Composites in the Emerging Domain of Automotive and Aerospace: A Converged Review. *Journal of The Institution of Engineers (India): Series D,* 1-18.

Rymansaib, Z., Iravani, P., Emslie, E., Medvidović-Kosanović, M., Sak-Bosnar, M., Verdejo, R., & Marken, F. (2016). All-polystyrene 3D-printed electrochemical device with embedded carbon nanofiber-graphite-polystyrene composite conductor. *Electroanalysis,* 28(7), 1517-1523.

Safai, L., Cuellar, J. S., Smit, G., & Zadpoor, A. A. (2019). A review of the fatigue behavior of 3D printed polymers. *Additive Manufacturing,* 28, 87-97.

Sanei, S. H. R., & Popescu, D. (2020). 3D-printed carbon fiber reinforced polymer composites: a systematic review. *Journal of Composites Science*, 4(3), 98.

Sang, L., Han, S., Peng, X., Jian, X., & Wang, J. (2019). Development of 3D-printed basalt fiber reinforced thermoplastic honeycombs with enhanced compressive mechanical properties. *Composites Part A: Applied Science and Manufacturing*, 125, 105518.

Saroia, J., Wang, Y., Wei, Q., Lei, M., Li, X., Guo, Y., & Zhang, K. (2020). A review on 3D printed matrix polymer composites: its potential and future challenges. *The International Journal of Advanced Manufacturing Technology,* 106, 1695-1721.

Sheoran, A. J., & Kumar, H. (2020). Fused Deposition modeling process parameters optimization and effect on mechanical properties and part quality: Review and reflection on present research. *Materials Today: Proceedings,* 21, 1659-1672.

Singh, N., Singh, R., & Ahuja, I. P. S. (2018). Recycling of polymer waste with SiC/Al2O3 reinforcement for rapid tooling applications. *Materials Today Communications,* 15, 124-127.

Slater, A. G., & Cooper, A. I. (2015). Function-led design of new porous materials. *Science,* 348(6238), aaa8075.

Tambrallimath, V., Keshavamurthy, R., Saravanabavan, D., Koppad, P. G., & Kumar, G. P. (2019). Thermal behavior of PC-ABS based graphene filled polymer nanocomposite synthesized by FDM process. *Composites Communications,* 15, 129-134.

Thiam, B. G., El Magri, A., Vanaei, H. R., & Vaudreuil, S. (2022). 3D Printed and Conventional Membranes—A Review. Polymers 2022, 14, 1023. *Polymers and Their Application in 3D Printing*, 159.

Tian, X., Liu, T., Yang, C., Wang, Q., & Li, D. (2016). Interface and performance of 3D printed continuous carbon fiber reinforced PLA composites. *Composites Part A: Applied Science and Manufacturing,* 88, 198-205.

Ventura, D. N., Stone, R. A., Chen, K. S., Hariri, H. H., Riddle, K. A., Fellers, T. J., ... & Acquah, S. F. (2010). Assembly of cross-linked multi-walled carbon nanotube mats. *Carbon*, 48(4), 987-994.

Vigolo, B., Coulon, C., Maugey, M., Zakri, C., & Poulin, P. (2005). An experimental approach to the percolation of sticky nanotubes. *Science,* 309(5736), 920-923.

Yang, L., Li, S., Zhou, X., Liu, J., Li, Y., Yang, M., ... & Zhang, W. (2019). Effects of carbon nanotube on the thermal, mechanical, and electrical properties of PLA/CNT printed parts in the FDM process. *Synthetic Metals,* 253, 122-130.

Yang, Z., Chabi, S., Xia, Y., & Zhu, Y. (2015). Preparation of 3D graphene-based architectures and their applications in supercapacitors. *Progress in Natural Science: Materials International,* 25(6), 554-562.

Zhang, H., Huang, T., Jiang, Q., He, L., Bismarck, A., & Hu, Q. (2021). Recent progress of 3D printed continuous fiber reinforced polymer composites based on fused deposition modeling: a review. *Journal of Materials Science,* 56(23), 12999-13022.

Zhou, L. Y., Fu, J., & He, Y. (2020). A review of 3D printing technologies for soft polymer materials. *Advanced Functional Materials,* 30(28), 2000187.

Zong, H., Guo, C., Wang, Z., Guo, R., Zhou, H., Hao, G., ... & Jiang, W. (2022). Preparation of TNT/HMX-based melt-cast explosives with enhanced mechanical performance by fused deposition modeling (FDM). *Journal of Energetic Materials*, 1-19.

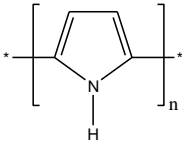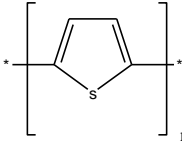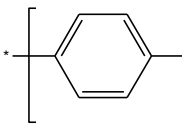# CHAPTER 3

CONDUCTING POLYMERS

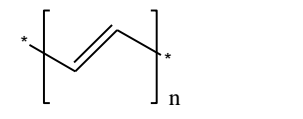Prof. Dr. Murat ATEŞ[1]
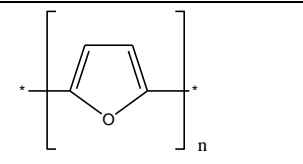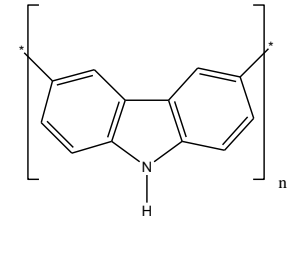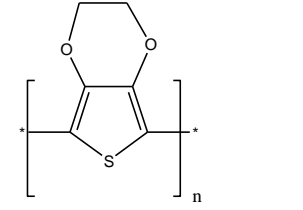
DOI: https://dx.doi.org/10.5281/zenodo.10030560

[1]Tekirdağ Namık Kemal Üniversity, Faculty of Arts and Sciences, Chemistry Department, Tekirdağ, Türkiye. mates@nku.edu.tr, Orcid ID: 0000-0002-1806-0330

1.INTRODUCTION

Polymers are called as macro-molecules formed by many different or the same type of monomers. In other words, these monomers are bonded to each other by covalent bonds, and by repeating small molecular units side by side in a skeleton are called as polymers. Polymers are classified concerning the terminology related to the monomer structure, crystallization, morphological aspects, etc (Meille et al., 2011). There are many usage areas of polymers. For example, they are used in the sheathing of cables due to their high electrical insulation and easy processing (Sacak, 2004). In the recent past, it has become possible to obtain conductive polymers with conductive properties by combining the superior properties of polymers and metals (Conwell, 1996). Some conductive polymers and their conductivity values were given in different dopants in Table 1.

Table 1. Some conductive polymers and their properties.

Polymer	Structure	Doped ion	Conductivity (S/cm)
Polypyrrole		BF_4^-, ClO_4^-	100
Polythiophene		ClO_4^-, $FeCl_4^-$, BF_4^-	10^{-3}-10^{-4}
Polyaniline		HBr	4.60×10^{-5}

Polyacetylene		Li, Na, Br$_2$, I$_2$, AsF$_5$	10^{-9} (cis) 10^{-5} (trans)
Polyfuran		ClO$_4^-$, BF$_4^-$	10^{-2}-10^{-5}
Polycarbazole		PTSA	9×10^{-4}
Poly(3,4-ethylenedioxythiophene)		PSS	8797

H. Shirikawa was firstly synthesized polyacetylene (PA) using the Zeigler-Natta catalyst. It was formed silver-colored films that had a metallic appearance but it was not doping process. The conductivity was increased by obtaining defect centers on the conjugated double bonds in the polymer chain. It has been reported that when PA films were doped by iodine, fluorine or chlorine vapors, the conductivity increases 10^9 times to 10^5 S/cm (Shirakawa et al., 1997). This value is close to the 10^6 S/cm level, which is nearly approach of the conductivity of metals such as Ag and Cu. H.Shirakawa, A.J. Heeger and A.G. MacDiarmid awarded for the Nobel prize in Chemistry in 2000 due to these important studies on conductive polymers.

Conductivity was supplied by 2 ways in polymers. One of them is to add metal particles into the polymer structure, as well as by filling the polymer with carbanous materials such as carbon black, acetylene black, carbon nanotubes etc. By incorporating metal particles into the polymer, conductivity was achieved through the metal phase. Second way is to add doped ions. Conductive polymer can be prepared by dissolving a suitable salt in the polymer chain and taking advantage of ionic conductivity. While conductivity is achieved in these methods, the polymer itself does not participate in conductivity; the polymer only provides conductivity and acts as a binding phase for the particles (Yılmaz, 2008). Conductive polymers are often called "synthetic metal" or "organic metal" due to the change in their structure. The main reason for metallic conductivity in unsaturated organic structures is the electrons in π bonds. Conductivity was supplied by these electrons. In saturated structures, these compounds show insulating properties because the splitting of sigma bond (σ) electrons and their transport along the chain requires high energy (approximately 7-10 eV) (Aydın, 2002).

1. HISTORY OF CONDUCTING POLYMERS

After giving Nobel prize in 2000, scientist know that most of the polymers can conduct electricity by changing the conjugation (single and double bonds) in the chain of carbon atoms by oxidation or reduction process. When the polymer was doped with strong electron acceptors such as iodide, the polymer achieved almost a metal conductivity (Heeger and MacDiarmid, 1982). Polyacetylene was firstly studied very intensively due to its practical and scientific

applications. Although PA shows very high conductivity in its doped form, it is not resistant to oxygen and moisture and degrades easily. For this reason, studies have focused on conducting polymers that can be synthesized from monomers such as aniline, pyrrole and thiophene, which have a cyclic structure that is more stable against oxidation (Kumar et al., 2017). New designed conducting polymers were presented in the the years with the hope of achieving better properties than PA. These new conducting polymers are polythiophene (PTh) (Guo et al., 2015; Wen et al., 2015), polyfuran (PF) (Yu et al., 2015; Sheberla et al., 2015, polypyrrole (PPy) (Liu et al., 2015), poly(p-phenylene) (Akbulut et al, 2015) (P-pP), poly(p-phenylene vinylene) (Kerry-Philips et al., 2014) and polyaniline (PANI) (MacDiarmid et al., 1985) etc. Although none of polymers show higher conductivity than PA, polymers are useful in the synthesis of new soluble and stable structures. Electron-rich heterocyclic polymers (PTh and PPy, etc) are very stable with p-type doping process. So, it can be mostly used in amongt the other polymers. PTh and PPy are stable because they have low oxidation potential (ox. pot order: PA>PTh>PPy).

Researchers' studies have focused on synthesis conditions that will increase the conductivity of synthesized polymers. The most important factors that increase the conductivity of the obtained polymers are: the type and rate of doping, type of solvent, temperature and acidic or basic nature of solution. It is easy wat to enhance mechanical and termal properties of polymers is to form composite or copolymer structures. Thus, the conductivity of materials have been improved.

2. CONDUCTIVITY THEORY AND DOPING PROCESS

Conducting polymers have sufficient electrical conductivity with the electrons with their lattice. In other words, there must be proper vacant places in the polymer structure that permit electrons to be transported along the polymer chain (Guimard et al., 2017). Conducting polymers have been distinquished than the other polymers with conjugation of their structure. Conductivity mechanisms in conductive polymers can be explained in two basic classes.

a) Ionic conductivity in conductive polymers,

b) Electronic conductivity in conductive polymers,

3. BAND THEORY

3.1. Ionic Conductivity in Conductive Polymers

Some polymer molecules are solid solvents for salts. By taking advantage of this feature, polymers that conduct electricity can be prepared through the mechanism. Ionic conductivity in such polymers can be explained based on the electrical conduction mechanism of KCl dissolved in water.
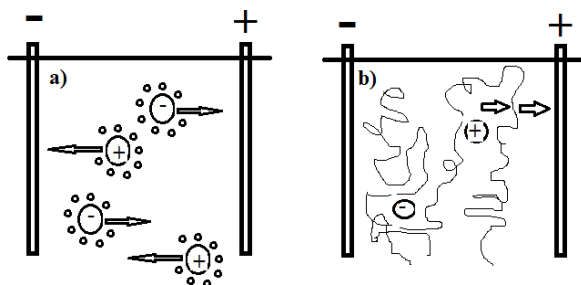

Figure 1. Comparison of the ionic conductity of the KCl salt in aqueous solution with the ionic conductivity of a salt dissolved in the polymer, a) Aqueous KCl, b) Salt dissolved in the polymer.

Electricity is transmitted by the migration of K^+ and Cl^- ions in KCl solution to opposite electrodes under the electric potential. Generally, polymers that show ionic conductivity have an electron donating group in their structure. In one or both of the anions or cations of the electrolyte used in the medium are weakly bound to the groups on the polymer chain, these groups will be tansported between the chains by the bending and twisting movement of the polymer under the influence of heat. This transport is in the form of ion transfer from a group on the polymer to a similar group on another polymer chain.

3.2. Electronic Conductivity in Conductive Polymers

The conductivity mechanism of polymers such as PA, PANI, and PPy, which conduct electricity electronically, has not yet been fully elucidated. Electrical conductivity provided by delocalized electrons in polymers, as in metals and semiconductor systems, can be explained by Band theory.

Two new energy levels were formed when obtaining a new bond formation,. These are called as the band energy levels where electrons are present (bonding orbitals) and the empty antibonding energy levels (antibonding orbitals). Each time a new atom is added to the molecule, a new bond and antibond energy level added to the electronic structure of the molecule. Substances whose electrons can rise to high-energy antibonding energy levels under the influence of heat or light conduct electricity. This teory is explained in Figure 2.
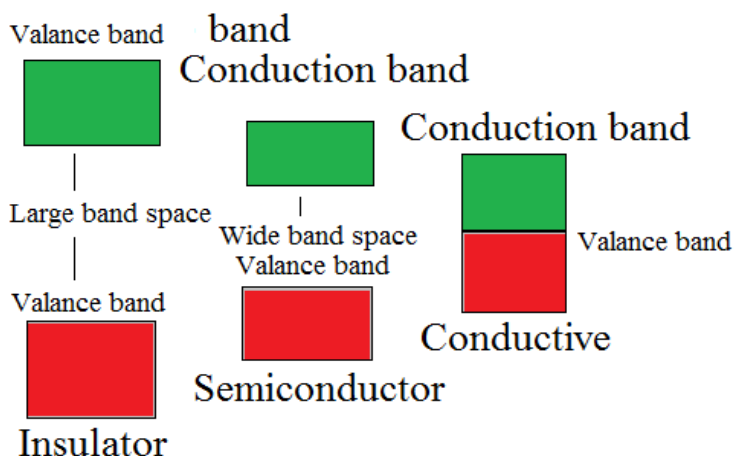
Fig. 2. Explanation of conductivity according to band theory.

As the molecular size increases, the number of bonding orbitals increases the difference between orbital energy levels decreases. At a point, instead of clearly seperated energy levels, a continuous energy bond forms. This bond is called band bond. This bond is called bond band. Electrons in the bond band can easily move within the band by changing their positions. The size of the bond threshold energy is important in order to group materials as insulator – semiconductor – conductor. According to this theory, substances with a wide energy gap between high-energy electrons and the conduction band are insulators. Insulators have gaps that are too large for electrons to pass through the band threshold and therefore do not conduct electricity.

Most conventional polymers are insulators. The band threshold energy is smaller than that of insulators. Their conductivity is in the range of 10^{-6} to 10^2 S/cm. They can conduct electricity because the energy level between the valance band nad conduction band can be renewed by heat or light energy. Polymers with a conjugated bond system in the main chain can show semiconductivity. The bond band of metals is partially filled and the

conduction band is empty. In addition, there is no band threshold that creates an obstacle for electron movement. They can easily conduct electron conduction. Metal electrons are in the low energy orbitals of the valance band. Morever, Vacant sides were obtained in higher energy levels that electrons can easily pass in the same band. In addition, conduction band can easily overlap the same band. They provide electron conduction through a partially filled valance or conduction band.

3.3. Doping Process

To prepare conductive polymers, it is carried out by reducing or oxidizing a polymer with conjugated π bonds with a suitable reagents (Trung et al., 2005). Polymers can be doped by the following techniques (Bernasik et al., 2005).

1- Gas phase doping,

2- Doping in solution medium,

3- Electrochemical doping,

4- Radiation-induced doping,

5- Ion-exchange doping.

The first three items of these techniques are preferred because they are lower cost. In gas phase doping, polymers are exposed to vapor of the dopant under vacuum. It can be achieved by doping in the solution environment and by using a solvent in which the additive can be dissolved (Gao et al., 2015). The ability to provide conductivity through doping can be explained as follows. In polymers, electrons in the valance shell can either be removed with an oxidizing reagent and the valance shell becomes positive or an electron can be given to the empty reduction band with a reducing reagent. These processes are

called p-type doping, corresponding to oxidation, and n-type doping, corresponding to reduction.

During the doping process, none of the doping molecules replace polymer atoms; doping molecules only help electrons paa through their energy shells. Doping substances or dopants are either strong reducing or oxidizing substances. These can be organic salts or compounds that can easily from ions, neutral molecules, organic dopants or polymeric dopants. The structure of dopants play a crusial effect on conductivity and stability of conductive polymers. The stability of conducting polymers can be increased with antioxidants such as benzoquinone, azobisisobutyronitrile or by ion grafting.

3.4. Soliton, Polaron, Bipolaron Formations

The conductivity of polymers can be enhanced by doping process (Cataldo and Maltese, 2002). Doping of a polymer occurs by preparing the salt of the polymer using a suitable reagent by chemical method or creating cations or anions by applying potential by electrochemical method. The conductivity of the polymer can be inclined by doping by ensuring that the valence or conductivity layers are not fully filled or fully empty as a result of doping in polymers (Khanna et al., 2005). The electrochemical change applied to doped the skeletal structure of polymers causes a change in the electronic state of the polymer. With this change, one of the charge gaps emerges. These are known as monovalent (polaron), bivalent (bipolaron) and soliton.

Free radical
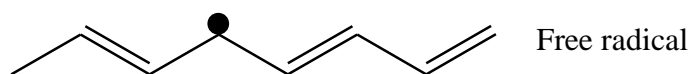
a) Neutral soliton

Carbocation
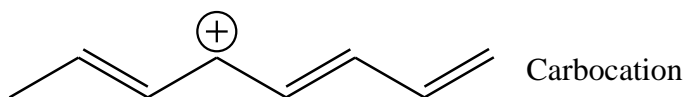
b) Positive soliton

Carboanion
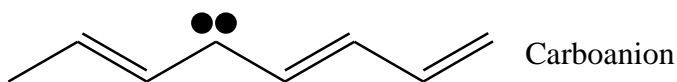
c) Negative soliton

Figure 3. Polaron, bipolaron and soliton structures.

A charge carrier can be blocked and move towards a certain point to form a new equilibrium state and become polarized. The charge carrier with this deformed structure is called "polaron" or "radical cation". Unlike soliton, polarons cannot move unless the initial energy barrier is overcome. Jumping movements can be made due to this reason. This creates an isolated charge-carrying polaron. A pair of these changes is called a "bipolaron".

REFERENCES

Aydın, A. (2002). Pirolün elektrokimyasal polimerizasyonuna organik asit etkilerinin incelenmesi. *Anadolu Uni., Fen Bilimleri Ens., Yüksek Lisans Tezi*, 61s, Eskişehir.

Akbulut, H., Endo, T., Yamada, S., Yagci, Y. (2015). Synthesis and characterization of polyphenylenes with polypeptide and poly(ethyleneglycol) side chains. *Journal of Polymer Science Part A-Polymer Chemistry,* 53(15), 1785-1793.

Bernasik, A., Haberko, J.,Wlodarczyk-Miskievicz, J.,Raczkowska, J., Lunny, W.,Budkowski, A.,Kowalski, K.,Rysz, J. (2005). Influence of humid atmosphere on phase separation in polyaniline-polystyrene thin films. *Synth. Met.,* 53, 516-522.

Cataldo, F., Maltese, P. (2002). Synthesis of alkyl and *N*-alkyl substituted polyanilines a study on their spectral properties and thermal stability. *European Polymer Journal*, 38, 1791-1803.

Conwell, E.M. (1996). Definition of exciton binding energy for conducting polymers. *Synth. Met.,* 83,101-102.

Gao, J., Stein, B.W., Thomas, A.K., Gareia, J.A.,Yang, J., Kirk, M.L., Grey, J.K. (2015). Enhanced charge transfer doping efficiency in J-aggregate poly(3-hexylthiophene) nanofibers. *Journal of Physical Chemistry C,* 119(28), 16396-16402.

Guo, C.X., Jiang, S.X., Zhu, W.X., Yang, X.X., Pei, M.S., Zhang, G.Y, (2015). Polythiophene based fluorescent probe for copper ions with high sensitivity. *J. Appl. Polym. Sci.,* 132(34), 42440.

Guimard, N.K.,Gomez, N, Schmidt, C.E. (2007). Conducting polymers in biomedical Engineering. *Prog. Polym. Sci.,* 32, 876-921.

Heeger, A.J.,MacDiarmid, A.G. (1982). Conducting polymers-Theoretical concepts and experimental results. *Abstracts of papers of the American Chemical Society,* 183,56-Poly.

Kerry-Philips, T., Srinivas, A.R.G., Travas-Sejdic, J. (2014). Electrospun substituted polyphenylene vinylene nanofibers. *Int. J. Nanotechnol.*, 11 (5-8), 626-635.

Khanna, P.K.,Singh, N., Charan, S., Viswanath, A. (2005). Synthesis of Ag/polyaniline nanocomposite via an in-situ photo-redox mechanism. *Materials Chemistry and Physics*, 92, 214-219.

Kumar, V., Kalia, S., Swart, H.C. (2017). Conducting polymer nanocomposites for sensor applications. *Conducting Polymer Hybrids, Springer Series on Polymer and Composite Materials,* 223-267.

Liu, X.J., Qian, T., Xu, N., Zhou, J.Q., Guo, J., Yan, C.L. (2015). Preparation of on chip, flexible supercapacitor with high performance based on electrophoretic deposition of reduced graphene/polypyrrole composites. *Carbon,* 92, 348-353.

MacDiarmid, A.G., Samasiri, N.L.D., Wu, Q., Mu, S.L. (1985). Electrochemical characteristics of polyaniline cathodes and liquid crystals. 121 (1-4), 187-190.

Meille, S.V.,Allegra, G.,Geil, P.H., He, J.S., Hess, M.,Jin, J.I., Kratochvil, P.,Mormann, W., Stepto, R. (2011). Definitions of terms relating to crystalline polymers. *IUPAC Recommendations Pure and Applied Chemistry,* 83(10),1831-1871.

Saçak, M. (2004). Polimer Kimyası. Gazi Kitabevi, Ankara, 525s.

Shirakawa, H., Louis, E.J., MacDiarmid, A.G.,Chiang, K.C.,Heeger, A.J. (1997). Synthesis of electrically conducting organic polymers halogen derivatives of polyacetylene, (CH)x. *Journal of Chem. Soc. Chem. Commun.*, 578-580.

Sheberla, D., Patra, S., Wijsboom, Y.H., Sharma, S., Sheynin, Y., Haj-Yahia, A.,Barak, A.H.,Gidron, O.,Bendikov, M. (2015). Conducting polyfurans by electropolymerization of oligofurans. *Chemical Science,* 6(1), 360-371.

Trung, T.,Trung, T.H.,Ha C. (2005). Preparation of cyclic voltammetry studies on nickel-nanoclusters containing polyaniline composites having layer by layer structures. *Electrochim. Acta,* 51, 984-990.

Wen, L., Jeong, D.C.,Javid, A.,Kim, S.,Nam, J.D.,Song, C.,Han, J.G (2015). Conductive polythiophene-like thin film synthesized using controlled plasma processes. *Thin Solid Films,* 587, 66-70.

Yılmaz, M. (2008). Çözünür polianilin, poli(*N*-etilanilin), poli(*N*-metilanilin) sentezi, karakterizasyonu ve membran uygulamaları, *Anadolu Uni., Fen Bilimleri Enst., Yüksek Lisans Tezi,* 76s, Eskişehir.

Yu, S.W., Frisch, J., Opitz, A., Cohen, E., Bendikov, M., Koch, J., Salzmann, I. (2015). Effect of molecular electrical doping on polyfuran based photovoltaic cells. Appl. *Phys. Lett.,* 106(20), 203301.

CHAPTER 4

THE UTILIZATION OF POLYOXOMETALATE(POM)/ CARBON NANOTUBE(CNT) HYBRIDS AS ELECTRODES IN LITHIUM-ION STORAGE APPLICATIONS

Mertcan TOPUZ[1], Prof. Dr. Mehtap EMİRDAG-EANES[2]

[1] İzmir Institute of Technology,Chemistry Department,Urla,İzmir,Türkiye, mertcantopuz@std.iyte.edu.tr,

[2] İzmir Institute of Technology, Chemistry Department,Urla,İzmir,Türkiye, mehtapdemirdag@iyte.edu.tr. Orcid ID: 0000-0002-2151-8242

1.INTRODUCTION

A group of metal oxides known as polyoxometalates (POMs) have distinct molecular structures of different sizes and shapes and a wide variety of related characteristics. In addition, POMs exhibit a remarkable variety of physicochemical features, as we have already described. However, POMs' distinctive electrochemical activity gives them their most significant utility. POMs have excellent redox state stability and can participate in quick, reversible multielectron-transfer processes. POMs' ability to behave as electron sponges or reservoirs makes them perfect for energy storage systems. The rapid and reversible electron-transfer kinetics of POMs are ideally adapted to high-power processes for the design of redox-active electrodes.

The crystal-structure definition of ultra-large clusters illustrates the POMs' explosive growth and quick evolution. POMs are often manufactured as minute crystals or powders, and because their structures are pH-sensitive, this restricts how easily they may be processed. POMs are modified and assembled with appropriate matrices, such as organic molecules, polymers, silica, and carbon materials, using a well-known solution technique to accomplish their improved stability and the synergistic functions of POMs and matrices (Genovese, Keryn, and Lian, 2017).

Carbon nanotubes (CNTs) are another material class that Redox actively uses. For more than 20 years, scientists have studied carbon nanotubes (CNTs), one of the carbon allotropes. They have exceptional mechanical, electrical, and thermal capabilities and a particular sp^2 structure with outstanding electrical qualities. Without any chemical reagents, graphene-carbon nanotube hybrid materials were effectively

created by C-C contact. The proportion of carbon nanotubes to graphene has been discovered to affect hybrid materials' aqueous solution state and shape significantly. This way, CNT-based hybrid materials can be easily used as electrodes in lithium-ion storage (Chen et al. 2012). Recent years have seen much interest in graphene, a new carbon nanomaterial made up of a monolayer of two-dimensional sp^2-bonded carbon atoms. These extraordinary properties include high mechanical stiffness, a sizable specific surface area, high thermal conductivity, and excellent carrier mobility. In addition, graphene serves as a stable matrix for assembling other elements, including tiny molecules, polymers, and inorganic nanoparticles, to create valuable nanocomposites. The huge specific area and excellent conductivity of graphene can improve several crucial POM features, including catalysis, capacitance, and lithium storage capacity. Thus, hybrids of graphene CNTs and POMs have an important role as cathode materials in LIB.

The electrons of the octahedral structure, which consists of three common points and four corners, can be reduced so that reverse electron reactions can be observed. The observed reactions are triangular, have W^{IV}-W^{IV} bonds, and form the POM lattice with the merging of molecular orbitals (MO).

$[PMo_{12}O_{40}]^{3-}$

P
Mo
O

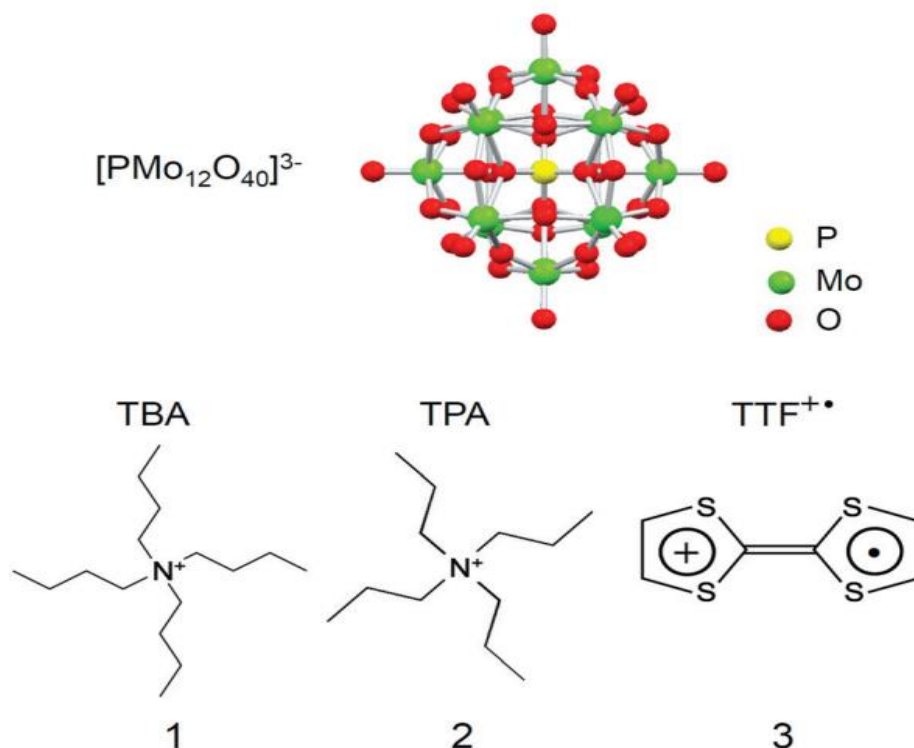TBA   TPA   TTF$^{+\bullet}$

1   2   3

Fig. 1. Polyoxometallates with different counter cations (Awaga et al. 2012).

Single-walled carbon nanotubes (SWNTs) and POMs were synthesized as nano-hybrid materials to be used as cathode materials in molecular cluster batteries (MCBs). The battery capacity and charging/discharging performance of the nano-hybrid MCBs were much higher than those of the microcrystal-POM MCBs. A new type of lithium battery called MCB has been developed to achieve high-performance batteries. As mentioned in (Awaga et al. 2012) MCB uses POMs and polynuclear metal complexes like Mn_{12} as the active cathode materials. The usage areas of POM and CNT hybrid materials, especially electrolytes, were examined (Figure 1).

1. PREPARATION OF POM & CNT MATERIALS

There are three basic approaches to preparing POM/nanocarbon composites, and their key benefits, drawbacks, and potential future possibilities are indicated.

2.1. Covalent Functionalization

The organo-functionalized alkoxides, phosphonates, imides, and silanes are the common functionalization groups that might be challenging to synthesize independently. No uniform functionalization method exists since each organic functionalization group just coupled a single cluster type. It is even more challenging for a non-expert to select the best synthetic strategy because the functionalization phase might be completed directly during cluster building or after the cluster synthesis. One of the main challenges facing contemporary POM research is the creation of generic functionalization pathways that lead to stable, long-lasting organic-inorganic hybrid materials.

2.2. Noncovalent Functionalization

POMs and nanocarbons can interact with one another in various ways to form noncovalent bonds.

2.2.1. Electrostatic interactions

The most advanced method for this is currently electrostatic interactions. Nanocarbons can be positively charged, whereas POMs can be negatively charged. Electrostatic interactions are made possible due to the opposing charges being attracted to one another. Covalent cation attachment and intermolecular interactions are the two basic strategies for the cationic functionalization of POMs. The particular application will determine the approach to use. Anionic POMs can be joined to

positively charged nanocarbons with the help of electrostatic interactions.

2.2.2. Interactions

A POM can be covalently connected to an extended aromatic system, such as pyrene, and then this hybrid molecule just coupled to nanocarbon through C-C bonding interactions.

2.2.3. Layer by layer (LbL) interactions

POMs and nanocarbons may be repeatedly stacked using wet-chemical deposition techniques to create LbL assemblies. Intense electrostatic forces may be employed to interact the alternated POM and nanocarbon layers by cationic alteration of the nanocarbon. (LbL) deposition is a simple and versatile method for fabricating energy conversion devices. However, it has some limitations, such as only being able to create layered structures and difficulty controlling layer thickness (Figure 2).
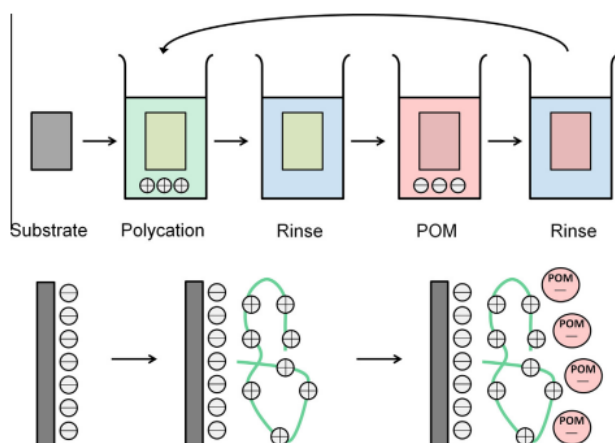

Fig. 2. Diagram illustrating the layer-by-layer (LbL) interactions (Genovese, Keryn Lian, 2017).

Despite these limitations, LbL deposition is still popular due to its ease of use, versatility, and cost-effectiveness. Researchers are working to overcome the limitations of LbL deposition by using other techniques and chemical modifications. As these efforts continue, LbL deposition will likely become an even more powerful tool for fabricating energy conversion devices. In short, LbL deposition is a valuable technique for fabricating energy conversion devices, but it has some limitations.

2. UTILIZATIONS OF POM & CNT COMPOSITES

POMs connected to nanocarbons can be used for electron transferring and energy storage processes due to their broad redox activity. The main areas of study in POM/nanocarbon composites will be reviewed in the following parts, along with a look at the difficulties and prospects for the future.

3.1.Electrocatalysis

POMs are flawless for the transfer of electrons according to their intense redox activity. This is especially desirable for multielectron transfer processes, frequently constrained by large excessive potentials that result in poor overall conversion efficiencies. POMs may be altered with redox-active materials, making them the perfect candidates to remedy this problem.
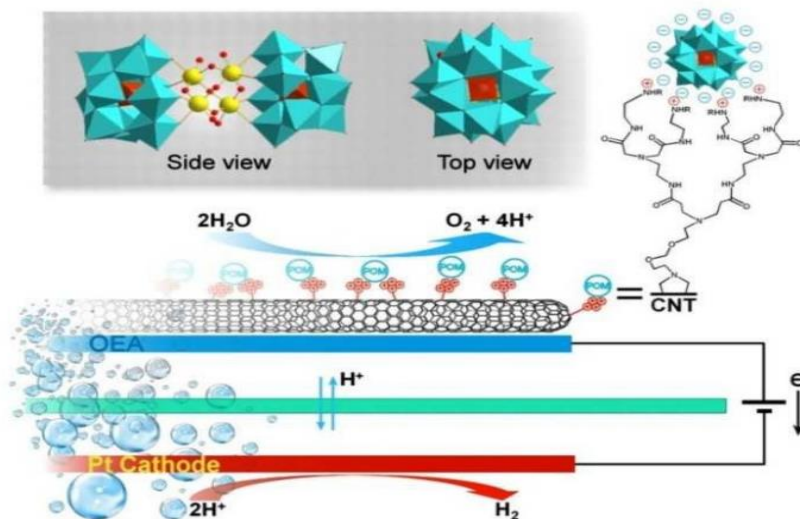
Fig. 3. A Diagram for Water oxidation (Huang et al. 2015).

3.2. Water Oxidation

Most articles agree that water oxidation is the most difficult part of the water-splitting process. Even when noble metals like platinum are used as electrodes, significant overpotentials are frequently seen (Figure 3).

- Pyrene-based cationic species: These molecules contain a pyrene ring, a sizeable aromatic compound with a high affinity for π-electrons.

- π–π interactions: These are weak interactions between two aromatic compounds caused by the attraction between their π-electron clouds. At the same time, that attractions cause aggregation in aromatic groups (Figure 4).

- Solvent-free microwave procedure: This method uses microwaves instead of a solvent to carry out a chemical

reaction. Microwaves can heat substances very quickly, speeding up reaction times and improving yields.

- Volatile organic solvents: These solvents evaporate quickly and can harm human health and the environment.

- Electrocatalysts: These are materials that can accelerate the rate of electrochemical reactions. They are essential for various applications, including energy storage and water splitting.
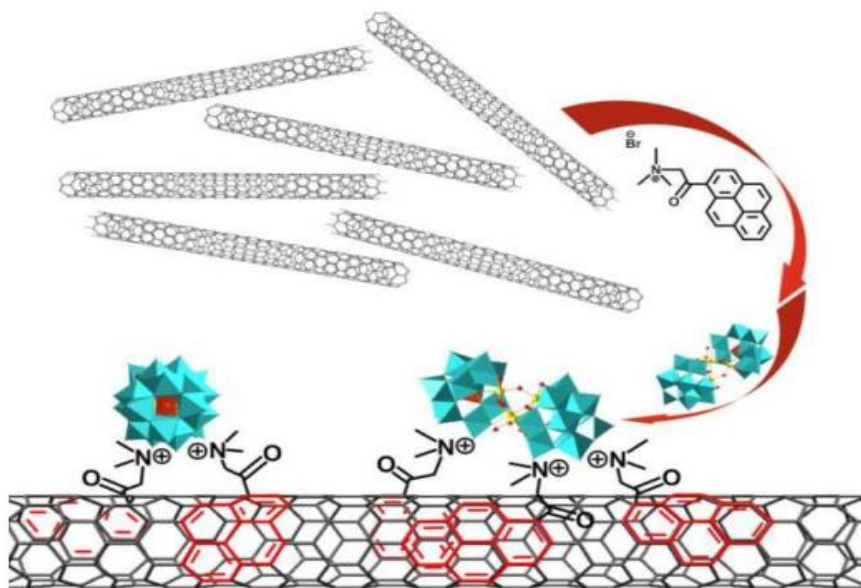
Fig. 4. A demonstration of the CNT-bound POM catalyst in a schematic. By "C-C" stacking, an amphiphilic cationic pyrene derivative is added to CNTs (Huang et al. 2015).

Graphene is superior to carbon nanotubes in terms of stability and conductivity making them perfect for electrochemical processes requiring immobilized catalysts. Graphene material is utilized as the catalyst support, electrocatalytic performance has been found to improve significantly. As mentioned above, graphene's enormous specific area

and excellent conductivity can be used to improve various crucial POM features, including catalysis, capacitance, and lithium storage capacity. POMs are built onto reduced graphene oxide (rGO) via various reduction techniques, such as POM-catalyzed photochemical reduction, using graphene oxide (GO) as the precursor.

The reduction of GO can be accomplished using various techniques, such as chemical, photochemical, thermal, flash, laser, electron-beam, and electrochemical reduction. Electrochemical reduction, one of them, combines the benefits of simple, clean, and efficient technology for mass manufacturing, making it a potential strategy. However, an electrochemical reduction is only used in a few situations and is often to a create graphene-based electrode films-an electrochemical reduction procedure using a POM catalyst. The typical POM is $H_4SiW_{12}O_40$ (SiW_{12}), a commercially available material. As seen in Figure 5, SiW_{12} is electrochemically reduced during the reduction process, getting one or more electrons.
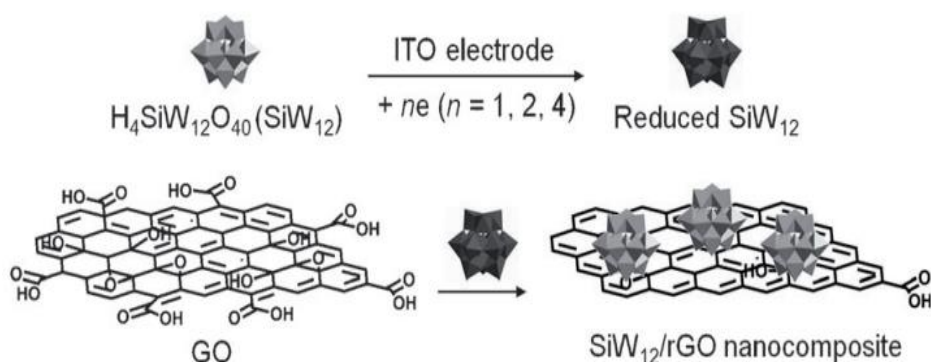

Fig. 5. The production of nanocomposite material based on SiW_{12} & rGO composites (Feng, 2013).

On the other hand, it has been proven that polyoxometallates with CNT or graphene are conceptually viable catalysis for effective water oxidation. Graphene is superior to carbon nanotubes in terms of stability, conductivity, and surface area-to-volume ratio, makes the material of choice for electrochemical processes requiring immobilized catalysts. The functionalized electrostatic interactions in Figure 6 can be given as an example to support these properties of graphene-based materials.
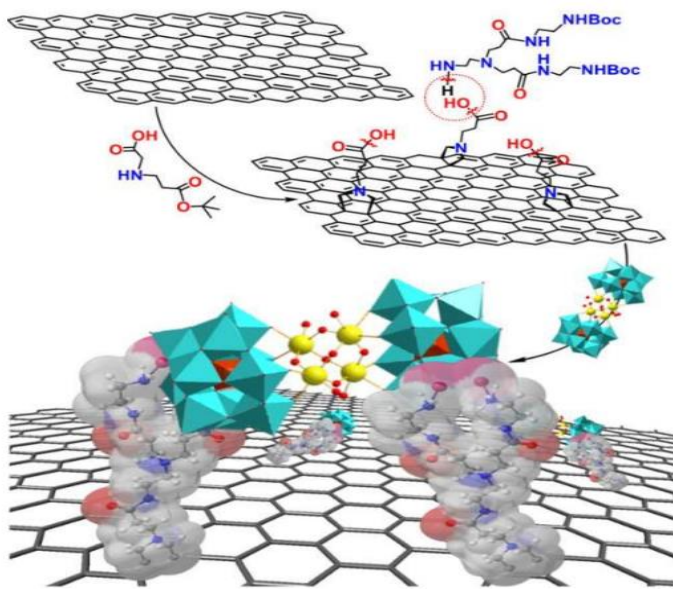
Fig. 6. Cationic graphene nanoplatforms supporting (SiW_{10}) were created. $(SiW_{10})^2$ is bound to graphene by electrostatic interactions after covalently functionalizing with organic cations (Huang et al. 2015).

3.3. Methanol Oxidation

Since methanol is employed in methanol fuel cells (DMFCs) as an electron donor and energy carrier, methanol's electrocatalytic oxidation employing plenty of metal catalysts has garnered much attention. In most

modern systems, the anode material is commonly made of noble metals, frequently platinum (Figure 7).

Palladium and platinum are the most commonly used catalysts for methanol oxidation in DMFCs. These metals have high electrocatalytic activity for methanol oxidation, but they are also susceptible to poisoning by the reaction intermediates CO, COH, and HCO. These intermediates are formed when methanol is oxidized on the catalyst surface. They can bind to the catalyst surface and block the active sites, decreasing the catalyst's activity. One way to deal with this is to include POMs in the electrode materials. The clusters have exceptional chemical and thermal durability. (Chen et al. 2006).

Increasing the surface area of the catalysts is an alternative strategy for improving methanol oxidation efficacy. The $PtSnPMo_{12}$/CNTs catalyst's electrochemical surface area was much more significant than various reference systems. That's ascribed to a better distribution of smaller Pt particles and the existence of POM, which may function as a co-catalyst for the oxidation of methanol and stabilize tiny Pt particles during their production.
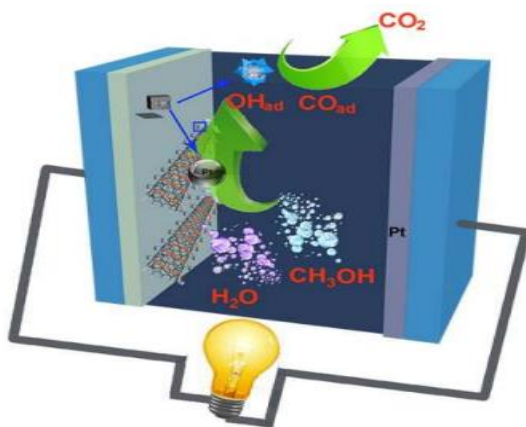

Fig. 7. Electrochemical processes in DMFCs (Huang et al. 2015).

As mentioned in the introduction, molecular cluster batteries (MCBs) mainly consist of nanohybrid materials such as Keggin POMs and SWNTs.

- **Single-walled carbon nanotubes (SWNTs)** are one-dimensional nanomaterials with a high surface area and excellent conductivity.
- **Molecular cluster batteries (MCBs):** These are battery types that use molecular clusters as the active material. Molecular clusters are small, organized groups of atoms that have unique properties.

3.4. Nanohybridization

Due to their unique qualities, including as high mechanical strength, good gas adsorption, vast surface areas, and particular electrical conductivity, carbon nanomaterials have received much interest.

One-dimensional nanomaterials called single-walled carbon nanotubes (SWNTs) have been used extensively in several areas of materials research, including biomedicine, catalysis, and sensor technology. Since SWNTs may offer a quick transport channel for electrons and ions, their use as nanostructured electrodes is particularly promising. Recently, we created Keggin-type POMs, $TBA_3[PMo_{12}O_{40}]$ ($TBA = (C_4H_9)_4N^+$), that were especially adsorbed on the surfaces of SWNTs in order to be used as the cathode active components of MCBs. High battery capacity and fast charging/discharging are possible with MCBs. The ($Mn_{12}O_{12}(CH_3COO)16(H_2O)_4$) is used to make MCB because it performs a multielectron redox reaction (Figure 8).
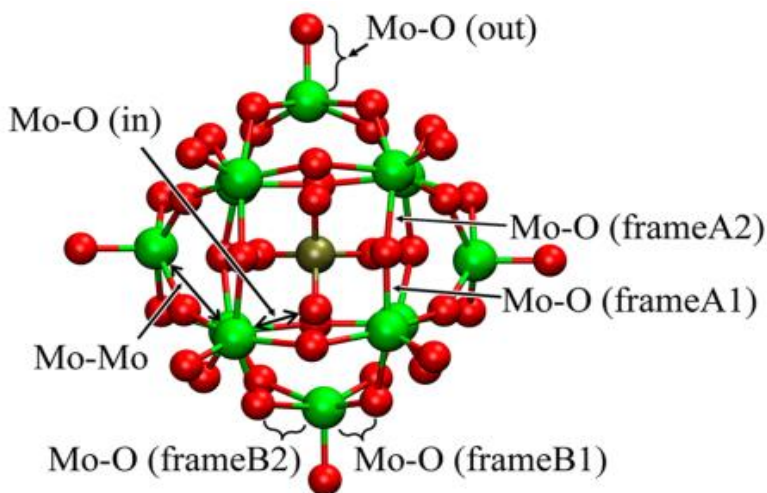
Fig. 8. Optimized Structure of $[PMo_{12}O_{40}]^{3-}$ (Awaga et al. 2012).
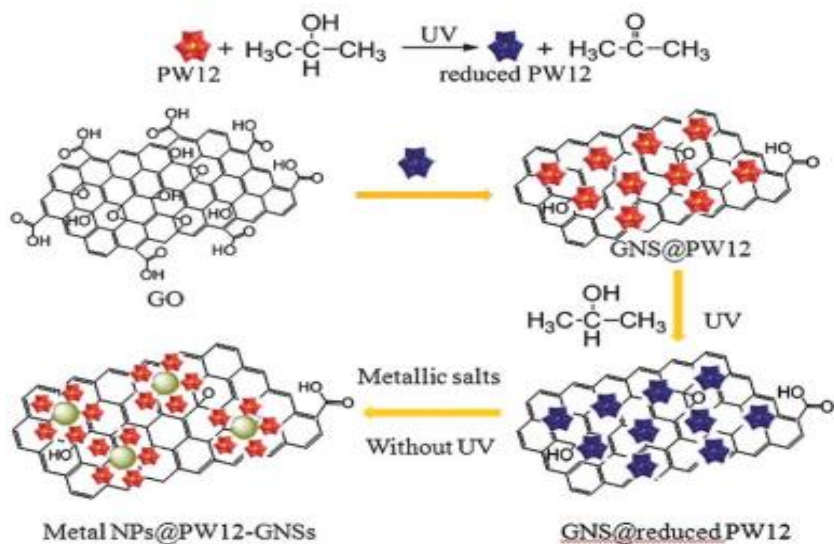
Fig. 9. Schematic procedure of the NPs@POM–GNS nanohybrids (Li et al. 2012).

POMs display many characteristics, including luminescence, catalysis, and magnetism. Rechargeable batteries have also used their reversible multielectron redox activity; some POMs, including

[PMo12O$_{40}$] and [PW12O$_{40}$]^3, can serve as the cathode-active components of lithium batteries with significant energy density (Figure 9). There has yet to be any information about POM-integrated SWNTs being used as battery cathodes, although they have been created for spintronics and catalysis. On the other hand, the mentioned characteristics can be seen in the production phases of SWNTs (Figure 10).
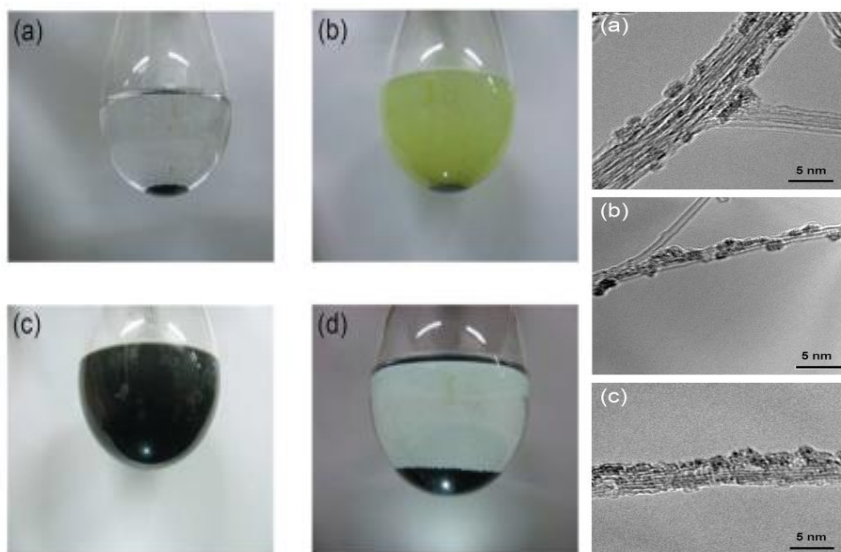
Fig. 10. Pictures documenting the SWNT-1 preparation phase. (a) A purified SWNTs solution in toluene. (b) Following the addition of 1.5% acetonitrile solution. (c) As the mixture is being vigorously stirred. (d) Their TEM images were one hour after allowing the mixture to stand (NAGASHIMA et al. 2002).

3.5. Oxygen Reduction

To solve the problems caused by high overpotentials, fuel cells also need effective oxygen reduction catalysts and MeOH oxidation. Despite their high cost, noble metals like Pt and Pd are frequently used as catalysts. Therefore, significant attempts are being made to find easily

reached-resources on Earth. An electrocatalyst with Pd, Pd@POM/PDDA/MWNT, was introduced for use as a successful catalyst for the reduction process in fuel cells instead of Pt. This was accomplished by positively charging PDDA-MWNTs by functionalizing MWNTs with polydiallyldimethylammonium chloride (or PDDA). After reductive Pd deposition, POMs were connected to the MWNTs electrostatically (Figure 11). As mentioned by (Jiang et al. 2010) that's crucial in optimizing the performance of an electrode because oxygen desorption and bubble formation can considerably boost the excessive potential.
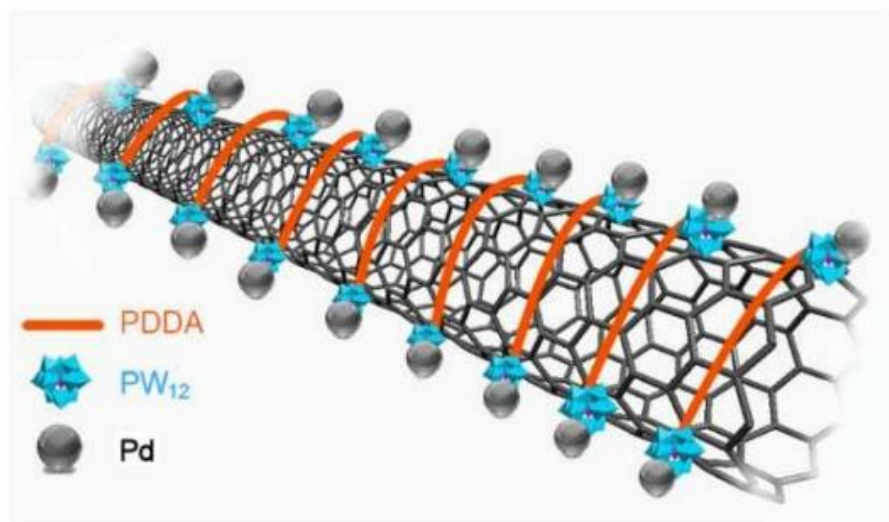
Fig. 11. Keggin-type POMs on PDDA-functionalized MWNTs (Huang et al. 2015).

Initial measures have recently been launched to switch out the expensive noble metal particles used in the ORR with less expensive metals. The researchers have developed a new method by reacting acidized MWNTs with $AgNO_3$ and adding reduced Keggin anion to

produce silver nanoparticles decorated with CNTs. The interaction between these materials resulted in high electrocatalytic-reducing activity. Comparing the POM functionalized system to non-functionalized CNTs, considerably higher oxygen reduction current densities were found. The team employed $H_7[PMo^V 4Mo^{VI}8O_{40}]$ as a reducing agent to deposit Ag nanoparticles on graphene (Figure 12). These composites demonstrated significant electrocatalytic activity in conjunction with the Ag NNs' high catalytic activity and the GNs' outstanding electron transfer capabilities, further strengthened by leftover POM units and components resulting from their breakdown.
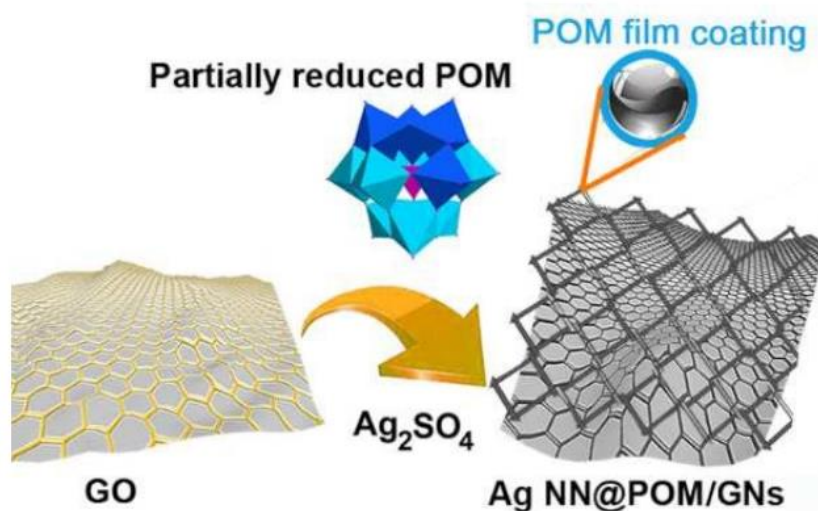
Fig. 12. Ag NN@POM/GNs composites using $H_7[\beta PMo^V 4Mo^{VI} 8O_{40}]$ material (Zhang et al. 2011).
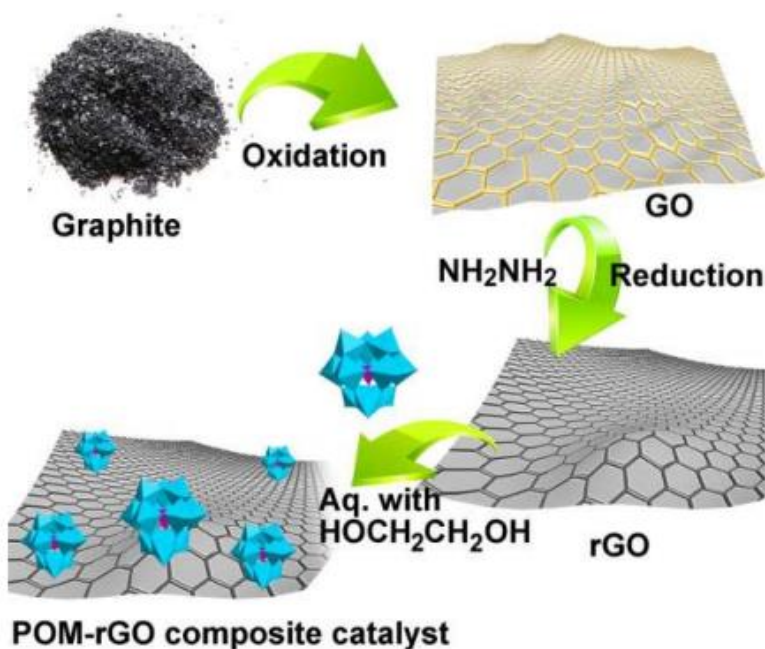
Fig. 13. Demonstration of the production of POM-rGO (Huang et al. 2015).

In the end, POM/CNT are extremely durable and adaptable systems that can be used in various techniques for significant electrocatalytic reactions, allowing for the targeted development of future applications in numerous fields. As an example of these studies, composite materials obtained as a result of Redox reactions on graphite was demonstrated (Figure 13).

3. ENERGY STORAGE and LITHIUM-ION BATTERIES

Electrochemical energy storage is one of most interesting areas of study utilizing nanostructured hybrid materials. Batteries, which rely on chemical redox processes for energy storage and release, and supercapacitors, which store energy using a mix of electrostatic and electrochemical charge separation, are the two most capable methods for

electrochemical energy storage. POMs provide excellent electrochemical energy storage possibilities to obtain high electronic conductivity.

Studies on the enhanced performance of energy storage and conversion devices are exploding due to rising energy demand and significant utilization of nonrenewable energy sources. Lithium-ion batteries (LIBs) are now commonly used in smartphones, computers, wearable technology, and other electronic devices. However, demands for greater LIB performance have steadily risen for new applications, including grid energy storage and electric vehicles. LIBs perform poorly in terms of power and energy due to their low theoretical capacity when employed as an anode material. Therefore, finding innovative substitute materials with improved specific capacity and high-rate performance for LIB anodes is urgently needed. Because they undergo repeated oxidations throughout the charge/discharge process and have relatively high specific capacities, transition-metal oxides have attracted much interest from a wide range of well-researched materials (Yang et al. 2020). As an anode for LIBs, for instance, $Co_3O_4/CoMoO_4$ was effectively synthesized by a solvothermal method and paired with a thermal treatment, and it demonstrated superior electrochemical capabilities over $CoMoO_4$ (Figure 14).
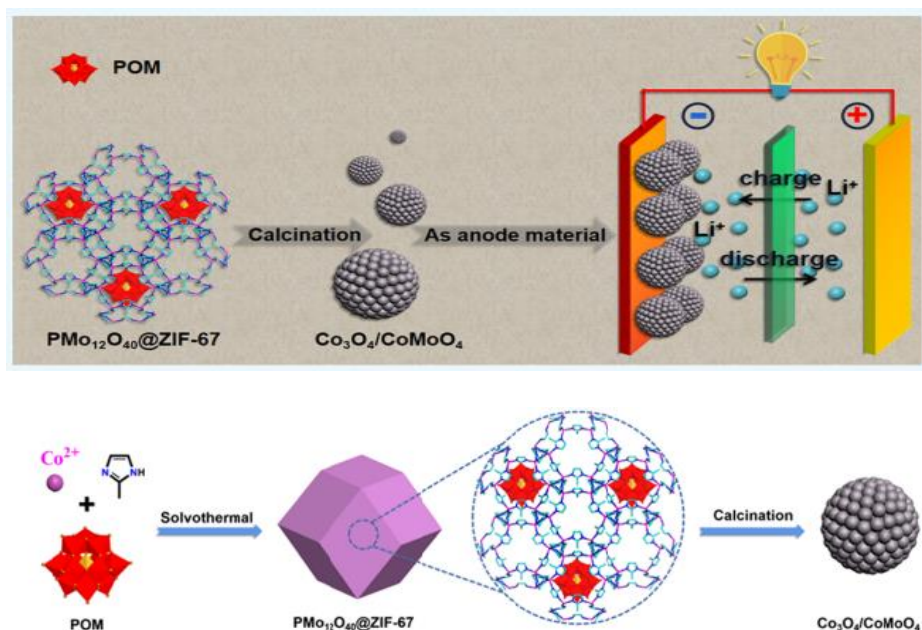
Fig. 14: Schematic demonstration of $Co_3O_4/CoMoO_4$ preparation & $Co_3O_4/CoMoO_4$ based LIB (Yang et al. 2020).

Based on typically controlled porosity architectures for the well-defined structure and large surface areas, metal-organic frameworks (MOFs) and polyoxometalate (POM)-based MOFs have gained significant research attention in LIBs and supercapacitors A viable strategy for creating high-capacity energy storage devices combines reducing POMs with nano-hybrid composites (Figure 15). In conclusion, recent advancements of polyoxometallates with carbon nanotubes or graphene as electrode materials demonstrate major improvement in LIB (Huang et al. 2015).

Recently, integrating POMs into LIB system have been made advances in cutting-edge battery development. The investigation has been focused on POM with Kegging of Well-Dawson cluster hybridized with carbon nanotubes.
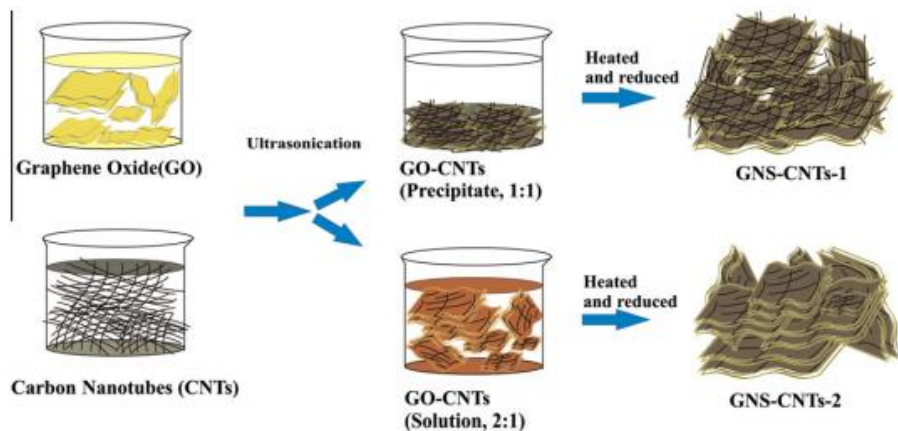
Fig. 15. Preparation of CNT & GO hybrid materials for LIB process (Chen et al. 2012).

Molecular cluster batteries (MCBs) were first studied using a nanocomposite of $(_nBu_4N)3[PMo12O_{40}]$/SWNTs for electrochemical energy storage. Electrostatic interactions were used to attach the cluster to the SWNTs. Anionic POM was bound by SWNTs, which produced positive surface charges. The POM clusters were successfully molecularly dispersed, resulting in efficient lithium-ion diffusion and smooth electron transfer. POMs are affixed to SWNTs for enhanced charge transfer. SWNTs containing $[SiW11O_{39}]^{7-}$ clusters that have been organofunctionalized. In order to assemble $PySiW_{11}$/SWNT/ nanocomposite materials, pyrene units were connected covalently to the cluster by silanol bonds, and these clusters were bonded to the SWNTs by C-C bonding (Figure 16).
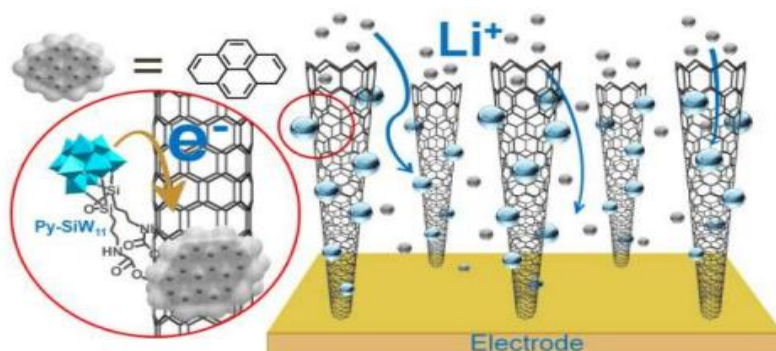
Fig. 16. Connection of functionalized POM clusters with the SWNTs by stacking interactions in the nanocomposite Py-PW$_{11}$/SWNTs shown schematically (Huang et al. 2015).

A new strategy was proposed to increase electrical interactions between POM and CNT. POM with aluminum as a metal and layered GO created an ordered nanostructure attractive for high-capacity electrodes, as battery experiments show that Al$_{13}$-intercalated GO displays a considerably improved mutual capacity due to the pristine GO.
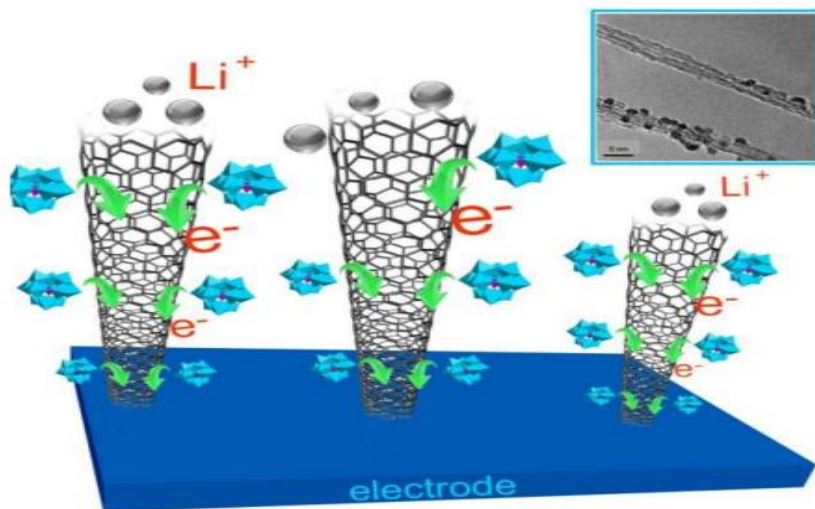
Fig. 17. Schematic demonstration of MCB formed on POM/SWNTs composites (Huang et al. 2015).

The reduction techniques assisted with POM significantly enhancing the electronic association of GO materials, leading to noticeably enhanced electronic conductivity. The preliminary findings on POM battery electrodes emphasize the requirement for chemically redox-tuneable, highly cycle-stable, and highly redox-active molecular materials.

It has been mentioned how crucial metal-metal bonding is within the POM cluster and how counterions may balance charges by encircling it. Future MCB cathode materials must possess the following structural and electrical characteristics (Awaga et al. 2014).

First, there must be many oxygen atoms outside the cluster. Second, transition metal atoms should not occupy degenerate d levels. Third, these metal atoms must be geometrically close to one another to form metal-metal bonds. Fourth, Li+ counterions must be able to move into the negatively charged outer oxygen shell at least partially in order to balance the repellent Coulomb forces brought on by the excess charges. Theoretically, oxidation can change, and the findings indirectly infer that creating Mo–Mo bonds is a multi-step process. As mentioned above, POM-carbon composites have also been researched as promising Li-ion battery lithium storage materials. Molecular cluster battery with a lithium metal anode and a cathode active material of PMo_{12} combined with carbon black as The POM-MCB showed a substantial capability (Figure 17).
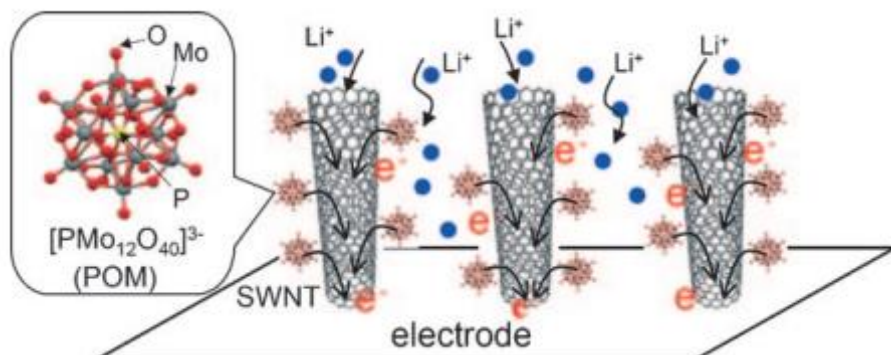
Fig. 18. Battery reactions in POM&SWNT Hybrids (Awaga et al. 2012).

4. CONCLUSION

In conclusion, POM/graphene nanocomposites can be constructed quickly, sustainably, and at scale using the POM-catalyzed electrochemical reduction process. The synergistic qualities of POMs and graphene matrices are responsible for the nanocomposites' improved lithium-storage capacity. The battery performances of the POM/MCB were demonstrated to be exactly dependent on the ratio of POM enclosed of the cathodes; the capacity of discharging decreases while the ratio of POM increases.

Researchers have developed new methods for assembling POM/graphene nanocomposites using a POM-catalyzed electrochemical reduction process. This method is simple, environmentally beneficial, and convenient production. The resulting nanocomposites exhibit enhanced lithium-storage capacity, attributed to the interdependent features for POMs and graphenes. The large surface area and excellent conductivity of graphenes can also be used to enhance other POM properties, such as their catalysis and capacitance, making the current electrochemical reduction method a promising general method for the

production of different functionalized POM/graphene hybrid materials for use in catalysis, electronics, and energy storage (Figure 18).

In other words, the researchers have developed a new method for making POM/graphene nanocomposites that is easy to do, environmentally friendly, and can make many nanocomposites simultaneously. The resulting nanocomposites have a higher capacity for storing lithium than pure POMs, which is attributed to the fact that the POMs and graphene matrices work together to improve the lithium-storage properties.

5. FUTURE STUDIES

Several pillars support POM/nanocarbon materials' future development. Investigating devoloped POMs, where unique reactivity, stronger stability, and varied reactivity might be anticipated, is an apparent and, in the authors' opinion, auspicious approach. Where target systems are concerned, an interdisciplinary approach is vitally needed. Nanocarbon materials are coupled with POMs that can interact with these targets. New methods for constructing POM/nanocarbon composites are needed to reach electrode materials with high stability and reactivity because this material combination is currently tricky. The creation, synthesis, and reactivity of brand-new POM/nanocarbon nanocomposite materials formed on graphene or carbon nanotubes that have been POMfunctionalized. They were more effective electrocatalysts when used as electrodes for Li-ion batteries than the reference system. The applications above are not the only ones that POM/nanocarbon composites will see in the future. POM/nanocarbon composites have the potential to solve significant technical problems.

Therefore, collaborative studies that combine the knowledge of polyoxometalate chemists, nano carbons, and experts in device manufacturing might one day result in actual devices made of self-assembled POM and nanocarbon components (Huang et al. 2014).

REFERENCES

Chen, S., Yeoh, W., Liu, Q., & Wang, G. (2012). Chemical-free synthesis of graphene–carbon nanotube hybrid materials for reversible lithium storage in lithium-ion batteries. *Carbon,* 50(12), 4557–4565. DOI:10.1016/j.carbon.2012.05.040

Feng, C., Zhang, L., Yang, M., Song, X., Zhao, H., Jia, Z., … Liu, G. (2015). One-Pot synthesis of copper sulfide nanowires/reduced graphene oxide nanocomposites with excellent lithium-storage properties as anode materials for lithium-ion batteries. *ACS Applied Materials & Interfaces,*7(29), 15726–15734. DOI:10.1021/acsami.5b01285

Genovese, M., & Lian, K. (2015). Polyoxometalate modified inorganic–organic nanocomposite materials for energy storage applications: A review. *Current Opinion in Solid State and Materials Science,* 19(2), 126–137. DOI:10.1016/j.cossms.2014.12.002

Hutin, M., Rosnes, M. H., Long, D.-L., & Cronin, L. (2013). Polyoxometalates: Synthesis and structure – from building blocks to emergent materials. *Comprehensive Inorganic Chemistry II,* 241–269. DOI:10.1016/b978-0-08-097774-4.00210-2

Ji, Y., Huang, L., Hu, J., Streb, C., & Song, Y.-F. (2015). Polyoxometalate-functionalized nanocarbon materials for energy conversion, energy storage, and sensor systems. *Energy & Environmental Science,* 8(3), 776 –789. DOI:10.1039/c4ee03749a

Jin, S., & Wang, C. (2014). Synthesis and first investigation of excellent lithium storage performances of Fe_2GeO_4 / reduced graphene oxide

nanocomposite. *Nano Energy,* 7, 63–71. DOI:10.1016/j.nanoen.2014.04.011

Kawasaki, N., Wang, H., Nakanishi, R., Hamanaka, S., Kitaura, R., Shinohara, H., Awaga, K. (2011). Nanohybridization of polyoxometalate clusters and single-wall carbon nanotubes: Applications in molecular cluster batteries. *Angewandte Chemie International Edition,* 50(15), 3471–3474. DOI:10.1002/anie.201007264

Liu, R., Li, S., Yu, X., Zhang, G., Zhang, S., Yao, J., & Zhi, L. (2012). A general green strategy for fabricating metal nanoparticles / polyoxometalate / graphene tri-component nano hybrids: Enhanced electrocatalytic properties. *Journal of Materials Chemistry,* 22(8), 3319. DOI:10.1039/c2jm15875b

Long, D.-L., Tsunashima, R., & Cronin, L. (2010). Polyoxometalates: Building Blocks for Functional Nanoscale Systems. *Angewandte Chemie International Edition,* 49(10), 1736–1758. DOI:10.1002/anie.200902483

Nakashima, N.,Tomonari, Y., & Murakami, H., *Chem. Lett.,* 2002, 31,638.

Nishimoto, Y., Yokogawa, D., Yoshikawa, H., Awaga, K., & Irle, S. (2014). Super-reduced polyoxometalates: Excellent molecular cluster battery components and semipermeable molecular capacitors. *Journal of the American Chemical Society,* 136(25), 9042–9052. DOI:10.1021/ja5032369

Wang, G., Wang, B., Wang, X., Park, J., Dou, S., Ahn, H., & Kim, K. (2009). Sn/graphene nanocomposite with 3D architecture for enhanced reversible lithium storage in lithium-ion batteries.

Journal of Materials Chemistry, 19(44), 8378. DOI:10.1039/b914650d

Wang, H., Kawasaki, N., Yokoyama, T., Yoshikawa, H., & Awaga, K. (2012). Molecular cluster batteries of nano-hybrid materials between Keggin POMs and SWNTs. *Dalton Transactions*, 41(33), 9863. DOI:10.1039/c2dt30603d

Wang, S., Li, H., Li, S., Liu, F., Wu, D., Feng, X., & Wu, L. (2013). Electrochemical-reduction-assisted assembly of a polyoxometalate /graphene nanocomposite and Its enhanced lithium-storage performance. *Chemistry-A European Journal,* 19(33), 10895–10902. DOI:10.1002/chem.201300319

Wang, H., Yamada, T., Hamanaka, S., Yoshikawa, H., & Awaga, K. (2014). Cathode composition dependence of battery performance of polyoxometalate (POM) molecular cluster batteries. *Chemistry Letters*, 43(7), 1067–1069. DOI:10.1246/cl.140233

Wei, T., Zhang, M., Wu, P., Tang, Y.-J., Li, S.-L., Shen, F.-C., … Lan, Y.-Q. (2017). POM-based metal-organic framework/reduced graphene oxide nanocomposites with hybrid behavior of battery-supercapacitor for superior lithium storage. *Nano Energy,* 34, 205–214. DOI:10.1016/j.nanoen.2017.02.028

Yan, Y., & Wu, L. (2011). Polyoxometalate-incorporated supramolecular self-assemblies: Structures and functional properties. *Israel Journal of Chemistry,* 51(2), 181–190. DOI:10.1002/ijch.201000077

Yang, X.-L., Ye, Y.-S., Wang, Z.-M., Zhang, Z.-H., Zhao, Y.-L., Yang, F., … Wei, T. (2020). POM-based MOF-derived $Co_3O_4/CoMoO_4$

nanohybrids as anodes for high-performance lithium-ion batteries. *ACS Omega*. DOI:10.1021/acsomega.0c03929

Yao, Z., Xia, X., Zhong, Y.,Wang, Y., Zhang, B., Xie, D., … Huang, Y. (2017). Hybrid vertical graphene/lithium titanate – CNTs arrays for lithium-ion storage with extraordinary performance. *Journal of Materials Chemistry A,* 5(19), 8916–8921. DOI:10.1039/c7ta02511d

Yue, Y., Li, Y., Bi, Z., Veith, G. M., Bridges, C. A., Guo, B., … Dai, S. (2015). A POM–organic framework anode for Li-ion battery. *Journal of Materials Chemistry A,* 3(45), 22989–22995. DOI:10.1039/c5ta06785e

Zhang, Y., Liu, J., Li, S.-L., Su, Z.-M., & Lan, Y.-Q. (2019). Polyoxometalate-based materials for sustainable and clean energy conversion and storage. *Energy Chem,* 100021. DOI:10.1016/j.enchem.2019.100021

CHAPTER 5

2D-, 3D-BORON CARBON NITRIDE ADSORPTION

Assist. Prof. Dr. Nilgün ONURSAL[1]

DOI: https://dx.doi.org/10.5281/zenodo.10030567

[1] Siirt University, Faculty of Education, Department of Mathematics and Physical Sciences Education, Physical Sciences Education, Siirt, Türkiye, Email: nilgun.onursal@gmail.com, Orcid ID: 0000-0002-2460-6475

1.INTRODUCTION

Diamond, graphite, boron carbide (B_4C), boron nitride (BN), and carbon nitride (C_3N_4) are a few of the industrially significant phases in the ternary boron carbon nitride system. Among these covalently bonded materials, diamond, cubic boron nitride (c-BN), and B_4C are the hardest known materials on earth. Both graphite and hexagonal boron nitride (h-BN), which have layered structures, are significant industrial materials. While h-BN is utilised in electrical insulators, lubricants, and refractories, graphite is frequently employed for electrodes in lithium ion batteries, as a steel toughening agent, and as a component in high-strength composites. Therefore, it has been predicted that boron, carbon, and nitrogen hybridization with a regulated composition will result in novel materials with multifunctional capabilities. Due to its versatility in modifying a variety of chemical, optical, and electrical properties, two-dimensional boron carbon nitride is a complex system that has recently received a lot of interest. For various energy-related applications, including supercapacitors, lithium ion batteries, electrocatalysts, and sensors, boron carbon nitride structures have been the subject of intense research during the past ten years. There are critical global technological and scientific concerns related to the availability and accessibility of clean and secure water supplies. Due to global water shortages, wastewater treatment and reuse are being considered as practical alternatives to using fresh water for domestic, industrial, and agricultural reasons. Nanosheets made of boron carbon nitride have recently been applied to the treatment of wastewater. Porous boron nitride materials have a wide range of potential applications in the disciplines of pollutant adsorption, gas absorption, and catalyst carrier adsorption. For various

organic pollutants, such as dyes, oils, aromatic molecules and solvents they have a good adsorption effect.

For a while, the development of new forms of carbon has generated a great attention for both solving environmental issues and the newest technological advancements. The structural diversity that results from carbon's combination with other elements makes carbon-based materials more versatile in terms of their properties and uses. Due to their covalent bonds, short bond lengths, and low atomic masses, compounds in the boron-carbon-nitrogen phase diagram, such as diamond (C), cubic boron nitride (c-BN), and boron carbide (B_4C), are particularly well known and have excellent thermal and mechanical strength (Nehate et al., 2020). Until now, carbonaceous substances like fullerenes, nanotubes, graphene, and nanodiamond have advanced science by allowing the synthesis of apparatuses with exceptional traits like large surface areas and porous structures. These substances have also attracted ongoing interest for their potential use in energy and waste treatment applications. Among them, effective, low-cost nanomaterials made primarily of carbon (C), nitrogen (N), or boron (B) have been utilised frequently for the adsorption of toxic chemicals. For a number of the identified pollutants, boron nitride (BN) nanosheets, which are graphene-like nanomaterials with alternating B and N atoms, have outstanding adsorption capabilities (Recepoglu et al., 2022).

To remove pharmaceuticals from water, a variety of techniques including membrane filtration, electrochemical catalysis, coagulation, biodegradation, photocatalysis, and ozonation have been utilised extensively. Adsorption technology has drawn more attention than the methods mentioned above for the removal of different types of

contaminants from water because of its advantages in terms of economy, regeneration, and flexibility. A greater focus has been placed on the special physical and chemical characteristics of boron nitride (BN), such as its high specific surface area, multiple structural flaws, low density, high thermal conductivity, chemical durability, and oxidation resistance. Because of these properties, porous boron nitride materials have a wide range of potential applications in the disciplines of pollutant adsorption, gas absorption, and catalyst carrier adsorption. For various organic pollutants, such as dyes, oils, aromatic molecules and solvents have a good adsorption effect. By pyrolysis at high temperatures or by stripping with organic solvents, BN nanosheets are frequently generated synthetically. The surface defect, doping and porous properties of nitrogen-based materials play an important role in adsorption. Boron carbon nitride (BCN), which consists of various B, C, and N components, is regarded as a hybrid material between C and BN (Sun et al., 2022).

For the past few decades, the removal of harmful organic and inorganic water and air pollutants has been mostly accomplished using photocatalysis using semiconductor materials. Strong light absorption, an appropriate band gap, a low cost, and the capacity to be easily machined into the desired forms are all qualities that these materials must possess. They also need to be stable, non-toxic, and non-expensive. The application of photocatalytic materials is also constrained by problems like a quick reaction time, a weak light source, ineffective pollutant interception, and secondary pollution, which are drawbacks of photocatalytic materials in the improvement of the efficacy of water pollution removal. Therefore, the removal efficiency of treating polluted

water may be improved by using an adsorption-degradation system and adsorbent photocatalyst materials. One of the most promising metal-free semiconductor materials among possible catalysts is carbon nitride (CN). The procedure for making CN is straightforward: typically, CN is made by thermally polymerizing organic compounds that include carbon and nitrogen, such as urea, melamine, thiourea, dicyandiamide, and cyanamide. In addition, it has an excellent photocatalytic action, a restricted bandwidth of around 2.7, and a high efficacy in eliminating viruses, heavy metals, and organic contaminants. As a result, CN-based photocatalysts and their applications may one day help to address challenges with energy and the environment. However, it has been discovered that CN has a low photocatalytic effectiveness under visible light, and it only absorbs 0.1% of the irradiated visible light. The use of CN is also restricted by the high rate of photogenerated electron-hole pairs recombining. As a result, numerous techniques have been constructed to enhance the characteristics of CN, such as photocatalytic efficiency, adsorptivity, and solar light utilisation. These techniques include doping with metallic or nonmetallic components, coupling with other materials, and altering the shape. It has garnered a lot of interest since the adsorptivity of CN is another crucial element that affects the effectiveness of removal. In general, the surface chemical properties and porous microtexture of an adsorbent have a significant impact on its adsorption capacity. Therefore, some investigations have used the acid treatment of CN or its precursor to improve the specific surface area. However, the acid treatment requires acid form, washing, drying, and calcining, which complicates the procedure. Most critically, the adsorption capacity of CN was not greatly increased by this technique.

In order to improve the adsorption-degradation ability of CN, a novel technique with easier stages is required. To enhance the photocatalytic performance, boron-doped polymeric CN has been explored as metal-free catalysts (Guo et al., 2019).

Covalent and porous organic polymers (COPs and POPs), hexagonal/porous boron nitride (h-BN), silica, polymeric materials, nitrogen-doped carbon compounds, metal-organic frameworks (MOFs), and metal oxide-based carbonaceous materials have all been proposed as alternatives for CO_2 uptake by adsorption on porous adsorbents. Porous BN compounds are among these adsorbents, and they appear to be the most effective due to their similar physiochemical properties, which include high thermal and chemical durability and conductivity, low density, tunable high specific surface area (almost identical to activated carbon), few morphological defects, and possession of higher ordered chemistry in comparison to carbonaceous adsorbents due to the presence of polar B-N bonds. These advantageous properties lend porous BN to be favorable for applications in various areas, such as for gas adsorption of H_2, removal of organic pollutants and dyes from water, and use as a catalytic support (Kamran et al., 2019).

2. BORON CARBON NITRIDE

Two-dimensional materials have recently been identified as the most promising options for the removal of new hazardous substances from the environment. Molybdenum disulphide, graphene, and silica have all gained attention in recent years due to their fascinating properties, including their high surface area, optical transparency, low bandgap, flexibility, and high tensile strength. Numerous additional

nanosheets, including boron nitride (BN), silicon carbide (SiC), and boron carbon nitride (BCN) nanosheets, have drawn interest since graphene was shown to be a viable adsorbent (Dindorkar et al., 2023a). Potential candidates for the adsorption of organic contaminants include monolayered materials including boron nitride, boron carbide, molybdenum disulphide, bismuth iodide, silicene, and phosphorous carbide. Adsorbents are outstanding adsorption materials because of their high surface area, low HOMO-LUMO energy gap, excellent carrier mobility, and light weight. It has been demonstrated that monolayer BCN, as a two-dimensional framework with a hexagonal arrangement similar to graphene, is capable of efficiently adsorbing a number of toxicants and pollutants. Depending on how the atoms in the constituent parts are arranged, BCN nanosheets can take on a variety of configurations (BxCyNz). The in-plane combinations of boron, carbon and nitrogen exhibit a great thermodynamically stability. Usually, monolayer BCN sheets are associated with a variety of defects such as point defects, interstitial atoms, dislocations, grain boundaries etc. Several studies have reported that point defects in the adsorbent material significantly affect the adsorption interaction (Yadav & Dindorkar, 2022).

According to Yan et al. (2010), the BCN shows excellent photocatalytic effectiveness for both RhB (Rhodamine B) and MO (Methyl Orange). According to Sagara et al. (2016), BH_3NH_3 and melamine were used to make B-doped carbon nitride. The surface of g-C_3N_4 and B-doped g-C_3N_4 was then coated with Au, Ag, or Rh as a co-catalyst using magnetron sputtering. They found that B-doped g-C_3N_4 coated with Rh has the highest photocurrent response under solar light

irradiation, its photocurrent being about 10 times larger than that of original g-C_3N_4.

It is thought of as a material intermediate between carbon and BN materials and is a ternary hybrid material made up of various B, C, and N components. The majority of BCN materials are generated by the use of carbon sources that are organic substances, such glucose. There are studies using melamine as a source of both carbon and nitrogen. BCN has good adsorption ability in addition to having great chemical stability because the incorporation of carbon into the BN skeleton weakens the conjugation between B (electron deficiency centre) and N (rich electron centre). BCN is mostly synthesised in an inert atmosphere, such as nitrogen gas (Guo et al., 2020). Most BCN hybrid materials are typically produced using urea or glucose as the carbon source (Sun et al., 2022).

For synthesing BCN films, plasma-enhanced chemical vapour deposition (PECVD) has proven to be especially beneficial. In the CVD processes, molecular precursors such as dimethylamine borane ($C_2H_{10}NB$), N,N′,N″-trimethylborazine ((CH_3)$_3N_3B_3H_3$), triethylamine borane ($C_6H_{18}NB$), (N-pyrrolidino)diethylborane ($C_8H_{18}BN$), pyridine-borane ($C_5H_5NBH_3$), and triazaborabicyclodecane ($BN_3H_2(CH_2)6$) have been used as boron, carbon, and nitrogen sources. Compared to dangerous and toxic gaseous precursors like B_2H_6 and BCl_3, these liquid molecular precursors are safer and simpler to manage. However, it is challenging to regulate the compositions of deposited films and prevent the incorporation of oxygen impurities when utilising such organic precursors. Due to boron's high reactivity with oxygen in CVD techniques, the oxygen incorporation has frequently been reported (Kida et al., 2009).

3. Boron carbon nitride nanomaterials

Two-dimensional boron carbon nitride nanosheets (BCNNs) have attracted a lot of interest recently in the field of adsorption of pollutants because to their huge specific areas, great thermal stability, and chemical inertness. The photoelectric and adsorption characteristics of boron nitride BN can be significantly enhanced by the production of BCNNs by adding carbon into BN. Wang et al. (2020) used boric acid, melamine, and glucose as the key starting materials to manufacture carbon-doped BN (BCN) nanosheets at 1100 °C using a molten salt technique. Typically, these sheets are several micrometers wide and have a few layers. The temperature of the post-treatment (remove carbon by oxidation) can affect the composition ratios of BN-C sheets (Han et al., 2011). Doping C atoms in a pure BNNS layer or inducing B and N atoms in a graphene layer are two popular ways to produce BNC hybrid nanosheets. For instance, substitutional carbon doping of BNNSs, nanotubes, and nanoribbons can be accomplished using in situ electron beam irradiation (Wei et al., 2011).

The combustion of fuels like petrol, wood, petroleum, coal, and natural gas results in the continual production of VOCs such toluene, xylene, benzene, formaldehyde, 1,3-butadiene, indole, etc. VOCs can be eliminated from the atmosphere using a number of methods, such as thermal plasma oxidation, biofiltration, adsorption, thermal oxidation, and catalytic oxidation. Two-dimensional (2D) materials offer interesting alternatives for clearing the environment of newly arising harmful substances. Due to their intriguing characteristics, including as high surface area, low energy gap, optical transparency, flexibility, and high tensile strength, they have attracted significant interest from both

fundamental and applied points of view. Graphene (GRA), boron nitride (BN), silicon carbide, boron carbon nitride (BCN), and molybdenum disulphide are some examples of 2D materials that have attracted attention for their intriguing features, including high surface area, low bandgap, optical transparency, flexibility, and high tensile strength. Recently, 2D versions of the materials BN, boron carbon nitride, silicon carbide, and phosphorus carbide have been developed. Since then, 2D materials have been the subject of substantial investigation. 2D materials like GRA, BN, and BCN are challenging to synthesise and experimental studies can be complex (Dindorkar et al., 2023b).

BCN nanoparticles' superior adsorption capacities have allowed them to be employed successfully for water treatment. The food, paper, leather, and textile sectors produce a huge amount of organic dyes, which are significant water pollutants. Dye wastewater has a complex composition, a high organic content and a significant amount of refractory compounds that need to be removed before to disposal. Malachite green (MG) from water has been treated using mesoporous BCN, which has a maximum adsorption capacity of 310 mg/g in the study of Recepoglu et al., (2022). Porous BCN nanosheets have additionally demonstrated outstanding photodegradation abilities for organic pollutant cleanup. BCN materials have also been used in the nuclear power industry to enrich uranium residues by reducing the uranyl ions, which are highly soluble and mobile ($U(VI)O_2^{2+}$), to sparingly soluble U(IV) as oxides/hydroxides with photocatalytic activities.

Wang et al., (2017) reported novel flower stamen-like porous BCN nanoscrolls for water cleaning. The porous BCN nanoscrolls with a high surface area of 890 m^2 g^{-1} displayed excellent dye adsorption

performances up to the adsorption capacity of 620 mg g^{-1} of Congo red and 250 mg g^{-1} of methylene blue, which have a great potential value for water cleaning applications.

4. GRAPHENE-LIKE BORON NITRIDE-CARBON HETEROSTRUCTURES

The adsorption of aromatic compounds on graphene has received a great attention recently. Scientists believe that their interactions serve as a good model for how graphene layers interact. For instance, while benzene and pyridine have moderate adsorption energies, aminotriazines can significantly be adsorbed on the surface of graphite. Naphthalene and benzophenone molecules only extremely weakly or never bond to graphene sheets. When, for instance, NH_2 groups are introduced to the aromatic core of graphene, the overall interactions between the adsorbed molecules and graphene can be dramatically altered by the addition of functional groups (Petrushenko & Petrushenko, 2017).

Scientists have worked extraordinarily hard to investigate the characteristics and phenomena of 2D nanomaterials that are not made of carbon and are similar to graphene, especially those that have only one or a few layers. This has been motivated by the rigorous studies of graphene. Several graphene-like 2D structures have been fabricated experimentally using a wide range of layered and nonlayered materials. These graphene-like structures have already demonstrated exceptional properties that will lead to new discoveries and inventiveness in the field of nanomaterials. Density-functional theory (DFT) calculations theoretically provide a strong tool to investigate the electronic structure of nanomaterials (primarily the ground state), to predict their intrinsic

properties, to help characterise and explain experimental results, as well as to explore their potential applications. By DFT computations, many graphene-like materials have been explored and designed, and fantastic properties are disclosed (Tang et al., 2015).

Graphene and hexagonal boron nitride (h-BN) are two-dimensional materials with hexagonal honeycomb lattice atomic layers. Graphene is a very good conductor, but h-BN is a good insulator, therefore despite their structural similarities, the two materials are fundamentally different in electrically (Gong et al., 2014). With a 2% difference in lattice constant, graphene and hexagonal boron nitride (h-BN) exhibit similar crystal structures. A superlattice of vertically stacked graphene and h-BN heterostructures is one of the possible configurations for graphene/h-BN hybrid structures (Liu et al., 2013).
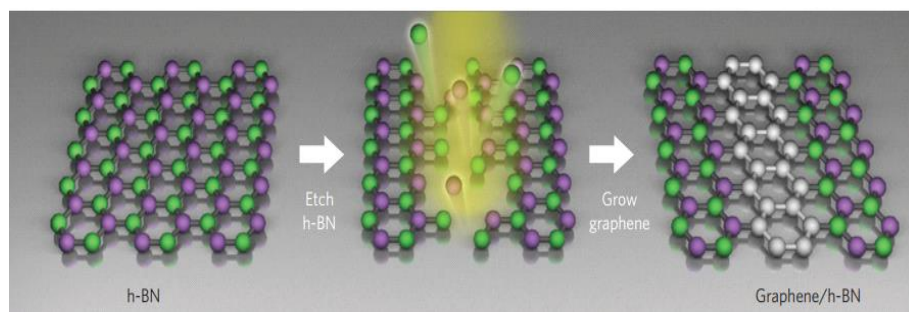
Fig. 1. Illustration of the fabrication procedure for in-plane graphene/h-BN heterostructures. Steps: preparation of h-BN films using the CVD method; partial etching of h-BN by argon ions to give predesigned patterns; subsequent CVD growth of graphene on the etched regions (Liu et al., 2013)

Previous studies have found that B–N and C–C bonds tend to segregate in the BCN systems. For instance, hexagonal BN (h-BN) and graphene can be synthesised as layer-by-layer composite structures because their lattice characteristics are so similar (Ci et al., 2010).

Because graphene and h-BN have structures that are similar, it is possible to combine the two in a single layer to form a hybrid 2D material. Recently, it was proposed and synthesised to synthesise graphene-like boron nitride-carbon heterostructures with various forms of h-BN embedded in graphene and vice versa (Petrushenko & Petrushenko, 2018).

The hybrid graphene-BN sheet is one of the highly researched 2D materials. Since graphene and BN sheets are the two most extensively researched 2D materials and they exhibit significantly different properties while having the least lattice mismatch with one another. As a result, the hybridization between them offers special tuning flexibility for the characteristics, which can change from semiconducting to half-metallic and from nonmagnetic to ferromagnetic. The most striking feature is that, unlike functionalized graphene and BN sheets for band engineering formed through hydrogenation, fluorination, or metal doping, the hybrid graphene-BN sheet retains its single-atomic structure. The hybrid sheet has a variety of functions that go beyond those of ordinary 2D materials due to the combinations of various patterns and sizes. Both graphene and BN nanosheets (BNNSs) can be produced using CVD methods. The secret to synthesising BNC hybrid nanosheets by CVD is building sources with an equal distribution of carbon, boron, and nitride atoms in the process. A carbon source is typically present in the reaction mixture in the form of graphite or gaseous phase, while sources of boron and nitride can take the form of ammonia borane, pyridine-BH_3, trimethylamine-BH3, boron imidazolate, pyrrolidine-borane, BCl_3, BBr3, ammonia, and other substances. Since large-area graphene and hexagonal BN are always grown on copper substrates, Ci

et al. (2010) declared the first substantial development on the successful synthesis of BNC hybrid nanosheets in that study. Methane and ammonia borane (NH_3BH_3) were used as B, C, N sources. By controlling the experimental conditions such as pressure, temperature, and gas flow rate, the atomic ratio of B, C, N can be tuned flexibly (Kan et al., 2016).

One of the pillars of contemporary materials research is the capability to regulate the emergence of interfaces between various materials. With the development of two-dimensional (2D) crystals, low-dimensional counterparts of traditional interfaces are now possible: line barriers dividing several materials that are incorporated into a single 2D sheet. To design such 2D heterostructures, graphene and hexagonal boron nitride present an attractive platform. Although they are isostructural, virtually lattice-matched, and isoelectronic, the integration of their various band structures promises to yield intriguing functional features. With the interfaces between monolayer graphene and boron nitride, first-principles calculations have predicted some unusual electronic characteristics, such as the opening of a variable bandgap, magnetism, special thermal transport characteristics, robust half-metallic behaviour without applied electric fields, and interfacial electronic reconstructions similar to those seen in oxide heterostructures. Methods for regulating the production of graphene-boron nitride interfaces within a single atomic layer are necessary to access these features. 2D material synthesis techniques on metal substrates have advanced, and variations of these techniques might promote the development of more intricate heterostructures (Sutter et al., 2012).

Both pure graphene and graphene oxide can be employed as the beginning sheet materials to transform a graphene-related layer into a

BNC hybrid nanosheet. B atoms can be obtained from B2O3 powder or boric acid, whereas N atoms are obtained from nitrogen or ammonia atmosphere. Han et al., (2011) generated pure, extremely crystalline BN and BNC hybrid nanosheets. In their experiment, graphene sheets were placed on top of B2O3 powder and heated for 30 minutes at 165 oC in a nitrogen atmosphere. The synthesised sheets were several micrometres wide and only a few layers thick, and the post-treatment temperature allowed for precise control of the BN and C composition ratios. Instead of beginning with graphene, Lin et al. (2012) employed graphene oxide. The boron and nitrogen atoms were integrated into the graphene lattice as randomly dispersed BN nanodomains by treating it with B2O3 and ammonia at 900–1100 ºC. Graphene or BN nanosheet islands were first formed on the substrate using the heteroepitaxial growth process, and then the other material was patched onto the exposed surface to form the BNC hybrid nanosheet material. Gao et al., (2013) used the two-step heteroepitaxial growth approach to generate the almost seamless BNC hybrid films in ultra-high vacuum (UHV) conditions on a chosen single crystalline Rh (1 1 1) substrate. In their work, the growth of graphene happened after the growth of discrete BN islands. The surface ratio of graphene domains could be easily modulated from 6.6 to 62% by controlling the growth time of BN islands.

5.   3D   HYBRID   BORON-NITRIDE-CARBON FRAMEWORKS

In order to form electrically heatable sorbents for economically significant adsorptive desulfurization applications, Xia et al. (2019) hybridised boron nitride particles with electrically-conducting carbon

nanotube aerogels. Specifically, by freeze-drying aqueous BN-precursor/CNT mixes and then subjecting them to high-temperature thermal treatment, carbon-doped boron nitride structures (BN) were incorporated within carbon nanotube (rCNT) aerogels. In comparison to pure BN powders, the resulting BN/rCNT aerogels demonstrated significantly improved desulfurization performance as demonstrated by a 50% increase in organosulfur uptake (up to 43 mg S/g BN) and significantly improved sorbent regeneration stability (90% performance retention after 5 regeneration cycles). As determined by electron microscopy, BET, EDX mapping, and post-sorption XPS, the improved desulfurization efficacy in the hybrid BN/rCNT hybrid aerogels was associated with significantly improved boron-sulfur interactions and higher meso-porosity. Importantly, the CNT scaffold's conductivity allowed for the resistive heating of BN to extremely high temperatures (up to 700 °C) with little energy input and extremely fast heating rates (up to 74 ºC/s). A number of regeneration cycles of depleted BN/rCNT adsorbents were used to demonstrate the value of resistive scaffold heating for energy-efficient thermal regeneration. In addition to increasing BN's already beneficial properties (sorption capacity, regeneration stability), the study also introduces new functions (direct electrical framework heating), highlighting the key benefits of combining BN with 3D nanocarbon networks.
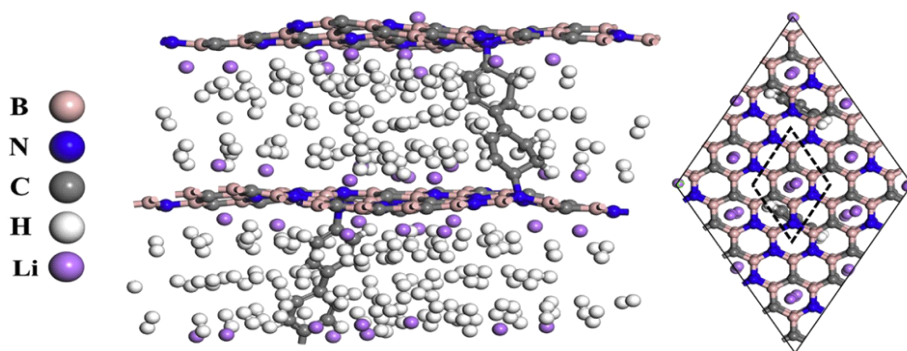
Fig. 2. 3D hybrid Boron-Nitride-Carbon frameworks (Bi et al., 2019)

Cui et al. (2023) built an interconnected three-dimensional (3D) polysulfone/hexagonal boron nitride-carbon nanofiber (PSF/BN-CNF) skeleton. This C/BN-CNF hybrid scaffold was built using a combination of salt-templated assembly and high-temperature post-treatment. It is lightweight, strong, and interconnected. Then, using a vacuum aided planetary mix process, the liquid epoxy matrix was infused into the 3D skeletons to form the matching composites.

Bi et al. (2019) have synthesised and optimised a new 3D hybrid Boron-Nitride-Carbon-interconnected framework (BNCIFs) made up of organic linkers with Li decoration. According to the results, replacing the N atom in pure BN with a C atom could significantly increase the metal binding energy. With an average binding energy of 0.24 eV, four H_2 molecules could be adsorbed by each Li atom.

These findings therefore have clear implications for a wide range of BN applications, including water treatment, carbon capture, energy storage and electro-catalysis.

6. CONCLUSIONS

Differently shaped materials made of boron carbon nitride are gaining popularity due to their wide range of potential uses. Materials

made of boron carbon nitride are famous for their adaptable mechanical behaviour, great chemical inertness, high thermal stability, and adaptable electrical properties, making them suitable for corresponding applications in difficult environments. Chemical vapour deposition, ion beam-aided deposition, magnetron sputtering, and pulsed laser deposition are frequently used synthesis methods for ternary boron carbon nitride compounds.

Boron carbon nitride compounds are suitable for a variety of severe environment applications, such as photocatalysts and adsorbents, as well as electrochemical reduction and capacitive deionization, due to their excellent mechanical strength, superb unreactivity, and significant stability.

REFERENCES

Bi, L., Yin, J., Huang, X., Wang, Y., & Yang, Z. (2019). A DFT study of H_2 adsorption on lithium decorated 3D hybrid Boron-Nitride-Carbon frameworks. *International Journal of Hydrogen Energy,* 44(29), 15183-15192.

Ci, L., Song, L., Jin, C., Jariwala, D., Wu, D., Li, Y., ... & Ajayan, P. M. (2010). Atomic layers of hybridized boron nitride and graphene domains. *Nature materials,* 9(5), 430-435.

Cui, Y., Xu, F., Bao, D., Gao, Y., Peng, J., Lin, D., ... & Wang, H. (2023). Construction of 3D interconnected boron nitride/carbon nanofiber hybrid network within polymer composite for thermal conductivity improvement. *Journal of Materials Science & Technology,* 147, 165-175.

Dindorkar, S. S., Patel, R. V., & Yadav, A. (2023a). Adsorption behaviour of graphene, boron nitride and boron carbon nitride nanosheets towards pharmaceutical and personal care products. *Computational and Theoretical Chemistry,* 1220, 113995.

Dindorkar, S. S., Sinha, N., & Yadav, A. (2023b). Comparative study on adsorption of volatile organic compounds on graphene, boron nitride and boron carbon nitride nanosheets. *Solid State Communications,* 359, 115021.

Guo, X., Rao, L., Wang, P., Zhang, L., & Wang, Y. (2019). Synthesis of porous boron-doped carbon nitride: adsorption capacity and photo-regeneration properties. *International Journal of Environmental Research and Public Health,* 16(4), 581.

Gong, Y., Shi, G., Zhang, Z., Zhou, W., Jung, J., Gao, W., ... & Ajayan,

P. M. (2014). Direct chemical conversion of graphene to boron- and nitrogen-and carbon-containing atomic layers. *Nature Communications,* 5(1), 3193.

Guo, Y., Yan, C., Wang, P., Rao, L., & Wang, C. (2020). Doping of carbon into boron nitride to get the increased adsorption ability for tetracycline from water by changing the pH of solution. *Chemical Engineering Journal,* 387, 124136.

Han, W. Q., Yu, H. G., & Liu, Z. (2011). Convert graphene sheets to boron nitride and boron nitride–carbon sheets via a carbon-substitution reaction. *Applied Physics Letters,* 98(20).

Kan, M., Li, Y., & Sun, Q. (2016). Recent advances in hybrid graphene-BN planar structures. *Wiley Interdisciplinary Reviews: Computational Molecular Science,* 6(1), 65-82.

Kamran, U., Rhee, K. Y., & Park, S. J. (2019). Effect of triblock copolymer on carbon-based boron nitride whiskers for efficient CO_2 adsorption. *Polymers,* 11(5), 913.

Kida, T., Shigezumi, K., Mannan, M. A., Akiyama, M., Baba, Y., & Nagano, M. (2009). Synthesis of boron carbonitride (BCN) films by plasma-enhanced chemical vapor deposition using trimethylamine borane as a molecular precursor. *Vacuum*, 83(8), 1143-1146.

Liu, Z., Ma, L., Shi, G., Zhou, W., Gong, Y., Lei, S., ... & Ajayan, P. M. (2013). In-plane heterostructures of graphene and hexagonal boron nitride with controlled domain sizes. *Nature Nanotechnology,* 8(2), 119-124.

Lin, T. W., Su, C. Y., Zhang, X. Q., Zhang, W., Lee, Y. H.,Chu, C.W., ... & Li, L. J. (2012). Converting graphene oxide monolayers into

boron carbonitride nanosheets by substitutional doping. *Small*, 8(9), 1384-1391.

Nehate, S. D., Saikumar, A. K., Prakash, A., & Sundaram, K. B. (2020). A review of boron carbon nitride thin films and progress in nanomaterials. *Materials Today Advances*, 8, 100106.

Petrushenko, I. K., & Petrushenko, K. B. (2017). Physical adsorption of N-containing heterocycles on graphene-like boron nitride-carbon heterostructures: a DFT study. *Computational and Theoretical Chemistry,* 1117, 162-168.

Petrushenko, I. K., & Petrushenko, K. B. (2018). Hydrogen adsorption on graphene, hexagonal boron nitride, and graphene-like boron nitride-carbon heterostructures: A comparative theoretical study. *International Journal of Hydrogen Energy,* 43(2), 801-808.

Recepoglu, Y. K., Goren, A. Y., Vatanpour, V., Yoon, Y., & Khataee, A. (2022). Boron carbon nitride nanosheets in water and wastewater treatment: A critical review. *Desalination,* 533, 115782.

Sun, Y., Bian, J., & Zhu, Q. (2022). Sulfamethoxazole removal of adsorption by carbon–Doped boron nitride in water. *Journal of Molecular Liquids,* 349, 118216.

Sagara, N., Kamimura, S., Tsubota, T., & Ohno, T. (2016). Photoelectrochemical CO2 reduction by a p-type boron-doped g-C3N4 electrode under visible light. *Applied Catalysis B: Environmental,* 192, 193-198.

Sutter, P., Cortes, R., Lahiri, J., & Sutter, E. (2012). Interface formation in monolayer graphene-boron nitride heterostructures. *Nano Letters,* 12(9), 4869-4874.

Tang, Q., Zhou, Z., & Chen, Z. (2015). Innovation and discovery of graphene-like materials via density-functional theory computations. *Wiley Interdisciplinary Reviews: Computational Molecular Science,* 5(5), 360-379.

Wang, H., Tian, L., Huang, Z., Liang, F., Guan, K., Jia, Q., ... & Zhang, S. (2020). Molten salt synthesis of carbon-doped boron nitride nanosheets with enhanced adsorption performance. *Nanotechnology,* 31(50), 505606.

Wang, J., Hao, J., Liu, D., Qin, S., Chen, C., Yang, C., ... & Lei, W. (2017). Flower stamen-like porous boron carbon nitride nanoscrolls for water cleaning. Nanoscale, 9(28), 9787-9791.

Wei, X., Wang, M. S., Bando, Y., & Golberg, D. (2011). Electron-beam-induced substitutional carbon doping of boron nitride nanosheets, nanoribbons, and nanotubes. *ACS Nano*, 5(4), 2916-2922.

Xia, D., Li, H., Huang, P., Mannering, J., Zafar, U., Baker, D., & Menzel, R. (2019). Boron-nitride/carbon-nanotube hybrid aerogels as multifunctional desulfurisation agents. *Journal of Materials Chemistry A,* 7(41), 24027-24037.

Yadav, A., & Dindorkar, S. S. (2022). Vacancy defects in monolayer boron carbon nitride for enhanced adsorption of paraben compounds from aqueous stream: a quantum chemical study. *Surface Science*, 723, 122131.

Yan, S. C., Li, Z. S., & Zou, Z. G. (2010). Photodegradation of rhodamine B and methyl orange over boron-doped g-C_3N_4 under visible light irradiation. *Langmuir,* 26(6), 3894-3901.

CHAPTER 6

THE USAGE OF ACTIVATED CARBON IN SUPER CAPACITORS

Assist. Prof. Dr. Hacer DOLAS[1]

[1]Harran University, Hilvan Vocational School, Program of Occupational Health and Safety, Şanlıurfa, Türkiye, hacerdolas@harran.edu.tr , Orcid ID: 0000-0002-8030-8560

1.INTRODUCTION

Supercapacitors are energy conversion devices that combine batteries based on electrochemical redox processes with capacitors that store energy according to physical principles. It is a type of capacitor that has the energy and power density between capacitors and batteries. Supercapacitors have advantages over secondary batteries due to their long life (>100 000 cycles), simple operation, short charging times, safety, and high power densities that are approximately ten times better.

A capacitor stores energy in the form of static charge, as opposed to an electrochemical reaction. To charge a capacitor, it is sufficient to apply a voltage difference to the positive and negative plates. There are three types of capacitors. super capacitors show higher capacitance than electrolytic capacitors. The super capacitor stores energy through frequent charge and discharge cycles at high current and in a short time. While the basic Electrochemical Double Layer Capacitor (EDLC) relies on the electrostatic effect, the Asymmetric Electrochemical Double Layer Capacitor (AEDLC) uses battery-like electrodes to achieve higher energy density, but with a shorter cycle life. Graphene electrodes promise improvements in super capacitors and batteries.

Various types of electrodes have been tried, and today the most common systems are built on the electrochemical double-layer capacitor, which has a carbon-based, organic electrolyte and is easy to manufacture. These structures have some advantages and disadvantages due to electrostatic formation. These are given in Table 1.

Table 1. The advantages and disadvantages of double-layer capacitor.

Advantages	Disadvantages
✓ Virtually unlimited cycle life; can be cycled millions of time	✓ Low specific energy; holds a fraction of a regular battery
✓ High specific power; low resistance enables high load currents	✓ Linear discharge voltage prevents using the full energy spectrum
✓ Charges in seconds; no end-of-charge termination required	✓ High self-discharge; higher than most batteries
✓ Simple charging; draws only what it needs; not subject to overcharge	✓ Low cell voltage; requires series connections with voltage balancing
✓ Safe; forgiving if abused	✓ High cost per watt
✓ Excellent low-temperature charge and discharge performance	

Electrodes are very important parts for super capacitors. For this reason, the material to be used in making electrodes must be easily accessible, cheap and have a high surface area. Activated carbons (ACs) are an excellent candidate as an electrode material, especially because they have the above-mentioned properties (Wang et al., 2013).

Oil and coal were used as raw materials in AC production (Zhang et al., 2013). However, environmental pollution and limited availability of fossil fuels led researchers to use biomass waste as raw material in AC production (Voloshin et al., 2016). AC prepared from various biomass

such as Pistachio shell (Dolas et al., 2011), pine nut shell (Chen et al., 2016), pepper stems (Dolas et al., 2023), plum kernels (Juang et al., 2000), arundo donax cane (Vernersson et. al., 2002), saw-dust (Kaczala et al., 2009), cotton stalk (Chen et al., 2013), seed shell (Amuda et al., 2009), coconut shell (Sarswat et al. , 2016), waste coffee ground (Yun et al., 2015), olive seeds (Ajuria et al., 2017), oil-palm shells (Guo et al., 2003) etc. has been reported in the literature.

The presence of heteroatoms in the carbon network (nitrogen, oxygen) is a promising way to increase capacitance, as it increases the charge density of the entire structure (Ahmed et al., 2018)**.**

Besides pore formation, the presence of hetero atoms also helps to improve the performance of AC materials. Recently, the effect of nitrogen doping on the specific capacitance of AC materials has been studied (Frackowiak et al., 2007; Lee et al., 2006; Lota et al., 2005; Guo et al., 2009). It provides an increase in capacitance because functional groups containing hetero atoms cause a faradaic reaction and wettability of the entire surface. At the same time, heteroatom doping also increases the conductivity of porous carbon materials (Seredych et al., 2008; Raymundo-Piñero et al., 2009; Béguin et al., 2005; Jeong et al., 2011).

In each of these processes there is primarily AC generation. At the end of this stage, the produced ACs are mixed with organic binders to make electrodes and the electrochemical performance of these electrodes is examined in the triple electrode system.

2.PRODUCTION OF AC

The raw material recorded for AC is first washed thoroughly to remove external dirt. The ground material is kept in the chemical solution

selected as an activator for a certain period of time. It is then subjected to carbonization in the selected atmosphere (N_2/CO_2) at a certain temperature for a certain period of time (Dolas et al., 2022; Chen et al., 2011). The product is sieved in a certain sieve size and taken to electrode preparation as AC.

3. PREPARATION OF ELECTRODE

To make the electrode, a slurry is prepared by mixing a certain amount of AC produced and a certain proportion of organic binders such as acetylene black, PVDF (polyvinilidene fluoride) and polytetrafluoroethylene. This slurry is impregnated with conductive structures such as nickel foam and used as a working electrode. and electrical measurements are taken in the triple electrode system (Figure 1).

Fig. 1. The triple electrode system.

In this system, other electrodes used are auxiliary and reference electrodes.

4.CHARACTERIZATION OF ELECTRODE

The resulting electrode is analyzed structurally by Fourier Transform Infrared Spectroscopy (FTIR), morphologically by Scanning electron microscopy (SEM), energy dispersive spectroscopy (EDX), X-ray spectroscopy and its electrical behavior by Cyclic voltammetry (CV), galvanostatic charge-discharge (GCD) and electron impedance spectroscopy (EIS).

5.ELECTROCHEMICAL PERFORMANCE OF ELECTRODE

The electrochemical performances of the electrodes are measured by cyclic voltammetry (CV), galvanostatic charge-discharge (GCD) and electrochemical impedance spectroscopy (EIS). Current versus current density graphs against applied potential are CV graphs (Figure 2).
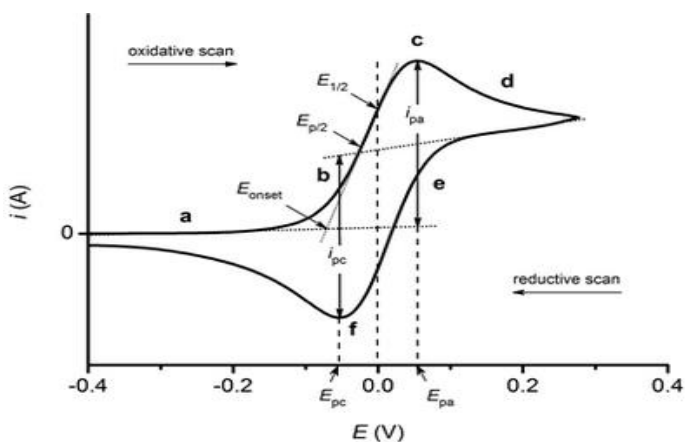
Fig. 2. A duck shape CV graph.

These measurements are conducted in an electrolyte solution at certain of scan rate and potential range. A general CV shape at a conductive electrode where oxidation and reduction reactions are observed is duck-shaped. On the other hand, the composition of a

material with high capacitiveness is similar. The triangle or rectangular shape of these graphs and the low or high current density give us information about the electrical reactivity. From CV graph The specific capacitance was calculated by using Eq. (1).

$$C_{sp} = \frac{\int i dV}{2.m.s.\Delta V} \tag{1}$$

here ∫idV is the integrated area of the CV curve, m (g) is the mass of AC, s is the scan rate (mV/s), and ΔV(V) is the potential value.

The EIS measurements are performed at certain of frequency range. Galvanostatic charge-discharge (GCD) measurements are performed at different current densities and specific capacitance was calculated using the below equation:

$$C_{sp} = \frac{i.\Delta t}{m.\Delta V} \tag{2}$$
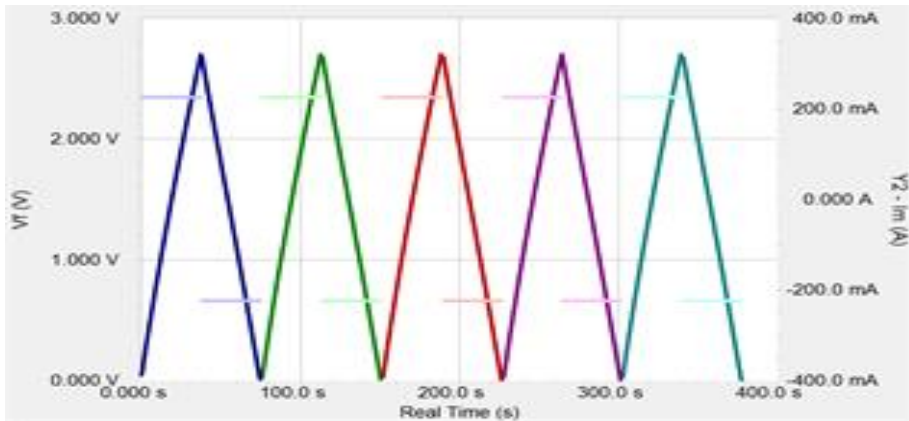
Fig. 3. GCD voltammogram

The electrochemical performance of the electrode prepared from activated carbons produced from agricultural wastes are examined in aqueous, organic and ionic liquid based electrolyte. For example, It was

found that the synthesized AC-based electrode from rotten carrot exhibited the highest specific capacitance (135.5 Fg^{-1} at 10mHz) and highest specific energy (29.1 $Whkg^{-1}$ at 2.2 Ag^{-1}) and specific power (142.5 $kWkg^{-1}$) in aqueous electrolyte in 2.2 Ag^{-1}in the ionic liquid-based electrolyte. This indicates the suitability of the synthesized material for use in energy storage applications (Pandey et al., 2023).

In another study, activated carbon (AC) was obtained from the waste material of peanut shells. Chemical activation was done with NaOH. Through Cyclic voltammetry and galvanostatic charge-discharge measurements taken with electrodes obtained from these ACs, it was observed that samples activated with 1:3 NaOH revealed the maximum specific capacitance value (263 F/g at 10 mV/s and 290 F/g at 0.2 A/g). The sample also achieves ~98% dominant efficiency from the 400th to the 1000th cycle with fast and nearly constant capacitance. As a result of electrochemical impedance spectroscopy (EIS), it was determined that the sample showed dominant electric double-layer capacitive (EDLC) behavior. The results obtained indicate that activated carbon derived from peanut shells is a potential candidate as electrode material for super capacitors (Pandey et al., 2023).

In study conducted by Bing et al., electrodes were obtained by adding nitrogen to activated carbons. The nitrogen content was 4 wt% and the surface area was 2900 m^2g^{-1}. In addition to excellent rate capability and cycling stability, the resulting electrodes exhibited a high specific capacity of 129 $mAhg^{-1}$ (185 Fg^{-1}) in an organic electrolyte at a current density of 0.4 Ag^{-1}. The hybrid type super capacitor assembled using NACs and Si/C electrode exhibited high material-level energy density of 230 $Whkg^{-1}$ at 1747 Wkg^{-1}. The hybrid device achieved 76.3% capacity retention after 8000 cycles tested at 1.6 Ag^{-1} (Li et al., 2016).

5.CONCLUSION

The electrodes of super capacitors can be made of AC material. It is also important that ACs have the desired surface area by changing the production conditions, as their electrochemical properties can be increased by adding heteroatoms or chemically incorporating them into the structure. For example, synthesized AC-based electrode from rotten carrot exhibited the highest specific capacitance (135.5 Fg^{-1} at 10mHz) and highest specific energy (29.1 $Whkg^{-1}$ at 2.2 Ag^{-1}) and specific power (142.5 $kWkg^{-1}$) in aqueous electrolyte in 2.2 Ag^{-1}in the ionic liquid-based electrolyte.

As a result of cyclic voltammetry and galvanostatic charge-discharge measurements made with electrodes obtained from ACs obtained from peanut shells, the maximum specific capacitance value (263 F/g at 10 mV/s and 290 F/g at 0.2 A/g) showed. The sample also achieved fast and nearly constant capacitance with ~98% dominant efficiency from the 400th cycle to the 1000th cycle.

Excellent rate capacity and cycling stability were achieved with another electrode with a nitrogen content of 4% by weight and a surface area of 2900 m^2g^{-1}. The hybrid type super capacitor assembled using NACs and Si/C electrode exhibited high material-level energy density of 230 $Whkg^{-1}$ at 1747 Wkg−1. The hybrid device achieved 76.3% capacity retention after 8000 cycles tested at 1.6 Ag^{-1}.

The results obtained indicate that activated carbon obtained from various shells is a potential candidate as electrode material for super capacitor. This indicates that the synthesized material is suitable for use in energy storage application and has high performance.

REFERENCES

Ahmed, S., Ahmed, A., & Rafat, M. (2018). Supercapacitor performance of activated carbon derived from rotten carrot in aqueous, organic and ionic liquid based electrolytes, *Journal of Saudi Chemical Society*, 22, 8, 993-1002.

Ajuria, J., Redondo, E., Arnaiz, M., Mysyk, R., Rojo, T., & Goikolea, E. (2017). Lithium and sodium ion capacitors with high energy and power densities based on carbons from recycled olive pits. *J. Power Sources*, 359, 17–26.

Amuda, O. S., Adelowo, F.E., & Ologunde, M.O. (2009). Kinetics and equilibrium studies of adsorption of chromium (VI) ion from industrial wastewater using chrysophyllum albidum (Sapotaceae) seed shells, colloids Surf. *B Biointerfaces*, 68, 184–192.

Béguin, F., Szostak, K., Lota, G., & Frackowiak, E. (2005). A self-supporting electrode for supercapacitors prepared by one-step pyrolysis of carbon nanotube/polyacrylonitrile blends. *Adv. Mater.,*17, 2380–2384.

Chen, D., Chen, X., Sun, J., Zheng, Z., & Fu, K. (2016). Pyrolysis polygeneration of pine nut shell: quality of pyrolysis products and study on the preparation of activated carbon from biochar. *Bioresour. Technol.,* 216, 629-636.

Chen, M., Kang, X., Wumaier, T., Dou, J., Gao, B., Han, Y., Xu, G., Liu, Z., & Zhang, L. (2013). Preparation of activated carbon from cotton stalk and its application in supercapacitor, *J. Solid State Electrochem.,* 17, 1005–1012.

Chen, Y., Zhang, X., Zhang, D., Yu, P. and Ma, Y. (2011). High performance supercapacitors based on reduced graphene oxide in aqueous and ionic liquid electrolytes. *Carbon,* 49, 573–580.

Dolas, H. (2022). Characterization of activated carbon produced from pistachio shell at different temperatures. *Bulgarian Chemical Communications,* 54, 3, 219-223. DOI: 10.34049/bcc.54.3.F001.

Dolas, H. (2023). Activated carbon synthesis and methylene blue adsorption from pepper stem using microwave assisted

impregnation method: Isotherm and kinetics. *Journal of King Saud University–Science,* 35, 102559.

Dolas, H., Sahin, O., Saka, C., & Demir, H. (2011). A new method on producing high surface area activated carbon: The effect of salt on the surface area and the pore size distribution of activated carbon prepared from pistachio shell. *Chemical Engineering Journal,* 166, 191–197.

Frackowiak, E. (2007). Carbon materials for supercapacitor application. *Phys. Chem. Chem. Phys.,* 9, 1774-1785.

Guo, H. & Gao, Q. (2009). Boron and nitrogen co-doped porous carbon and its enhanced properties as supercapacitor. *J. Power Sources,* 186, 551–556.

Guo, J., & Lua, A.C. (2003). Adsorption of sulphur dioxide onto activated carbon prepared from oil-palm shells with and without pre-impregnation. *Sep. Purif. Technol.,* 30, 265–273.

Jeong, H. M., Lee, J. W., Shin, W. H., Choi, Y. J., Shin, H. J., Kang, J. K., & Choi, J. W. (2011). Nitrogen-doped graphene for high-performance ultracapacitors and the importance of nitrogen-doped sites at basal planes. *Nano Lett.,* 11, 2472–2477.

Juang, R.S., Wu, F.C., & Tseng, R.L. (2000). Mechanism of adsorption of dyes and phenols from water using ACs prepared from plum kernels, *J. Colloid Interface Sci.,* 227,437–444.

Kaczala, F., Marques,M., & Hogland, W. (2009). Lead and vanadium removal from a real industrial wastewater by gravitational settling/sedimentation and sorption onto pinus sylvestris sawdust. *Bioresour. Technol.,* 100, 235-243.

Lee, J., Kim, J., & Hyeon, T. (2006). Recent progress in the synthesis of porous carbon materials. *Adv. Mater.,* 18, 2073–2094.

Li, B., Dai, F., Xiao, Q., Yang, L., Shen, J., Zhang, C., & Chai, M. (2016). Nitrogen-doped activated carbon for a high energy hybrid supercapacitor. *Energy Environ. Sci.,* 9, 102-106. DOI:10.1039/C5EE03149D.

Lota, G., Grzyb, B., Machnikowska, H., Machnikowski, J. & Frackowiak, E. (2005). Effect of nitrogen in carbon electrode on the supercapacitor performance. *Chem. Phys. Lett.,* 404, 53–58.

Pandey, L., Sarkar, S., Arya, A., Sharma, A. L., Panwar, A., Kotnala, R. K. & Gaur, A. (2023). Fabrication of activated carbon electrodes derived from peanut shell for high-performance supercapacitors. *Biomass Conversion and Biorefinery,* 13, 6737–6746.

Raymundo-Piñero, C. M. & Béguin, F. (2009). Tuning Carbon Materials for Supercapacitors by Direct Pyrolysis of Seaweeds. *Adv. Funct. Mater.,* 19, 1032–1039.

Sarswat, A., & Mohan, D. (2016). Sustainable development of coconut shell activated carbon (CSAC) & a magnetic coconut shell activated carbon (MCSAC) for phenol (2-nitrophenol) removal. *RSC Adv.,* 6, 85390–85410.

Seredych, M., Hulicova-Jurcakova, D., Lu, G. Q., & Bandosz, T. J. (2008). Surface functional groups of carbons and the effects of their chemical character, density and accessibility to ions on electrochemical performance. *Carbon,* 46, 1475- 1488.

Yun, Y.S., Park, M.H., Hong, S.J., Lee, M.E., Park, Y.W., & Jin, H.J. (2015). Hierarchically porous carbon nanosheets from waste coffee grounds for supercapacitors. *ACS Appl. Mater. Interfaces,*7, 3684–3690.

Vernersson, T., Bonelli, P.R., Cerrella, E.G., & Cukierman, A.L. (2002). Arundo donax cane as a precursor for activated carbons preparation by phosphoric acid activation. *Bioresour. Technol.,* 83, 95–104.

Voloshin, R.A., Rodionova, M.V., Zharmukhamedov, S.K., Veziroglu, T.N., & Allakhverdiev, S.I. (2016). Biofuel production from plant and algal biomass, *Int. J. Hydrogen Energy,* 41, 17257– 17273.

Wang, Y., & Xia, Y. (2013). Recent progress in supercapacitors: From materials design to system construction. *Adv. Mater.,* 25, 5336– 5342.

Zhang, L.L., Gu, Y., & Zhao, X.S. (2013). Advanced porous carbon electrodes for electrochemical capacitors*, J. Mater. Chem. A,* 1, 9395–9408.

CHAPTER 7

THE USAGE OF NANOPARTICLES AT ADSORPTION

Assist. Prof. Dr. Hacer DOLAS[1]

[1]Harran University, Hilvan Vocational School, Program of Occupational Health and Safety, Şanliurfa, Turkiye, hacerdolas@hotmail.com, hacerdolas@harran.edu.tr, Orcid ID: 0000-0002-8030-8560

1. INTRODUCTION

Adsorption, also known as adhesion, is a process in which molecules or ions of dissolved solids, liquids or gases are held on the surface by solids whose surface molecules are more active. Although this event is usually a physical event, it can sometimes occur chemically. There are many factors that affect adsorption. These; ambient temperature where adsorption takes place, solution pH, concentration of the adsorbent, physical and chemical properties of the adsorbent and the amount of adsorbent. For adsorption, which is a surface phenomenon, the surface properties of the adsorbent are of great importance. The higher the active surface of the adsorbent, the higher and more successful the adsorption.

Water is of vital importance to humanity. Lack of water or access to clean water resources will not only bring about the end of humanity, but will also bring about famine and various diseases. Water resources are polluted with various organic chemicals such as dirt, paint, inorganic and metallic chemicals due to various reasons such as increasing population, developments in industry and technology, urbanization, domestic and agricultural activities. In addition, releasing wastewater of such chemicals from cosmetics, pharmaceutical, textile, plastic and food factories into natural resources disrupts the ecological balance and causes pollution of water resources (Imran et al., 2006., Franklin et al., 1991; Droste, et al., 1997; John et al., 1990).

For these reasons, it is of great importance to remove these chemicals effectively and practically before they reach water resources or to convert them into less harmful products (Vererakumar et al., 2015). Coagulation/flocculation, ion exchange, flotation, membrane filtration,

chemical precipitation, electrochemical processing and adsorption are used to remove such toxic, harmful and dangerous chemicals from the environment (Femina et al., 2017). However, these methods are time-consuming, require more techniques and are expensive because the formation of other by-products is possible. At the same time, most of these methods are not useful because they are not practical to use (Demirbas et al., 2008). Over time, researchers have tended to develop simpler, practical, inexpensive and efficient methods. Adsorption is one of these methods. The method used to obtain adsorbents also plays an important role. The more abundant the raw material used to obtain adsorbents, the easier it is to access, and the higher the active surface area is obtained as a result of its processing, the more efficient adsorption is observed (Ewecharoen et al.,2009). For this purpose, carbonaceous materials such as lignin (Hayashi et al., 2000), coal and biomass were selected for active carbon production. For example, biomass such as Glebionis Coronaria L (Tounsadi et al., 2016; Liou et al., 2010) and biosorbents such as pistachio shell (Dolas et al., 2011), pepper stems (Dolas et al., 2023), plum kernels (Juang et al., 2000), arundo donax cane (Vernersson et al., 2002), oil-palm shells (Guo et al., 2003), saw-dust (Kaczala et al., 2009), seed shell (Amuda et al., 2009).

The fact that these materials are abundant in nature, cheap and have a carbonated cellulosic structure made them important as popular materials. However, to obtain activated carbon from these materials, various chemical and/or physical processes had to be applied. Since these processes involve methods such as activation in chemical solutions or carbonization at high temperatures, various toxicities may be possible (Sapana et al., 2021).

Recently, active substances containing nanoparticles have begun to be obtained by using plant extracts (Hassanien et al., 2018) that are more chemically and environmentally harmless. Since little or no chemicals are used during this process, it is called green synthesis. With this production technique, more effective and efficient applications have been made since the features are reduced to the nanoscale and the expected features in the nanostructure emerge (Duan et al., 2015). Parts of plants such as leaves, fruits, roots and seeds were used in nanoparticle synthesis because they contain reducing substances such as phytochemicals (Narayanan et al., 2011).

There are many different types of nanoparticles used in various fields. Antimicrobial activity (Sathishkumar et al., 2009) hence silver nanoparticles in the biological and pharmaceutical field magnolia Kabus (Lee et al.,2014), Capsicum annum (Li et al., 2007), cinamomum camphora (Huang et al., 2008), zea mays (Rajkumar et al., 2019) were synthesized by the green synthesis method.

Gold nanoparticles have been used in cancer treatment, especially for the destruction of cancer cells. Gold nanoparticles are of great importance in the pharmaceutical industry. It can be used as a biomarker for biological monitoring tests. It was found that the material prepared from the extract of Nerium oleander leaves with gold nanoparticles showed good antioxidant properties (Tahir et al., 2015). It was demonstrated that gold nanoparticles obtained from gymnocladus assamicus extract showed great catalytic activity in the reduction of 4 nitrophenols to 4 aminophenols (Tamuly et al., 2013). Gold nanoparticles from the extract of Sesbania grandiflora plant showed high catalytic performance in the reduction of methylene blue dye (Das et al.,

2014). The use of plant extracts in the removal of heavy metals from aqueous solutions has become increasingly important due to their environmental friendliness and good performance in removing dirt, dye, and toxic substances from waste (Femina et al., 2017). Also, Nanoparticles were especially used to remove various drugs and pharmaceuticals from aqueous media (Husein et al., 2019). In the study, Cu nanoparticle adsorbent was obtained from the aqueous extract of Tillia plant and the treatment of wastewater contaminated with pharmaceuticals such as ibuprofen, naproxen and diclofenac was examined. The best results were obtained at 298 K, pH 4.5, 10 mg Cu-NPs and 60 minutes. A removal success of 91.4% was achieved for Diclofenac, 86.9% for Naproxen and 74.4% for Ibuprofen. Another study conducted with nanoparticles in another adsorption field is copper oxide loaded activated carbon nanocomposite (Farooq et al., 2022). In the study, nanocomposite was obtained by loading CuO nanoparticles with activated carbon produced from Prosopis juliflora (Mesquite) pods using the Green Synthesis method. This nanocomposite was used in methylene blue adsorption. With this adsorbent, a removal of more than 97% was achieved with 0.1 g of adsorbent in 15 minutes at a concentration of 10 mg/L at 313 K in a neutral medium. It was found that methylene blue (MB) adsorption occurred as a monolayer and the adsorption capacity was 54.73 mg/g at 313 K. It was determined that MB adsorption was endothermic under the experimental conditions studied.

In another study prepared with iron nanoparticles, the adsorption of Eriochrome Black T, a toxic textile azo-dye, was carried out with magnetic graphene oxide nanocomposite prepared using iron oxide (Fe_2O_3) and graphene oxide (Khurana et al., 2018). In this study, the

adsorbent was obtained by mixing a certain amount of iron oxide and graphene oxide in methanol medium and keeping it at 60 ^{o}C for 10 hours and then treating it with hydrazine. This adsorbent showed higher adsorption capacity than other graphene oxide type adsorbents with a value of 210.53 mg/g. Adsorption followed the Langmuir adsorption isotherm. Therefore, it could be said that it was an adsorbent with a homogeneous surface. Therefore, monolayer adsorption was observed. With thermodynamic studies, it was determined that it was an exothermic and spontaneous process.

In green synthesis, plant extracts are obtained from certain parts of the plant by boiling. These parts are first washed to remove all dirt and boiled with distilled water. After filtration, the salt of the desired nanoparticle is added to the filtrate and mixed thoroughly. Evidence indicating nanoparticle formation is the color change during mixing. Meanwhile, metal ions are reduced by the functional groups of phytochemicals found in the structure of the plant. and nanoparticle formation is thus completed. We can separate the resulting nanoparticle.

The aim of this study is to review the use and benefits of adsorbents containing various nanoparticles obtained by green synthesis in adsorption. Information about adsorption theory was also given within the scope of the topics.

1. ADSORPTION EXPERIMENTS

The adsorption process is based on adding a certain amount of adsorbent to a solution containing a certain concentration of adsorbent at a certain temperature, at a certain pH value, and determining the

adsorbent remaining in the environment at certain time intervals in a constantly shaking situation, using appropriate methods.

After the concentration of the adsorbent remaining in the environment is determined by the appropriate method, the adsorbed amount can be obtained by subtracting it from the initial concentration value. The equation used in this calculation is given below.

$$q_e = \frac{(C_0 - C_t)V}{m} \tag{1}$$

Here, qe is the amount of substance in equilibrium (mg/g), C_0 is the initial concentration of naproxen (mg/L), and C_t is the equilibrium concentration of naproxen in solution (mg/L) at time t of adsorption. V represents the adsorption solution volume in mL and m represents the amount of adsorbent used in mg.

2. ADSORPTION THEORY

2.1. Adsorption Isotherms

Isotherms and kinetics are used when characterizing the adsorption process. Isotherms explain the adsorption between the adsorbent surface and the dyestuff by establishing a relationship between the amount adsorbed and the equilibrium concentration at certain time intervals at constant temperature during adsorption. Major isotherms used in adsorption; Freundlich (Freundlich et al., 1907) and Langmuir (Langmuir et al., 1918). An adsorbent that shows an adsorption phenomenon that complies with the Langmuir isotherm is said to show monolayer adsorption and therefore has a homogeneous surface in terms of activity.

The equation used is given below.

$$\frac{C_e}{q_e} = \frac{1}{q_L K_L} + \frac{1}{q_L} C_e \qquad (2)$$

Here, C_e expresses the equilibrium concentration (mg/L) as q_e (mg/g) adsorption capacity and K_L as adsorption energy constant (L/mg). In addition, R_L, which is the equilibrium parameter depending on the initial concentration (C_o) and K_L value, which expresses the applicability of isotherm. It was expressed by the following equation.

$$R_L = \frac{1}{1+(K_L C_o)} \qquad (3)$$

It gives information in the sense that the applied isotherm and adsorption conditions are unfavorable if the R_L value is greater than 1, linear if it is equal to 1, favorable if it is between 1 and 0, and irreversible if it is equal to 0 (Lakkaboyana et al., 2017).

On the other hand, if the surface is heterogeneous, that is, if it exhibits a regional behavior in terms of the active surface, then several layers of adsorption can be observed, unlike single layer adsorption. In this case, a Freundlich isotherm is mentioned for a surface and the behavior obeys this isotherm. The equation representing the isotherm is as given below.

$$q_e = K_F C_e^{1/n} \qquad (4)$$

and

It is graphed by taking its logarithm and the interpretation is made on this graph.

$$log q_e = \log K_F + \frac{1}{n} \log C_e \qquad (5)$$

This equation gives the amount of equilibrium substance (q_e, mg/g) adsorbed on the adsorbent surface used in adsorption and given its mass. Ce (mg/g) depends on the equilibrium concentration and from the graph drawn by taking the logarithm, the Freundlich constant (K_F) expressing the adsorption capacity and the data expressing the degree of adsorption efficiency (n) are obtained.

2.2. Adsorption Kinetics

In order to better understand the mechanism that the molecules follow during mass transfer to the adsorbent surface through adsorption, their kinetics were examined using various adsorption models. And the Lagergren (Lagergren et al., 1898) approximation for pseudo first order in calculations,

$$\log(q_e - q_t) = log q_e - \left(\frac{K_t}{2,303}\right) t \tag{6}$$

Ho-McKay (Ho et al., 1999) approach for pseudo second order,

$$\frac{t}{q_t} = \frac{1}{k_2 q_e^2} + \frac{1}{q_e} t \tag{7}$$

Weber-Moris (Weber et al., 1963) approach for intraparticle diffusion mechanism,

$$q_t = C + K_{int} t^{1/2} \tag{8}$$

After each equation is plotted, it is interpreted that the closer the R^2 value of the slope is to 1, the adsorption progresses according to the appropriate kinetics.

Thermodynamic data is determined by the following equation, depending on the change in enthalpy (ΔH) and entropy (ΔS) Gibbs free energy (ΔG).

$$\Delta G = \Delta H - T\Delta S \tag{9}$$

$$\Delta G = -RT \ln K_c, \tag{10}$$

$$\ln K_c = -\frac{\Delta G}{RT} = -\left(\frac{\Delta H}{RT}\right) + \frac{\Delta S}{R} \tag{11}$$

$$Kc = \frac{C_t}{C_e} \tag{12}$$

K_c represents to the ratio of a adsorbed matter concentration in the medium to the equilibrium concentration. When the equation, also known as the Van't Hoff equation, is plotted for 11 different temperatures, enthalpy and entropy changes are obtained from the slope and cut of the equation. From here, the Gibbs free energy is calculated.

3. CONCLUSION

Pollution of clean water resources as a result of developments is an inevitable consequence. The important thing is to minimize this pollution and not create pollution again by using effective, cheap and practical methods. While adsorption is the most effective method applied in this regard, nanoparticle structures, which have been at the attention of researchers in the last few years, appear as a more effective, cheap and practical method to obtain adsorbents. Since they serve as active sites for the adsorbent, they also help increase adsorption. It is hoped that obtaining nanoparticle structures through green synthesis will be very popular in the future as it will be cleaner, safer and contribute more to waste management.

REFERENCES

Amuda, O.S., Adelowo, F.E. & Ologunde, M.O. (2009). Kinetics and equilibrium studies of adsorption of chromium(VI) ion from industrial wastewater using Chrysophyllum albidum (Sapotaceae) seed shells. *Colloids Surf. B Biointerfaces,* 68, 184–192.

Das, J. & Velusamy, P. (2014). Catalytic reduction of methylene blue using biogenic gold nanoparticles from Sesbania grandiflora L. *J Taiwan Inst Chem Eng.,*

Demirbas, A. (2008). Heavy metal adsorption onto agro-based waste materials: a review, *J. Hazard. Mater.,* 157, 220–229.

Dolas, H., Sahin, O., Saka, C. & Demir, H. (2011). A new method on producing high surface area activated carbon: The effect of salt on the surface area and the pore size distribution of activated carbon prepared from pistachio shell. *Chemical Engineering Journal,* 166, 191–197.

Dolas, H. (2023). Activated carbon synthesis and methylene blue adsorption from pepper stem using microwave assisted impregnation method: Isotherm and kinetics. *Journal of King Saud University – Science,* 35, 102559.

Droste, R.L. (1997). Theory and practice of water and wastewater treatment. *John Wiley & Sons, New York.*

Duan, H., Wang, D., & Li, Y. (2015). Green chemistry for nanoparticle synthesis. *Chem Soc Rev,* 44, 5778–5792.

Ewecharoen, A., Thiravetyan P., Wendel E. & Bertagnolli H. (2009). Nickel adsorption by sodium polyacrylate-grafted activated carbon. *J. Hazard. Mater.* 171, 335–339.

Femina Carolina, C., Senthil Kumara, P., Saravanana, A., Joshibaa, G. J. & Naushad, Mu. (2017). Efficient techniques for the removal of toxic heavy metals from aquatic environment: A review. *Journal of Environmental Chemical Engineering,* 5, 2782–2799.

Franklin, L.B. (1991). Wastewater engineering: Treatment, disposal and reuse. *McGraw Hill, New York.*

Guo, J. & Lua, A.C. (2003). Adsorption of sulphur dioxide onto activated carbon prepared from oil-palm shells with and without pre-impregnation. *Sep. Purif. Technol.,* 30, 265–273.

Farooq, S., Al Maani, A. H., Naureen Z., Hussain J., Siddiqa A. & Al Harrasi, A. (2022). Synthesis and characterization of copper oxide-loaded activated carbon nanocomposite: Adsorption, of methylene blue, kinetic, isotherm and thermodynamic study. *Journal of Water Process Engineering,* 47, 102692.

Freundlich, H. (1907). About adsorption in solutions. J. *Phys. Chem.,* 57(1), 385-470.

Hassanien, R., Dalal, Z.H. & Al-Hakkani, M. F. (2018). Biosynthesis of copper nanoparticles using aqueous Tilia extract: Antimicrobial and anticancer activities *Heliyon,* 4, 01077.

Hayashi, J.,Kazehaya, A.,Muroyama, K. & Watkinson, A.P. (2000). Preparation of activated carbon from lignin by chemical the maximum specific surface areas, *Carbon*, 38, 1873–1878.

Ho, Y.S., & McKay, G. (1999). Pseudo-second order model for sorption processes. *Process Biochem.*, 34, 451-465.

Huang, J., Lin, L. & Li, Q. (2008). Continuous-flow biosynthesis of silver nanoparticles by lixivium of sundried Cinnamomum

camphora leaf in tubular microreactors. *Ind Eng Res.,* 47, 6081–6090.

Husein, D.Z., Hassanien, R. & Al-Hakkani, M. F. (2019). Green-synthesized copper nano-adsorbent for the removal of pharmaceutical pollutants from real wastewater samples. *Heliyon,* 5, e02339. doi:10.1016/j.heliyon.2019.e02339.

Imran, A. & Gupta, V. K., (2006). Advances in water treatment by adsorption technology. *Nature Protocols*, 1(6), 2661, doi:10.1038/nprot.2006.370.

John, D.Z. (1990). Handbook of drinking water quality: Standards and controls. *Van Nostrand Reinhold, New York*.

Juang, R.S.,Wu, F.C. & Tseng, R.L. (2000). Mechanism of adsorption of dyes and phenols from water using ACS prepared from plum kernels. *J. Colloid Interface Sci*., 227, 437– 444.

Kaczala, F.,Marques, M. & Hogland, W. (2009). Lead and vanadium removal from a real industrial wastewater by gravitational settling/sedimentation and sorption onto Pinus sylvestris sawdust. *Bioresour. Technol.,* 100, 235–243.

Khurana, I.,Shaw A. K., Bharti, Jitender, Khurana, M. & Kumar R. P. (2018). Batch and dynamic adsorption of eriochrome black T from water on magnetic graphene oxide: Experimental and theoretical studies. *Journal of Environmental Chemical Engineering,* 6, 468-477.

Lagergren, S. (1898). About the theory of so-called adsorption of soluble substances. *K. Sven. Vetenskapsakad. Handl.*, 24, 1-39.

Lakkaboyana, S.K., Khantong, S., Asmel, N.K., Yuzir, A. & Wan Yaacob, W.Z. (2019). Synthesis of copper oxide nanowires-

activated carbon (AC@CuO-NWs) and applied for removal methylene from aqueous solution kinetics, isotherms, and thermodynamics. *J. Inorg. Organomet. Polym. Mater.*

Langmuir, I.(1918). The adsorption of gases on plane surfaces of glass, mica and platinum. *J. Am. Chem. Soc.,* 40, 1361-1368.

Lee, SH., Salunke, BK. & Kim, BS. (2014). Sucrose density gradient centrifugation separation of gold and silver nanoparticles synthesized using Magnolia kobus plant leaf extracts. *Biotechnol Bioprocess Eng.,* 19, 169–174.

Li, S., Shen, Y. & Xie, A. (2007). Green synthesis of silver nanoparticles using capsicum annuum L. extract. *Green Chem.,* 9, 852–858.

Liou, T.-H. (2010). Development of mesoporous structure and high adsorption capacity of biomass-based activated carbon by phosphoric acid and $ZnCl_2$ activation, *Chem. Eng. Journal*., 158, 129–142.

Narayanan, K.B. & Sakthivel, N. (2011). Green synthesis of biogenic metal nanoparticles by terrestrial and aquatic phototrophic and heterotrophic eukaryotes and biocompatible agents. *Adv. Colloid Interface Sci.,* 169, 59–79.

Rajkumar, T.,Sapi, A. & Das, G. (2019). Biosynthesis of silver nanoparticle using extract of Zea mays (corn flour) and investigation of its cytotoxicity effect and radical scavenging potential. *J Photochem Silver nanoparticles from plants such as Photobiol B Biol,* 193, 1–7.

Sapana, J., Rizwan, A.,Kumari, J.N. & Kumar M.R. (2021). Green synthesis of nanoparticles using plant extracts: a review. *Environmental Chemistry Letters,* 19, 355–374.

Sathishkumar, M., Sneha, K. & Won, S.W. (2009). Cinnamon zeylanicum bark extract and powder mediated green synthesis of nano-crystalline silver particles and its bactericidal activity. *Colloids Surfaces B Biointerfaces.*

Tahir, K., Nazir, S. & Li, B. (2015). Nerium oleander leaves extract mediated synthesis of gold nanoparticles and its antioxidant activity. *Mater Lett.* 156,198-201.

Tamuly, C., Hazarika, M. & Bordoloi, M. (2013). Biosynthesis of Au nanoparticles by Gymnocladus assamicus and its catalytic activity. *Mater Lett.* 108(1), 276-279.

Tounsadi H., Khalidi A., Machrouhi A., Farnane M., Elmoubarki R., Elhalil A., Sadiq M. & Barka, N. (2016). Highly efficient activated carbon from Glebionis coronaria L. biomass: Optimization of preparation conditions and heavy metals removal using experimental design approach. *J. Environ. Chem. Eng.* 4, 4549 - 4564.

Vererakumar, P.,Chen, S.M.,Madhu, R.,Veeramani, V.,Hung, C.T. & Liu, S.B. (2015). Nickel nanoparticle-decorated porous carbons for highly active catalytic reduction of organic dyes and sensitive detection of Hg(II) ions. *ACS Appl. Mater. Interfaces,* 7, 24810-24821.

Vernersson, T., Bonelli, P.R., Cerrella, E.G. & Cukierman, A.L. (2002). Arundo donax cane as a precursor for activated carbons preparation by phosphoric acid activation. *Bioresour. Technol.,* 83, 95-104.

Weber Jr, W. J. & Morris, J.C. (1963). Kinetics of adsorption on carbon from solution. *J. San. Eng. Div. Am. Soc. Civil Eng.,* 89, 31-58.5.

CHAPTER 8

EPOXY RESINS AND TOUGHENING METHODS OF EPOXY RESINS

Dr. Barış KURT[1],

Dr. Murat EVCİL[2*],

Assoc. Prof. Dr. Mehmet Fırat BARAN[3]

[1]Muş Alparslan University, Department of Chemistry, Faculty of Science and Literature, Muş, Türkiye, bariskurt007@gmail.com, Orcid ID: 0000-0002-1406-0915
[2*]Dicle University, Department of Chemistry, Science Faculty, Diyarbakır, Türkiye, muratevc@gmail.com, Orcid ID: 0000-0002-4646-8042
[3]Batman University, Food Technology Programme, Batman, Türkiye, mehmetfirat.baran@batman.edu.tr, Orcid ID: 0000-0001-8133-6670

ABBREVIATIONS

ALR	Acrylate Liquid Rubber
ATBN	Amine-Terminated Butadiene Acrylonitrile
BCPs	Block Copolymers
CSP	Core-Shell Polymers
CSR	Core-Shell Rubber
CTBN	Carboxyl-Terminated Poly(Butadiene-Co-Acrylonitrile)
CTPB	Carboxyl-Terminated Polybutadiene
EPE80	poly(ethylene glycol)-b-poly(propylene glycol)-b-poly(ethylene glycol)
EPs	Epoxy Resins
ETBN	Epoxy-Terminated Butadiene Nitrile Rubber
GIC	Critical Strain Energy Release Rate
GPG	Poly(Glycidyl Methacrylate)-B-Poly(Propylene Glycol)-B-Poly(Glycidyl Methacrylate)
HTBN	Hydroxyl-Terminated Butadiene Acrylonitrile Copolymer
KIC	Fracture Toughness
LCPs	Liquid Crystal Polymers
LCPSi	Liquid Crystal Hyperbranched Polysiloxane
LCTS	Liquid Crystal Thermosetting Polymers
PBA	Poly (Butyl Acrylate)
PEEKMOH	Hydroxyl Terminated Poly(Ether Ether Ketone) Oligomers Based On Methyl Hydroquinone
PEO	Poly (Ethylene-Oxide)
PEP	Poly (Ethylene-Alt Propylene)
PES	Polyethersulfone
PI	Polyisoprene
PMMA	Poly(Methyl Methacrylate)
PSO	Polysiloxane
PU	Polyurethane
PU2	Polyurea-2
RAFT	Reversible Addition-Fragmentation Chain Transfer
SLR	Stereolithography Resin
Tg	Glass Transition Temperature
TPs	Thermoplastics

1.INTRODUCTION

Epoxy resins (EPs) stand at the forefront as the preeminent thermosetting materials, owing to their inherent stability, both mechanically and chemically, coupled with resistance attributes to heat, corrosion, and electrical challenges (Zhao et al., 2022; Sukanto et al., 2021; Kim et al., 2018; Chen et al., 2020). Their distinct chemical make-up has rendered them indispensable in sectors ranging from construction and transportation to aerospace and electronics. The burgeoning automotive industry worldwide has witnessed a significant surge in demand due to epoxy-matrix composites, which underpin numerous industrial applications. While China leads in consumption with 51%, consumption in the West remains notably limited. Alongside regions such as the United States, Western Europe, South Korea and the West has conspicuously consumed less epoxy resin (Seo et al., 2019; Qiu et al., 2019). Historical data reveals intriguing insights. For instance, the period from 1950 to 1973 saw the genesis of EP toughening via the introduction of rubbers and thermoplastics. The subsequent decades witnessed a proliferation of methodologies, from block copolymers to bio-based materials. A noteworthy revelation from 1998 to 2009 was the induction of hyperbranched polymers as a viable toughening method for EPs. Such a trend suggests that second-phase toughening has garnered immense interest in the research realm recently (Merz et al., 1956). In fact, as of 2019, the world saw a production surge, with the global EPs capacity soaring to 4.69 million tons. This trajectory is likely to persist, underpinned by the expanding horizons of end-use industries like aerospace, marine coatings, and more (Chenthamara et al., 2019; Intelligence, 2023).

As seen above, the identification of the toughening methods of epoxies has dramatically increased their areas of application. Now, one must ask: What drives these toughening methods? It's the symbiotic or individual action of various toughening mechanisms. Tracing back to the 1950s, the inception of such mechanisms took root, and ever since, the landscape has evolved, embracing mechanisms based on blends, organic particles, and inorganic compounds (Merz et al., 1956; Peng et al., 2022).

One of the Achilles' heels of these resins is their susceptibility to cracks, a setback predominantly rooted in their highly cross-linked structure. The solution? Researchers are exploring a variety of uniform and diverse methods to enhance the durability of EPs. By introducing a secondary phase into the epoxy matrix, the toughness of cured EPs can be significantly bolstered (Parameswaranpillai et al., 2017). Such groundbreaking work has birthed myriad toughening methods for EPs, encompassing everything from rubbers and nanomaterials to topological structures and bio-based materials (Mi et al., 2022; X.-F. Liu et al., 2022).

In the modern context, the research on EP toughening has hit unprecedented milestones. Two metrics, impact toughness and fracture toughness, have emerged as the yardsticks to gauge the toughness of these composites. Such parameters aid in discerning the ability of these materials to absorb energy during a fracture or prevent crack progression (Kishi et al., 2011; KIM et al., 1992).

Conclusively, the enhancement of EP toughness remains a domain of vast potential and unending exploration. Whether through the lens of

heterogeneous toughening methods, or through the lens of homogeneous strategies, the goal remains crystal clear: crafting resilient, high-performance epoxy resins to support the ever-evolving demands of modern industries (Zerda & Lesser, 2002; Su et al., 2023).

Certainly, here is a concise summary of the provided sections:

2.1. Rubbers in Epoxy Toughening

Rubbers have been traditionally used to toughen epoxies. There are two categories for rubber toughening (Mi et al., 2022):

1. Reactive Liquid Rubbers

Reactive liquid rubbers, such as CTBN, HTBN, and ATBN, dissolve in epoxy. As the epoxy solidifies, phase separation occurs creating a secondary phase.

Various other rubber structures have been developed, like ALR, CTPB, and ETBN, each having unique effects on the toughness of cured materials (Kamar & Drzal, 2016; Zhou et al., 2019).

2.Rubber Particles

The introduction of rubber enhances impact strength but may reduce flexural strength, tensile strength with flexural modulus of the resulting composite. In particular, excessive CTPB content can reduce these material properties due to particle agglomeration and associated defects. CSR particles are another method to toughen epoxies (Quan et al., 2017).

The balance between toughness and strength is crucial, with considerations on interface with the matrix, rubber content and size (Mi et al., 2022).

2.2. Thermoplastics in Epoxy Toughening

Thermoplastics (TPs) are another phase introduced into epoxies to improve toughness, offering potential advantages over rubbers. Incorporating TPs can enhance resilience while still maintaining their structural rigidity and thermal stability. Examples of TPs used for toughening include polyurethane (PU), polyethersulfone (PES), polysiloxane (PSO), and others.

Specific findings include:

- PU2 enhances tensile strength,
- Young's modulus,
- Fracture energy release

Incorporating polyethersulfone (PES) into epoxy resin can enhance its resistance to stretching, its ability to elongate before breaking, and its capacity to withstand impacts.

Epoxy-based composites have increased fracture toughness when modified with PB or PC. The epoxy/PEEKMOH system shows a significant improvement in fracture toughness depending on the content of PEEKMOH8 (Li et al., 2018). Incorporating polyamide (PA) can boost fracture toughness. TPs can increase the fracture toughness of epoxies in comparison to rubbers without significantly influencing other mechanical properties. The objective when using TPs is to reach a morphology that is both interlinked and inverted in phase for optimal enhancements in toughness. Maintaining thermal stability and solubility in uncured epoxy resin is crucial for TPs. The curing process results in a structure with multiple phases. It's vital to ensure thorough curing to circumvent vulnerabilities from lingering active groups. TPs have shown greater efficacy in enhancing the toughness of extensively

networked materials, and raising the molecular weight of the thermoplastic can augment this toughness, though ease of processing may pose challenges.

2.3. Core-Shell Polymers in Toughening Epoxy Resins

CSPs represent distinct outcomes arising from the polymerization process in emulsions initiated by various monomers. These particles are distinct because of their ability to possess double or multi-layer structures by controlling the composition of their inner and outer components. A characteristic feature of CSPs is their size - they are submicron, often even nanosized. These particles generally consist of a soft core and a rigid shell. This combination leads to an enhancement in the toughness of epoxy resins due to the rubber core, while the plastic shell ensures compatibility with the epoxy polymers (EPs). The shell is frequently made up of poly(methyl methacrylate) (PMMA), while the core comprises various materials including butadiene, acrylates, polyurethanes, and siloxane.

CSPs play a pivotal role in determining the mechanical properties of epoxy matrices. An illustrative experiment using aqueous emulsion polymerization produced five distinct (co)polymers. The study found that core/shell nanoparticles were superior in toughening effect compared to homopolymers and copolymers. The optimal toughening was achieved with a nanoparticle having a polar PMMA shell and a soft PBA core. These findings suggest that the proper choice of core and shell can have significant implications on the properties of the resulting composite.

Further advancements in this field have been achieved by functionalizing CSR particles to enhance compatibility with the matrix and improve the toughening effect. For instance, CSPs with epoxy groups have been utilized to enhance the toughness of SLR in 3D printing applications. Another novel method involved creating reactive core–shell particles using RAFT microemulsion polymerization. These particles exhibited a remarkable toughening effect on EPs (Li et al., 2018).

However, the actual toughening magic happens when the CSPs have a soft rubber shell and a rigid core. The thickness of this rubber shell, known as Ts, has a profound effect on the mechanical properties of the resulting composite. A transition threshold, called Tsbd, denotes a shift from brittle to ductile behavior. However, there's a limitation to increasing Ts, as this can potentially compromise the composite's modulus and strength (Declet-Perez et al., 2015).

Despite the evident advantages and versatility of CSPs as tougheners, challenges persist in commercializing them. High production costs and intricate manufacturing processes pose significant barriers to their widespread adoption.

2.4. Liquid Crystal Polymers in Toughening Epoxy Resins

Liquid crystal polymers (LCPs) have emerged as a reliable material for toughening EPs. Thermotropic LCPs, with their rigid mesocrystalline elements and flexible intervals, bring a combination of high strength, modulus, and self-enhancement to the table. They offer dual means to toughen EPs. The first involves blending liquid crystal copolymers or curing agents with EPs, embedding the ordered structure

of the polymer into the EPs network during the curing process. The second strategy entails synthesizing liquid crystal epoxy resins directly.

Amino end-capped aromatic LCP has been shown to increase the impact strength of EPs. Similarly, Liquid crystalline elastomers (LCEs) have proven their worth as ideal tougheners. The combination of the entropy elasticity of elastomers and the self-organization of rigid interfaces brings significant benefits.

However, there are challenges. Notably, LCPs tend to have difficulties mixing with epoxy resins due to their narrow or excessive phase transition temperature range. There is a constant push in research to develop LCPs with a broad transition temperature range. Liquid crystal hyperbranched polysiloxane (LCPSi) is a recent breakthrough in this direction. The advantage of LC thermosetting polymers (LCTs) is their potential to deliver desired properties in various directions. The orientation of LC domains and the plastic deformation within these domains contribute to improved strength and elongation. This orientation can be gauged by the alignment of LC polydomains.

In summary, while thermotropic LCPs offer excellent potential as tougheners, they present challenges. They are hard to disperse evenly in matrices, are expensive, and involve complex molding processes. However, the prospects of improving compatibility with EPs, streamlining the production process, and reducing costs make the pursuit of LCPs in this context worthwhile.

3. BLOCK COPOLYMERS AND EPOXY TOUGHENING

Epoxy resins, pivotal in industries ranging from aerospace to electronics, are frequently in search of advancements that improve their

toughness. One route to achieving this goal is via the inclusion of block copolymers (BCPs).

3.1. BCP Morphologies and Integration into Epoxy Resins

BCPs are unique in that their molecular structures allow for the creation of various phase morphologies at the nanoscale, such as spherical, rod-shaped, and lamellar structures. There are two primary types of BCPs used in epoxy resins for toughening purposes: non-reactive and reactive.

3.1.1. Non-reactive BCPs

These BCPs develop nanostructures via intrinsic organization or due to phase differentiation triggered by reactions. (Vijayan P. et al., 2017; George et al., 2013). This results in structures like spherical micelles and bilayer vesicles, each producing different toughening effects. An example of this would be the non-reactive EPE80. Its inclusion in epoxy resins saw a significant increase in tensile strength and elongation at break (J. (Daniel) Liu et al., 2010). However, there were trade-offs, as Young's modulus and Tg (glass transition temperature) showed a decrease.

3.1.2. Enhancing epoxy resin mechanical properties through reactive BCPs: The role of covalent bonding and GPG variants

They can react or crosslink with epoxy resin. The significant advantage here is that these copolymers can form covalent bonds with the epoxy resins, ensuring maximal fracture toughness. An exemplary reactive BCP is the GPG. When incorporated into epoxy resins, it resulted in the enhancement of various mechanical properties without

compromising the Young's modulus. Another version of GPG with short reactive blocks (Lreactive) showed even better improvements in mechanical properties.

3.2. Nanostructural Influence on Epoxy Resin Toughening: Insights from Block Copolymers Morphologies

The creation of suitable nanostructures within these blends is pivotal to achieving the desired toughening. Studies on epoxy resins combined with PEO-PEP and PEO-PI BCPs have provided valuable insights. Results have shown that vesicle morphology displays superior toughening effects compared to spherical morphology. Interestingly, the G_{IC} (critical strain energy release rate) isn't significantly dependent on the micelle's radius in spherical morphologies. However, the vesicle morphology greatly impacts G_{IC}, with substantial improvements observed with specific block copolymers.

Further investigations have shown that wormlike micelles provide more toughness to epoxy resins than their spherical counterparts. The inclusion of just a small amount of PEP-PEO block copolymer wormlike micelles resulted in commendable improvements in tensile strength and K_{IC} (fracture toughness). The mechanisms contributing to this toughening include debonding, crack tip blunting, limited shear yielding, crack bridging and cavitation

3.3. Advancements in BCPs for Epoxy Toughening

A fascinating approach in epoxy resin toughening is the use of BCPs that have one block miscible with epoxy and another that isn't. These types of BCPs offer the possibility of microphase separation, creating ordered or disordered microstructures before the curing

process. This eliminates the need to rely solely on cure kinetics to induce a two-phase morphology. By manipulating the composition and architecture of BCPs, various morphologies can be produced, leading to significant improvements in toughness.

In essence, the incorporation of BCPs into epoxy resins holds the promise of delivering tougher epoxy resins, which could be revolutionary for many industries. By understanding and manipulating the nanostructures formed by these copolymers, it's possible to design epoxies with tailored properties to meet specific demands.

REFERENCES

Chen, B., Wu, Q., Li, J., Lin, K., Chen, D., Zhou, C., Wu, T., Luo, X., & Liu, Y. (2020). A novel and green method to synthesize a epoxidized biomass eucommia gum as the nanofiller in the epoxy composite coating with excellent anticorrosive performance. *Chemical Engineering Journal*, *379*, 122323. https://doi.org/10.1016/j.cej.2019.122323

Chenthamara, D., Subramaniam, S., Ramakrishnan, S. G., Krishnaswamy, S., Essa, M. M., Lin, F.-H., & Qoronfleh, M. W. (2019). Therapeutic efficacy of nanoparticles and routes of administration. *Biomaterials Research*, *23*(1),20. https://doi.org/10.1186/s40824-019-0166-x

Declet-Perez, C., Francis, L. F., & Bates, F. S. (2015). Deformation Processes in Block Copolymer Toughened Epoxies. *Macromolecules*, *48*(11), 3672–3684. https://doi.org/10.1021/acs.macromol.5b00243

George, S. M., Puglia, D., Kenny, J. M., Causin, V., Parameswaranpillai, J., & Thomas, S. (2013). Morphological and Mechanical Characterization of Nanostructured Thermosets from Epoxy and Styrene- block -Butadiene- block -Styrene Triblock Copolymer. *Industrial & Engineering Chemistry Research*, *52*(26), 9121–9129. https://doi.org/10.1021/ie400813v

Intelligence, M. (2023). *Epoxy resins market size & share analysis - growth trends & forecasts (2023 - 2028)*.

Kamar, N. T., & Drzal, L. T. (2016). Micron and nanostructured rubber toughened epoxy: A direct comparison of mechanical,

thermomechanical and fracture properties. *Polymer*, *92*, 114–124. https://doi.org/10.1016/j.polymer.2016.03.084

KIM, J., BAILLIE, C., POH, J., & MAI, Y. (1992). Fracture toughness of CFRP with modified epoxy resin matrices. *Composites Science and Technology*, *43*(3), 283–297. https://doi.org/10.1016/0266-3538(92)90099-O

Kim, Y.-J., Chun, H., Park, S.-Y., Park, S.-J., & Oh, C. H. (2018). Preparation and curing chemistry of ultra-low CTE epoxy composite based on the newly-designed triethoxysilyl-functionalized ortho-cresol novolac epoxy. *Polymer*, *147*, 81–94. https://doi.org/10.1016/j.polymer.2018.05.073

Kishi, H., Kunimitsu, Y., Imade, J., Oshita, S., Morishita, Y., & Asada, M. (2011). Nano-phase structures and mechanical properties of epoxy/acryl triblock copolymer alloys. *Polymer*, *52*(3), 760–768. https://doi.org/10.1016/j.polymer.2010.12.025

Li, M., Heng, Z., Chen, Y., Zou, H., & Liang, M. (2018). High Toughness Induced by Wormlike-Nanostructure in Epoxy Thermoset Containing Amphiphilic PDMS–PCL Block Copolymers. *Industrial & Engineering Chemistry Research*, *57*(39), 13036–13047. https://doi.org/10.1021/acs.iecr.8b02336

Liu, J. (Daniel), Thompson, Z. J., Sue, H.-J., Bates, F. S., Hillmyer, M. A., Dettloff, M., Jacob, G., Verghese, N., & Pham, H. (2010). Toughening of Epoxies with Block Copolymer Micelles of Wormlike Morphology. *Macromolecules*, *43*(17), 7238–7243. https://doi.org/10.1021/ma902471g

Liu, X.-F., Xiao, Y.-F., Luo, X., Liu, B.-W., Guo, D.-M., Chen, L., & Wang, Y.-Z. (2022). Flame-Retardant multifunctional epoxy resin

with high performances. *Chemical Engineering Journal*, *427*, 132031. https://doi.org/10.1016/j.cej.2021.132031

Merz, E. H., Claver, G. C., & Baer, M. (1956). Studies on heterogeneous polymeric systems. *Journal of Polymer Science*, *22*(101), 325–341. https://doi.org/10.1002/pol.1956.1202210114

Mi, X., Liang, N., Xu, H., Wu, J., Jiang, Y., Nie, B., & Zhang, D. (2022). Toughness and its mechanisms in epoxy resins. *Progress in Materials Science*, *130*, 100977. https://doi.org/10.1016/j.pmatsci.2022.100977

Parameswaranpillai, J., Hameed, N., Pionteck, J., & Woo, E. M. (Eds.). (2017). *Handbook of Epoxy Blends*. Springer International Publishing. https://doi.org/10.1007/978-3-319-40043-3

Peng, X., Liu, W.-C., & Wu, G.-H. (2022). Strengthening-toughening methods and mechanisms of Mg–Li alloy: a review. *Rare Metals*, *41*(4), 1176–1188. https://doi.org/10.1007/s12598-021-01874-2

Qiu, Y., Qian, L., Chen, Y., & Hao, J. (2019). Improving the fracture toughness and flame retardant properties of epoxy thermosets by phosphaphenanthrene/siloxane cluster-like molecules with multiple reactive groups. *Composites Part B: Engineering*, *178*, 107481. https://doi.org/10.1016/j.compositesb.2019.107481

Quan, D., Murphy, N., & Ivankovic, A. (2017). Fracture behaviour of epoxy adhesive joints modified with core-shell rubber nanoparticles. *Engineering Fracture Mechanics*, *182*, 566–576. https://doi.org/10.1016/j.engfracmech.2017.05.032

Seo, J., Yui, N., & Seo, J.-H. (2019). Development of a supramolecular accelerator simultaneously to increase the cross-linking density and ductility of an epoxy resin. *Chemical Engineering Journal*,

356, 303–311. https://doi.org/10.1016/j.cej.2018.09.020

Su, C., Guo, J., Cheng, J., Zhang, J., & Gao, F. (2023). Heterogeneous Epoxidation of Microcrystalline Cellulose and the Toughening Effect toward Epoxy Resin. *Industrial & Engineering Chemistry Research*, 62(6), 2671–2686. https://doi.org/10.1021/acs.iecr.2c03919

Sukanto, H., Raharjo, W. W., Ariawan, D., Triyono, J., & Kaavesina, M. (2021). Epoxy resins thermosetting for mechanical engineering. *Open Engineering*, 11(1), 797–814. https://doi.org/10.1515/eng-2021-0078

Vijayan P., P., Puglia, D., Al-Maadeed, M. A. S. A., Kenny, J. M., & Thomas, S. (2017). Elastomer/thermoplastic modified epoxy nanocomposites: The hybrid effect of 'micro' and 'nano' scale. *Materials Science and Engineering: R: Reports*, *116*, 1–29. https://doi.org/10.1016/j.mser.2017.03.001

Zerda, A. S., & Lesser, A. J. (2002). Organophosphorous additive for fortification, processibility, and flame retardance of epoxy resins. *Journal of Applied Polymer Science*, *84*(2), 302–309. https://doi.org/10.1002/app.10329

Zhao, S., Liu, Q., Yuan, A., Liu, Z., Zhou, S., Fu, X., Lei, J., & Jiang, L. (2022). Intrinsic toughened conductive thermosetting epoxy resins: utilizing dynamic bond and electrical conductivity to access electric and thermal dual-driven shape memory. *Materials Chemistry Frontiers*, *6*(14), 1989–1999. https://doi.org/10.1039/D2QM00509C

Zhou, L., Fu, Y., Yin, T., & Luo, Z. (2019). Synergetic effect of epoxy resin and carboxylated nitrile rubber on tribological and

mechanical properties of soft paper-based friction materials. *Tribology International*, *129*, 314–322. https://doi.org/10.1016/j.triboint.2018.08.020

CHAPTER 9

ADSORPTION KINETICS AND METHODS TO CALCULATE ACTIVATION ENERGY

Dr. Mehmet Can DAL[1]

[1]National Education Directorate, Kayapınar, Diyarbakır, Turkiye, mcandal123@gmail.com, Orcid ID: 0000-0001-6474- 6053

1.INTRODUCTION

Adsorption is a cheap and effective separation method compared to other separation methods. Historical documents show that ancient Egyptians was used adsorption to decolorize charcoal (Dabrowski, 2001; Dal, 2022). Adsorption is often discussed together with environmental or catalysis issues. Adsorption studies are carried out on various subjects, especially CO_2 (Aktı, 2018) and H_2 adsorption (Koçer Kızılduman, 2023), heavy metal adsorption (Onursal, 2022; Onursal et al., 2022; Uçar et al., 2014; Onursal et al., 2019; Uçar, 2019; Uçar et al., 2015; Onursal and Dal, 2021; Uçar et al., 2020; Onursal, 2019; Uçar et al., 2020), drugs (Maged et al., 2020; Wu and Hong, 2013; Baytar, 2019 ; Ağlamaz et al., 2022), composites and adsorption of dyes (Kul et al., 2014; Kul et al., 2016).

Nowadays, new materials are synthesized and studies on the adsorption properties of these materials are frequently carried out. The popularity is increasing especially in the use of nanomaterials, biomaterials and composites as adsorbents. Adsorption studies can be classified as adsorption isotherm, thermodynamics and adsorption kinetics.

2.DEFINITION AND NATURE OF ADSORPTION

Adsorption is the phenomenon of hold of the mass from the gas phase or aqueous solution to the surface of the solid called the adsorbate. According to another definition, adsorption is as follows: Adsorption is a physical or chemical phenomenon that occurs when atoms, molecules or ions bond together between the surface of the adsorbing material and the adsorbed substance. Adsorbent; It is defined as the substance that

holds molecules in the liquid or gas phase on the surface, and adsorbed is defined as the substance that holds on the surface of the solid. It is possible to divide adsorption into two: physical and chemical. Physical adsorption is called physisorption and chemical adsorption is called chemisorption. Chemical adsorption, like all other chemical phenomena, is selective. If it is not clear whether the type of adsorption is physical or chemical, then the phenomenon is called sorption.

3. KINETICS AND ADSORPTION KINETICS

Before talking about adsorption kinetics, it will be useful to consider the concept of kinetics:

3.1. Kinetics

Kinetics is a concept related to the rate of change. Examines the process. Many things in nature are in a state of change. Growth, development, maturation and aging are a process. Consider the decay of an apple torn from its branch: The apple breaking off from its branch is the beginning of the end. In other words, the degradation process started from that moment on. In this process, kinetics deals with all factors that slow down or accelerate the process, especially the speed of change between the beginning and the end. Kinetics can be defined as the science that studies the speed and mechanism of an event. Kinetics, by its nature, does not deal with the moment of equilibrium. Because there is no change in the equilibrium at the macro level. For example; Let's say that substances A and B combine to form substances C and D. At the beginning of the event, there are only items A and B. With the formation of substances C and D, change begins and therefore the field of investigation of kinetics arises. On the one hand, the amount of A and B

(concentration for solutions, partial pressure or volume in gases) decreases, on the other hand, the presence of C and D in the environment increases. There are two possibilities for the 'fate' of the process; Either A and B will be completely finished and turn into C and D, or it will not be completely finished and will remain in the same environment as C and D. This second phenomenon is called equilibrium. If the equilibrium is chemical, the phenomenon is called chemical equilibrium.

The reason for the formation of chemical equilibrium is that the concentrations of the reactants, which initially had high concentrations, decrease in the process and the reaction rate decreases in parallel, while the concentrations of the forming products C and D increase from the first moment . In parallel with this, the reaction rate increases, and as a result, the reaction rates of the starting matters and products become equal. Once the speeds are equalized, the quantities of inputs and products are also fixed. This situation is shown in figure 1. Equilibrium is not a static state. In other words, with equilibrium, the destruction of reactants and the formation of products do not stop, they continue because the speed of both is not zero. However, since the velocities are equal, the amounts of matter formed and consumed are also equal.
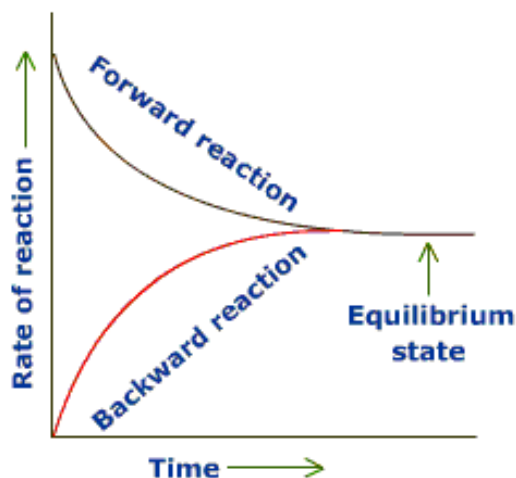
Fig. 1. Time-dependent change plot of forward and reverse reactions (URL 1)

Therefore, the ratio of the amount of products to the amount of reactants is constant. Because of this situation, the equilibrium is also called dynamic balance. The area of interest of kinetics is up to this point. In kinetics, the rate of change is generally considered as a function of time. Velocity is the change in the amount of matter or a property of matter due to change in time.

Adsorption kinetics examines the change in adsorption from the initial moment to the equilibrium moment. It is important to underline the following here: While in kinetics, rate calculations are calculated based on the concentration of the entering substances (pressure for gases), that is, the concentrations of the products are not included in the calculation, in adsorption kinetics, the calculation is based on the instantaneous amount (q_t) of the product, just like the turnover number in enzyme kinetics. Fig. 2 gives a typical graph of adsorption kinetics. As can be seen, the qt value, which increases rapidly at the beginning,

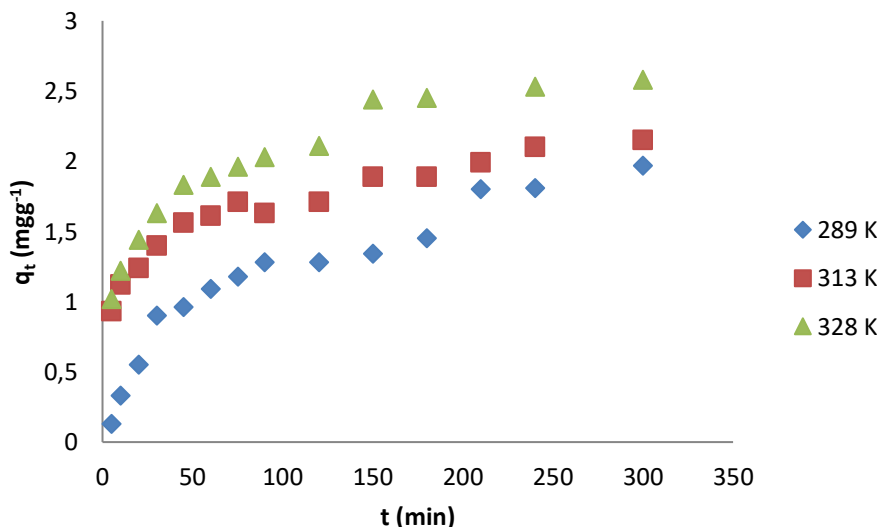stabilizes over time. In other words; The speed, which is initially high, converges to zero over time.

Fig. 2. Effect of adsorption contact time of Cu (II) on Karacadağ scoria at different temperatures (Dal et al., 2021).

4.REACTION SPEED AND ACTIVATION ENERGY

According to collision theory, the reacting substances must have sufficient kinetic energy. The amount of energy in the shape of the peak seen in Figure 3 is a threshold that in front of the reactant particles must exceed. The kinetic energies of particles in an environment are not the same. This is why temperature is defined as 'mean kinetic energy'. Particles with higher energy exceed this threshold more easily. Figure 4 depicts the situation of particles that can and cannot exceed this threshold. In cases where the activation energy is lowered, it becomes easier to exceed the threshold energy. In this case, the particles passing the threshold increase and the rate of the reaction increases.
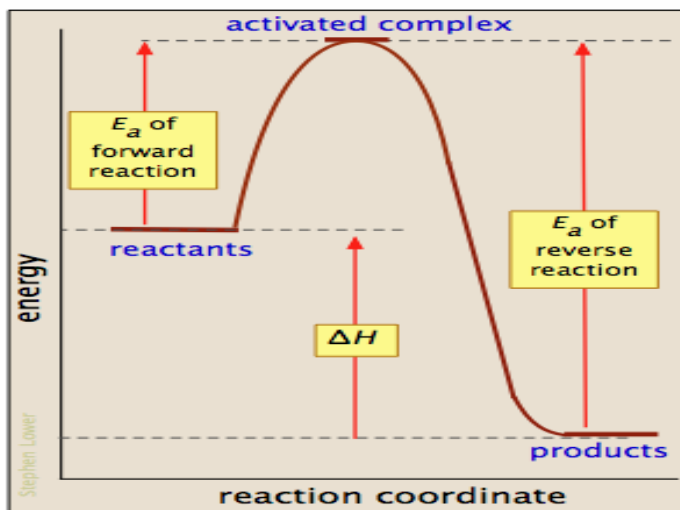
Fig. 3. Activation energies of forward and reverse reactions (URL 2).
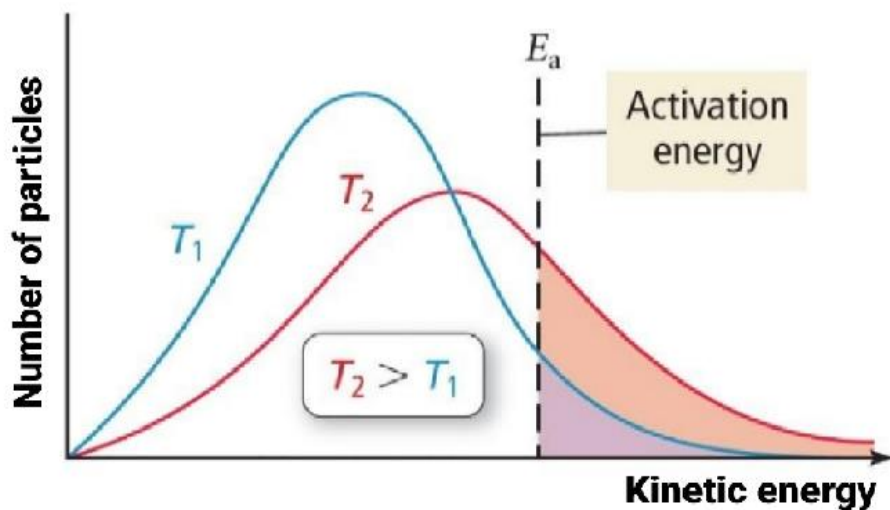

Fig. 4. Effect of temperature on particles exceeding the activation energy threshold (URL 3).

As can be seen, there is a clear inverse correlation between the rate of the reaction and the activation energy. If the reaction is multistage,

there is activation energy equal to the number of stages. In Figure 5, the activation energies belong to multistage reaction are given representatively. Since the slowest step determines the rate of the reaction, the highest activation energy determines the reaction rate. Activation energy can be reduced thanks to catalysts. Catalysts carry out the reaction through a different mechanism.

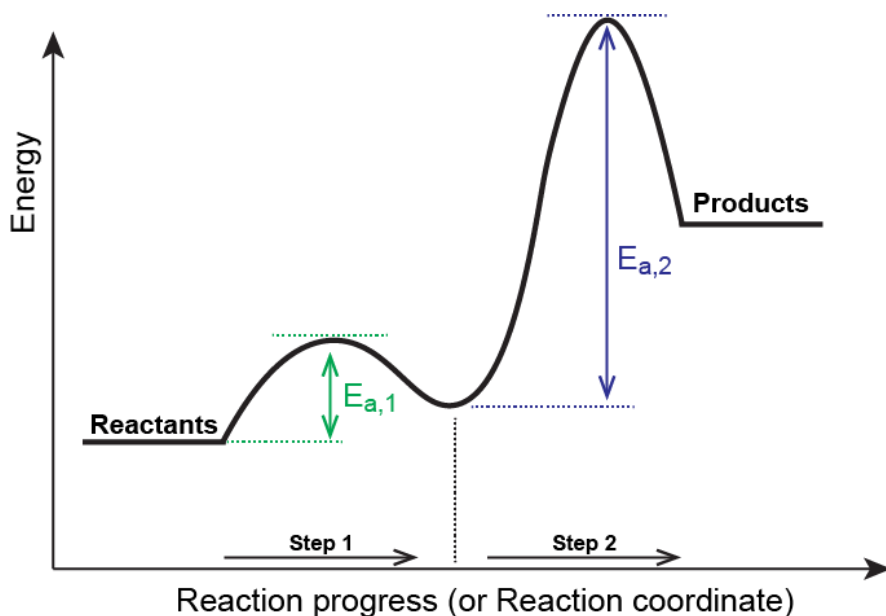
Fig. 5. Activation energies of multistep reactions (URL 4).

Knowing the activation energy gives us an idea about the reaction rate. The Arrhenius relation is used for this.

5. CALCULATION OF ACTIVATION ENERGY

5.1. Arrhenius Relation

It was proposed by Swedish chemist Svante Arrhenius in 1889 (Dou, 2023). The relation can be expressed as (27):

$$K = Ae^{\frac{-Ea}{RT}} \tag{1}$$

Here is;

K= Reaction rate constant (unit varies depending on the degree of reaction)

A: Frequency factor (unit varies depending on the degree of reaction)

e: Natural logarithm base,

Ea: Activation energy (Jmol^{-1})

R: Rydberg constant (8,314 Jmol^{-1}K^{-1})

T: Absolute temperature (K).

When the logarithm of Eq.1 is taken, linear Eq.2 is obtained:

$$lnK = \frac{-E_a}{R}\frac{1}{T} + lnA \tag{2}$$

However, the equation does not always give a line in practice.

5.2. Using K Constant

The k constants of kinetic models are used for the K constant used for the Arrhenius equation. There are various models in the literature for adsorption kinetics (Lagergren, 1898; Ho and McKay, 2000; Ho, 2006; Weber et al.,1963; Chien and Clayton, 1980). However, in order to find the E$_a$ value of adsorption,probably because it is related to chemical adsorption, the k$_2$ constant of the pseudo-second kinetic order model is used. Let's examine the model: The differential form of the pseudo-second-order equation derived can be written as follows (Ho and McKay, 2000);

$$\frac{dq}{dt} = k_2(q_e - q_t)^2 \tag{3}$$

$$q_t = \frac{q_e^2 k_2 t}{1 + q_e k_2 t} \tag{4}$$

Ho created a linear form of this equation:

$$\frac{t}{q_t} = \frac{1}{K_2 q_e^2} + \frac{1}{q_e} t \tag{5}$$

Equation, refers to;

q_e; the amount of substance adsorbed per gram by the adsorbent at equilibrium (mgg^{-1}),

q_t; the amount of substance adsorbed per gram by the adsorbent at time t (mgg^{-1}),

k_2; kinetic rate constants of pseudo-second rate order (min^{-1})

t; the contact time (min)

However, there are 6 types of pseudo-second kinetic order in the literature. These (Onursal, 2022):

Type 1: $\qquad \dfrac{1}{q_e - q_t} = \dfrac{1}{q_e} + k_2 t \tag{6}$

Type 2: $\qquad \dfrac{1}{q_t} = \dfrac{1}{q_e} + \dfrac{1}{K_2 q_e^2} \dfrac{1}{t} \tag{7}$

Type 3: $\qquad q_t = q_e - \dfrac{1}{K_2 q_e} \dfrac{q_t}{t} \tag{8}$

Type 4: $\qquad \dfrac{q_t}{t} = k_2 q_e^2 - k_2 q_e q_t \tag{9}$

Type 5: $\frac{1}{t} = -k_2\,q_e\ +\ k_2 q_e^2\,\frac{1}{q_t}$ (10)

Type 6: $\frac{t}{q_t} = \frac{1}{K_2 q_e^2} + \frac{1}{q_e}\,t$ (5)

6. CALCULATION METHOD IN ADSORPTION KINETICS

Type 6 is the most well-known linear equation. However, the equations of each type provide an opportunity to understand the adsorption kinetics. One q_e and k_2 constants are obtained from each equation. These k_2 constants are not used directly in the Arrhenius equation. Because these constants were obtained under a single temperature condition. However, the Arrhenius equation aims to find the activation energy, which remains constant in a changing 'narrow temperature range', with the K constants changing with these temperatures. Let's examine the equation:

$$lnK = \frac{-E_a}{R}\frac{1}{T} + lnA$$ (2)

As can be seen, there are three constants in this first-order equation: R, Ea and A. The constant R is a general constant that is independent of the equation and whose value is known. To find the other two constants, the lnK value is plotted against the 1/T value. The K value here is the k_2 value obtained from the pseudo-second order equation. However, gmg⁻¹min⁻¹ unit is used in classical kinetic calculations. Whereas, since the unit of activation energy is Jmol⁻¹, in kinetic calculations to obtain the k_2 constant, the qt value should be calculated

in gmol^{-1}, not gmg^{-1}. In this case, the unit of the k_2 constant will be gmol^{-1}min^{-1} and thus the Ea value can be calculated in Jmol^{-1}.

Let's take type 6 equation as an example to calculate the constant k_2. Type 6 equation;

Type 6: $\qquad \dfrac{t}{q_t} = \dfrac{1}{K_2 q_e^2} + \dfrac{1}{q_e} t$ $\qquad\qquad$ (5)

In this equation, $y = mx + n$, t/q_t represents y, $1/(k_2 q_e^2)$ represents n, $1/q_e$ represents m, and t term represents x. The inverse of the slope in the equation gives the constant q_e:

$$m = \frac{1}{q_e} \qquad\qquad (11)$$

From here, it is seen that the inverse of the slope according to multiplication gives the constant q_e:

$$q_e = \frac{1}{m} \qquad\qquad (12)$$

Shift of Eq.5;

$$n = \frac{1}{k_2 q_e^2} \qquad\qquad (13)$$

If the term m is written instead of $1/q_e$ and the equation is rearranged, the constant k_2 becomes;

$$k_2 = \frac{m^2}{n} \qquad\qquad (14)$$

If the square of the slope of the Type 6 equation is divided by the shift, the constant k_2 is obtained.

The slope of the line obtained when the $\ln k_2$ value is plotted against 1/T;

$$m = \frac{E_a}{R} \tag{15}$$

If E_a is withdrawn from here;

$$E_a = mR \tag{16}$$

When the slope of the equation is multiplied by the value of the R constant, 8.314, the value of the activation energy is found.

7. RESULTS AND DISCUSSION

Adsorption is a well-established separation method. Adsorption kinetics is an important sub-branch of adsorption science and deals with issues such as rate, amount deposited at equilibrium, temperature and activation energy. There is an inverse relationship between the rate of adsorption and activation energy. In this regard, knowing the value of activation energy is important as it will give an idea about the adsorption rate. In this context, kinetics, activation energy, Arrhenius relation, adsorption kinetics, pseudo-second order and the method of finding the constants of the linear equations of this model were discussed. It is hoped that the study will serve as a guide for researchers interested in this subject.

REFERENCES

Dabrowski, A., (2001). Adsorption- from theory to practice. *Advances in Colloid and Interface Science,* 93, 135-224.

Dal, M.C. (2022). Fen Bilimleri ve Matematik Alanında Yeni Trendler. Duvar yayınları. Aralık, 389-401.

Aktı, F. (2018). Düşük Sıcaklık CO_2 adsorpsiyonu için Panı/Sba-15 sorbentlerin sentezi ve yapısal özelliklere sentez parametrelerinin etkisi. *Uludağ Üniversitesi Mühendislik Fakültesi Dergisi*, 23(3).

Kızılduman, B.K. (2023). Kaolinit kilinin hidrojen depolama amaçlı kullanımı için modifikasyonu ve karakterizasyonu. *Balıkesir Üniversitesi Fen Bilimleri Enstitüsü Dergisi,* 25(1), 186-202.

Onursal, N. (2022). Removal of Ni (II) Ions from aqueous solutions with Siirt Koçpınar mixed type clay (SKMTC) ınvestigation of ısotherm, thermodynamic and kinetic parameters. Desalination and Water Treatment.

Onursal N., Altunkaynak Y., Baran A, Dal M.C., 2023. Adsorption of nickel (II) ions from aqueous solutions using Malatya clay: Equilibrium, kinetic, and thermodynamic studies. *Environ Prog Sustainable Energy,* e14150.

Uçar, M., Evcin, A.,Ünverdi, H.,Uçar, S. (2014). 4-Klorofenolün Al_2O_3 katkılı hidroksiapatit ile sulu ortamdan uzaklaştırılması. *Afyon Kocatepe Üniversitesi Fen ve Mühendislik Bilimleri Dergisi,* 14(3), 225-232.

Onursal, N., Dal, M., Kul, A., Yavuz, Ö. (2019). Cu (II) iyonlarının doğal karışık tipteki kil ile sulu ortamdan uzaklaştırılması, izoterm, kinetik ve termodinamik parametrelerin incelenmesi. *Euroasia*

*Journal of Mathematics, Engineering, Natural & Medical Sciences,*7(9), 58-103.

Uçar, M. (2019). Adsorption of chlorophenolic compounds on activated clinoptilolite. *Adsorption Science & Technology,* 37(7-8), 664-679.

Uçar S., Evcin, A.,Uçar M.,Alibeyli, R.,Majdan, M. (2015). Removal of phenol and chlorophenols from aquatic system using activated clinoptilolite. *HJBC,* 43(3), 235-249.

Onursal, N., Dal, M.C.(2021). Altı tip yalancı-ikinci dereceli kinetik denkleminin malahit yeşilinin siirt kili ile adsorpsiyonunda karşılaştırmalı doğrusal yöntemler. *International Siirt Scientific Research Congress,* Siirt, s. 399-409.

Uçar, M., Kayıran, D. & Evcin, A. (2020). Modifiye nanobentonitle sulu ortamdan fenol ve 4-klorofenolün giderilmesi. *Avrupa Bilim ve Teknoloji Dergisi,* 20, 760-768.

Onursal, N. (2019). Malahit yeşilinin sulu çözeltilerden karışık tip kil ile sulu çözeltilerden uzaklaştırılması. *3.Anadolu Uluslararası Uygulamalı Bilimler Kongresi* (s.644-657). Diyarbakır: UBAK Publications.

Uçar, M., Erçolak, K., and Uçar, S. (2020). Removal of phenol and nitrophenols from aquatic system with cibacron blue F3GA attached mPHEMA. *El-Cezeri,* 7(3), 1518-1528.

Maged, A.,Iqbal, J.,Kharbish, S.,Ismael, I.S.,Bhatnagar, A. (2020). Tuning tetracycline removal from aqueous solution onto activated 2:1 layered clay mineral: Characterization, sorption and mechanistic studies. *Journal of Hazardous Materials,* 384,121320.

Wu, Q.,Li, Z., Hong, H., (2013). Adsorption of the quinolone antibiotic nalidixic acid onto montmorillonite and kaolinite. *Applied Clay Science,* 74, 66-73.

Baytar, O.(2019). Antideprasan ilaçların etken maddelerinin adsorpsiyonu: Kinetik ve izotermi. *Uluslararası Mühendislik Araştırma ve Geliştirme Dergisi.*

Ağlamaz, M.D., Şarkaya, K., Türkmen, D., Uçar, M., Denizli, A., (2022). Removal of amoxicillin via chromatographic monolithic columns: comparison between batch and continuous fixed bed. *Turk J Chem.,* (1), 88-100. PMID: 37720859; PMCID: PMC10504016.

Kul, A. R., Selçuk, A., Ocak, S., Alacabey, İ., Onursal, N.(2014). Sulu ortamdaki tekstil boyarmadde kirliliklerinin adsorpsiyon tekniği ile uzaklaştırılması. *Ulusal Katı Atık Yönetimi Kongresi (UKAY)* (s. 63). Van: Van Yüzüncü Yıl Üniversitesi.

Kul, A. R.,Benek, V.,Selçuk, A., Onursal, N. (2016). Using natural stone pumice in van region on adsorption of some textile dyes. *28.Ulusal Kimya Kongresi.* Mersin: Mersin Üniversitesi Yayınları.

https://haygot.s3.amazonaws.com/questions/306335_255140_ans.gif

Dal, M. C., Onursal, N., Arıca, E., & Yavuz, Ö. (2021). Diyarbakır Karacadağ Kırmızı Tepe Skoryası ile Cu (II) Adsorpsiyon Kinetiğinin İncelenmesi. *DÜMF Mühendislik Fak. dergisi*, 337-346.

https://useruploads.socratic.org/HpDdyGF3TeitDzEnO2EP_EaPlot1.

https://pbs.twimg.com/media/Ea81EieU8AADKfI.jpg

https://wisc.pb.unizin.org/app/uploads/sites/557/2020/10/M13Q10_slo wsecond-1.png

Dou, R. (2023). Deriving the Arrhenius equation and the pre-exponential factor. *Preprints,* 2023040215.

https://doi.org/10.20944/preprints202304.0215.v1

https://qsstudy.com/explain-differentiation-of-the-arrhenius-equation

Lagergren S. (1898). Zur theories der sogenannten adsorption gelöster stoffe. kungliga svenska vetenskapsakademiens. *Handlingar*, 24, 1-39.

Ho, Y.S., McKay, G.,Waseand, D.A.J.,Forster, C.F. (2000). Study of the sorption of divalent metal ions on to peat. *Adsorption Science & Technology,* 18(7), 639-650.

Ho, Y.S. (2006). Review of second-order models for adsorption systems. *Journal Of Hazardous Materials*, 681-689.

Weber, J.W.,Morris, J.C., and Sanit, J. (1963). Kinetics of adsorption on carbon from solution. *Journal of the Sanitary Engineering Division, American Society of Civil Engineers*, 89, 31-38.

Chien S.H.,Clayton W.R.(1980). Application of Elovich equation to the kinetics of phosphate release and sorptionin soils. *Soil Sci. Soc. Am. J.*, 44,265-268.

Onursal, N. (2022). Kinetic model validation with experimental data using linearized 6-type equations obtained from the pseudo-second kinetic model for Ni (II) ion adsorption with Siirt Koçpınar mixed type clay. *International Journal of Pure and Applied Sciences,*8(2), 441-448.

CHAPTER 10

NANOTECHNOLOGY AND APPLICATIONS

Prof. Dr. Murat ATEŞ[1]

DOI: https://dx.doi.org/10.5281/zenodo.10030596

[1]Tekirdag Namik Kemal University, Faculty of Arts and Sciences,Department of Chemistry, Tekirdag, Türkiye, mates@nku.edu.tr, Orcid ID: 0000-0002-1806-0330

1. INTRODUCTION

Today, scientists are trying to design nano-matrials, methods, tools, and structures that can replicate, monitor, control and repair themselves. A nanometer is one billionth of a meter $(1/10^9)$. For example, when measured at the nanoscale, a hair strand is observed to be approximately 50.000 nanometers, while a bacterial cell is a few hundred nanometers. 1 nanometer is only 10 times the diameter of a hydrogen atom (Rodriquez-Gomez et al., 2023).

It is aimed to obtain functional products with high level of benefit.

1- Analysis and fabrication of nanometer scale structures,

2- Development of nanoscale devices,

3- Characterizations of nanometer sized devices.

Nanomaterials, which are the building blocks of products that are rediscovered every day, such as dirt-repellent paint, dirt-proof socks, bullet-proof fabric, and microsensor, are among the most striking topics of recent years. Nanomaterials can be in the form of metal ceramics, polymers or composites. Nanotechnology is the discovery of brand new properties of matter vy engineering it at the atomic-molecular level; it is the development of functional materials, devices and systems for the purpose of understanding (Kokotovich et al., 2021). It is the branch of science that aims to create new substances by bringing atoms together. Thanks to nanotechnology, matter can be structured on an atomic scale. Nanomaterials with new properties can be obtained. A road map has been planned for our country within the framework of nanotechnology studies within the framework of TUBITAK's 2023 vision programme

centers such as UNAM, Gebze Advanced Institude Technology and MAM were established for this purpose.

2. RESULTS AND DISCUSSION

2.1. Applications of Nanotechnology

2.1.1. Nanotechnology in paint field

Paint is defined as liquid or powder materials that can be spread on a solid surface and dry and harden, adhering to that surface and forming a decorative and protective film. Surfaces painted with nanotechnology are protected against damage caused by acid rain and pollutants. Nanomaterials kill bacteria and viruses on the surface and in its immediate surroundings (www.yasarboya.com.tr). They also prevent them from sticking to the surface easily. In addition, they ensure the dissolution of organic substances on the surface (such as oil and grafiti). Nanotechnological paints have features such as fire retardants, self-cleaning, better conduction of heat and electricity, sound isolation and resistance to sunlight (www.gelecegindunyasi.com).

Table 1. Comparison between traditional coating and nano coating.

Traditional coating	Nano coating
Physical, chemical, thermal, electrical and mechanical properties	It is an improved version of traditional coating features.
There is a high probability of moisture formation.	It minimizes moisture.
Surface rougness is ~5μ depending on particle size.	It reduces the surface roughness vy 1 nm to prevent good dirt retention.
It is micron scale.	It is nano scale.
There is high contact voltage between the water droplet and the coating layer.	Contact stress decreases (water repelency)

Nanopaints utilize the photocatalytic structure of titanium dioxide, which is a nano-sized semiconductor. When TiO_2 is exposed to UV light (<388 nm), they form electron and hole pairs on the surface. This gap forms an energy gap of 2.8-3.2 eV (http://kimya.uzerine.com). Nanomaterials includes TiO_2, silicon etc. supply an improved functionalities like water , stain resistance, stratch resistance, etc (Varma et al., 2019).

2.1.2. Nanotechnology in the automotive industry

The automotive industry is one of the most significant sector in the world in a budget of nearly 2 trillion euros. It is the world's second largest industry branch investing in research development. Nowdays, electric hybrid cars have been developed activity being conducted by many automotive companies (Wang et al., 2011). Thanks to nanotechnology, which allows the production of much more useful parts for automobiles, more durable and lighter metals, self-cleaning and not easily scratched metallic paints, parts that reduce friction, extent engine life and save engine oil are new being produced.

New battery technologies such as lithium ion, lithium iron phosphate ($LiFePO_4$) etc. in electric and hybrid vehicles significantly affect the cost and affordability of automobiles. In addition, hydrogen storage systems and efficient and low cost fuel cells are important as these systems are alternatives to batteries in electric vehicles. Research studies are continuing to improve hydrogen storage with the use of carbon nanotubes. By using carbon nanotubes in automobile tires with a nano-technological approach, it is expected to achieve much more durability and reliability than steel with the use of technology in

automobile windows. The glasses are made much thinner and more durable. In addition, self-cleaning glasses ensure that sticky dirt is washed way in a short time. Thanks to the new features developed, even overheating of the interior of a vehicle packet under the sun can be prevented with the development of bottom-up production, one of the nanofabrication methods, molecular structures that will serve as machine elements can be obtained (Presting et al. 2003).

2.1.3. Nanotechnology in the food and packaging industry

In recent years, great progress has been made in many areas such as the development of newly developed packaging products, the transport and controlled release of bioactive substances, and the detection of pathogens through nanosensors and indicators. Applications of nanotechnology in the field of food can be grouped under two main headings (Pal and Mahendra, 2015; Pal, 2017).

1- Food applications

Protection from oxidation, masking taste, identification of pathogens in the food system, food safety and quality analysis, controlled release of encapsulated nutrients (moisture of pH triggering) (Hemavathi and Siddaramalah, 2019).

2- Food packaging applications

Extending shelf life with active packaging nano additives, smart packaging, antibacterial packaging. While studies on keeping food fresh for longer are carried out by those working in the packaging industry, consumers want to see the freshness of the food without opening the package. Today's studies have shown that both are possible with nanotechnology.

Nanotechnology is used in 3 different categories for food packaging.

1- Biodegradable nanocomposite packaging materials,

2- Antimicrobial active and smart nano packaging,

3- Nanocomposite packaging materials are used as filler materials in the field of clay, silicates, SiO_2, $CaCO_3$ and TiO_2.

There are some safety regulations and management of nano food packaging in developing countries (Bumbudsonpharoke and Ko, 2015).

2.1.4. Nanotechnology in textile field

In the field of textile applications of nanofibers, non-woven surfaces consisting of nanofibers are obtained by the electrospinning method. The resulting non-woven surfaces have found wide use in textile sector. Features that determine the effectiveness and performance of the non-woven surface in textile applications;

a) Total porosity,

b) Average pore size,

c) It is the specific surface area. All these parameters can be characterized by Brunauer-Emmett-Teller (BET) analysis.

Electrospinning technique, which is quite different from nano fiber production technique in which fibers are obtained in a complex surface format, will open many doors in textiles once (Stoe and Aileni, 2022). It has some advantages such as applicability on a wide range of materials, cheaper, and simplicity. Micro and nano level fibers supply a high porosity, surface functionality, high surface to volume ratio, etc. (Doğan et al., 2019). Anti-bacterial textile fabrics are formed by the electrospinning method. Furthermore, with the use of less chemicals

compared to the completing process, studies that are economically advantages and reduce environmental pollution are carried out. Another advantage is that the resulting coatings are small enough to be examined under a microscope.

3. CONCLUSIONS

With the help of nanotechnology, new materials and nano-devices are used in many areas, such as paint, automotive, food and packaging, textile, etc. Nano level of materials affect the mechanical, thermal or electrical properties of materials. In the textile section, electrospinning technique can be used to obtain nanofibers. As a result, there are many useful areas for apllication of nanotechnology.

REFERENCES

Bumbudsonpharoke, N., Ko, S. (2015). Nano-food packaging: An overview of market, migration research, and safety regulations. 80(5), R910-R923.

Doğan, Y.K., Demirural, A.,Baykara, T. (2019). Single-needle electrospinning of PVA hollow nanofibers for cure-shell structures. *In: SN Applied Sciences*, 1, 5.

Hemavathi, A.B., Siddaramalah, H. (2019). Food packaging: Polymers as packaging materials in food supply chain. *Encylopedia of Polymer Applications*, Vols I-III, Edited by Mishra M, pp. 1374-1397.

http://www.yasarboya.com.tr/yasar/boya/akilli-boyalar/nanoteknolojik-ic-dis-cephe-duvar-boya-ve-astarlari

http://kimya.uzerine.com/index.jsp?objid=1078

Kokotovich, A.E., Kuzma, J., Cummings, C.L., Grieger, K. (2021). Resposnsible innovation definitions, practices and motivations from nanotechnology researchers in food and agriculture. *Nanoethics,* 15 (3), 229-243.

Pal, M. 2017. "Nanotechnology: a new approach in food packaging", Journal of Food: Microbiology, *Safety and Hygiene*, 2, 121.

Pal, M., Mahendra, R. (2015). Sanitation in food establishments. *Lambert Academic Publishers*, Saarbrucken.

Presting, H., König, U. (2003). Future nanotechnology developments for automotive applications. *Materials Science and Eng. C.,* 23, 737-741.

Rodriquez-Gomez, F.D., Penon, O., Monferner, D., Rivera-Gill, P. (2023). Classification system for nanotechnology-enabled health product with both scientific and regulatory application. *Frontiers in Medicine,* 10, 2212949.

Stoe, C.E., Aileni, R.M. (2022). An overview on nanomaterials with magnetic properties used in the textile sector. *Industria Textila*, 73(3), 317-326.

Varma, A., James, A.R., Daniel, S.A. (2019). A review on nano TiO_2- a repellent in paint. *National Conference on structural engineering and construction management,* Secon 2019: Proceedings of SECON'19, pp. 909-918.

www.gelecegindunyasi.com/nanoteknoloji.html

Wang, B.H., Luo, Y.G. (2011). Application study on a central strategy for a hybrid electric public bus. *Int. J. Automotive Technology,* 12(1), 141-147.

CHAPTER 11

EFFECTS OF PHYSICAL AND CHEMICAL PROPERTIES ON BIODIESEL EMISSIONS

Sinem KAYA[1*]

[1] Ministry of Environment, Urbanization and Climate Change, General Directorate of Environmental Impact Assessment, Permit and Inspection, Center Directorate of Clean Air for Central Black Sea Samsun, Türkiye. sinem.kaya@csb.gov.tr ORCID: 0000-0002-5468-9662
* Corresponding Author

INTRODUCTION

With the increasing population in the world, it is seen that the demand for energy is increasing due to rapid population growth. Accordingly, the use of biodiesel instead of fossil fuels to reduce greenhouse gases to produce energy comes to the fore [1]. Being safe and economical are among the main benefits of biodiesel. They are also considered an alternative to fossil fuels because they emit lower levels of carbon monoxide (co), hydrocarbons, and particulate matter into the atmosphere. The non-toxic nature of biodiesel provides optimum advantage in use. Biodiesel production is directly related to parameters such as oil raw material potential, climate and geographical location in the region. A wide variety of comprehensive methods exist for the production of biodiesel, such as the supercritical fluid method, emulsification, pyrolysis and transesterification. Among these methods, the transesterification method maintains its superiority due to its process simplicity and high conversion efficiency. Homogeneous based catalysts such as sodium hydroxide (naoh) and potassium hydroxide (koh) are mainly used in the transesterification process [2,3]. Then, as a result of the transesterification reaction, biodiesel is produced as the main product and glycerol is produced as a by-product [4,5]. Biodiesel has a wide range of advantages but faces the disadvantage of commercialization and applicability. Biodiesel requires special attention in terms of storage capacity and fuel protection under special standard conditions. While biodiesel fuel becomes rancid (oxidation) within a week, conventional diesel fuels have higher oxidation stability. The cumulative accumulation of oxidation-related end products (insoluble gums) in biodiesel causes blockages or clogging in fuel filters [6,7]. In addıtıon to

the disadvantages mentioned above, biodiesel is tendency to degrade in radical chemical reactions.

Figure 1. Biodiesel Life Cycle [8].

Achieving sustainable development goals emphasizes alternative fuel strategies that prioritize biodiesel production [9,10]. Biodiesel is the methyl esters obtained as a result of the reactions of long-chain fatty acids, generally found in the structures of vegetable and animal oils, in the presence of various catalyst types and alcohol). Biodiesel production from renewable energy sources is largely preferred due to its environmentally friendly and cost-effective economic benefits. However, there are various limitations in the use of biodiesel that affect its efficiency. The most important of these limitations is oxidation, which negatively affects the lifespan of biodiesel and, accordingly, engine performance. During biodiesel production, free radical

compounds prone to oxidation are formed in the environment as a result of chemical reactions after repeated chain modifications. For this reason, it is important to determine the physicochemical properties of biodiesel and keep them under control at standard values [11,12].

It is possible to group the sources of pollutant emissions into the environment into two groups: natural and anthropogenic. These pollutants are present in the atmosphere in particulate and gaseous form. The sources of those in particulate form are volcanic eruptions, forest fires, combustion processes, smoke released as a result of industrial activities, road transportation and biological creatures living in the sea. Pollutants commonly found in the atmosphere are carbon monoxide, nitrogen oxides, sulfate oxides, particulate matter, volatile organic carbon, ozone, greenhouse gases, carbon dioxide, methane, chlorofluorocarbon and nitric acid and are shown in Table 1 [13].

Gases resulting from incomplete combustion due to exhaust fumes in transportation (polycyclic aromatic hydrocarbons), carbon monoxide, nitrogen oxide, particulate matter and ozone are other important sources.

Studies conducted with polycyclic aromatic hydrocarbons have shown that biodiesel fuels release these compounds less [14]. However, since conflicting results were obtained, it was understood that more research was needed. As mentioned in previous sections, the reason why nitrogen oxide emissions from biodiesel are high is that it is present everywhere.

There is no single source of nitrogen oxides released as a result of biodiesel combustion. Biodiesel fuel types and properties are mentioned in Table 2. The reason why biodiesel is so effective in emissions is its physicochemical properties. It has been observed that these properties

affect the combustion temperature, residence time of the combustion mixture and the amount of nitrogen oxide. [15]. On the other hand, it can be said that fuel properties such as oxygen content, cetane index, kinematic viscosity, density, heat capacity (calorific value), degree of saturation, surface tension and thermal conductivity shown in Table 3 also contribute to emissions.

Table 1. Common pollutants in the atmosphere and their causes [13]

| Pollutants	Outputs	Inputs
CO	Traffic and industry	Usage of vehicles without catalytic converters
NO_x	Traffic and industry	Combustion at high and low temperatures
SO_x	Traffic and industry, (chemical, paper, refineries, and boilers)	Vehicles using high sulfur content fuels Usage of fuels with high sulfur content
PM	Traffic and industry	Transportation, agriculture and construction
	Traffic and industry	Construction and agricultural applications
VOC	Chemical industry, traffic, fuel depots and car workshops	İnşaat malzemelerinin işlenmesi, çözücüler ve diğer faaliyetler
O_3	NO_x, VOC veya CO	Birincil kaynak kirleticiler arasındaki kimyasal reaksiyonlar (Örnek: trafik, endüstriler, depolama alanları, boyalar ve solventler (VOC), ormanlar ve diğer kaynaklar
CO_2	Fuels	The use of fossil fuels, deforestation and change in land use
N_2O	Human activities	Energy production and consumption, Fertilizer use, acid production and burning biomass and fossil fuels
HNO_3	Human and economic activities	Wood combustion, fossil fuels, chemical composition of fertilizers and microbes
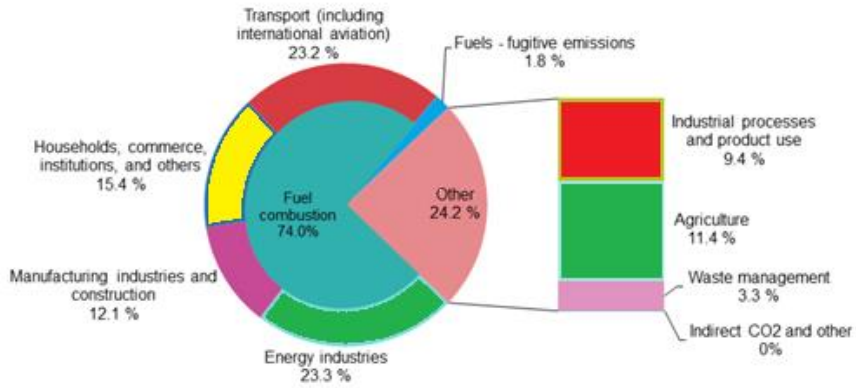
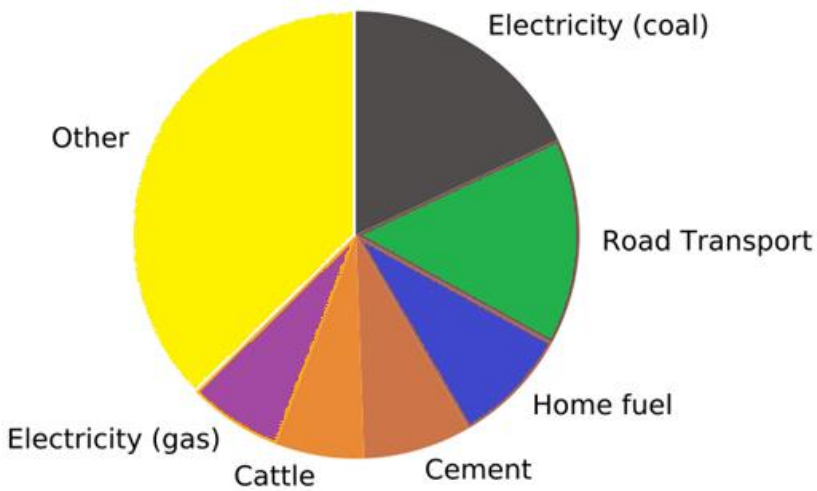**Figure 2.** Greenhouse Gas Emissions from EU Transport [8].

Figure 3. Greenhouse Gas Emissions from Transportation in Turkey [8].

Table 2. Fatty acid profiles of soybean, cottonseed, palm, jatropha and sunflower [16].

Fatty acid	Formıla	Structure	Soy bean	Flaxseed	Palm	Jatropa	Sun flower
Lauric	$C_{13}H_{26}O_2$	$C_{12}:0$	-	-	1.0	-	-
Myristic	$C_{15}H_{30}O_2$	$C_{14}:0$	0.2	0.8	2.1	0.1	-
Palmitic	$C_{17}H_{34}O_2$	$C_{16}:0$	10.2	22.9	44.3	14.2	-
Marganic	$C_{18}H_{36}O_2$	$C_{17}:0$	-	-	-	-	-
Stearic	$C_{19}H_{38}O_2$	$C_{18}:0$	4.6	3.1	2.2	7.0	-
Oleic	$C_{19}H_{36}O_2$	$C_{18}:1$	22.2	18.5	44.4	44.7	-
Linoleic	$C_{19}H_{34}O_2$	$C_{18}:2$	54.6	54.2	5.2	32.8	-
Linolenic	$C_{19}H_{32}O_2$	$C_{18}:3$	8.2	0.5	0.2	0.2	-
Arachidic	$C_{21}H_{42}O_2$	$C_{20}:0$	-	-	-	0.2	0.3
Gadoleic	$C_{21}H_{40}O_2$	$C_{20}:1$	-	-	-	-	-
Behenic	$C_{23}H_{46}O_2$	$C_{22}:0$	-	-	-	-	-
Lignoceric	$C_{25}H_{50}O_2$	$C_{24}:0$	-	-	-	-	-

Table 3. Physical properties of biodiesel [17].

Properties	Unit	Limits	Standart
Appearance	-	Açık/kahverengi	Görünür
Density (20 °C')	kg/m³	838.8	ASTM D1298
Kinematic Viscosity (40 °C)	cSt	2.32	ASTM D445
Flame point	°C	56.0	ASTM D93
Setan Index	-	46	ASTM D4737
Hydrogen	%	12.38	ASTM D7171
Copper Corrosion (3 hour)	100 °C	-	ASTM D130
Carbon	%	74.99	ASTM D7662
Oxygen	%	12.45	ASTM D5622
Sulphur Content	%	< 0.0124	ASTM D4294
Flash point	°C	160	ASTM D86
Distillation Temperature	°C	353.5	ASTM D86
Coating	%	-	-
Residue Loss	%	-	-
Gross Calorific Value	kj/kg	44.84	ASTM D4868

EFFECTS OF THE COMPRESSIBILITY BULK MODULE

Bulk modulus is the material's ability to resist compression. It is volumetric elasticity and is inversely proportional to compressibility. Bulk modulus increases with increase in pressure and decreases with increase in temperature. Figure 4 shows the change in bulk modulus of various hydrogenated vegetable oils (HBY) and biodiesel blended fuels with pressure. In addition, the bulk modulus of biodiesel is affected by the density and sound speed of biodiesel.
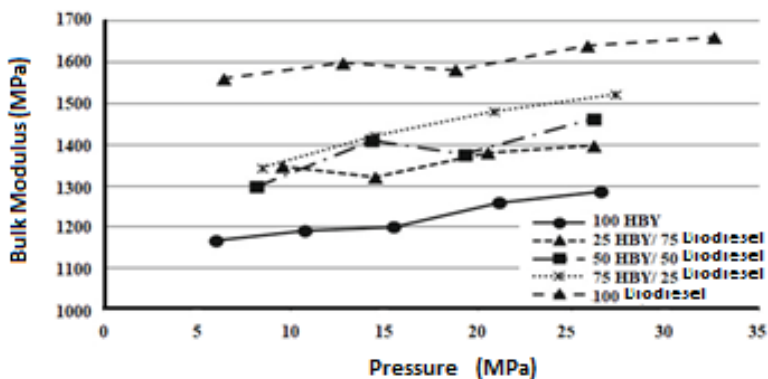

Figure 4. Variation of average bulk modulus with pressure for HBY/biodiesel blends [18]

The volume modulus has a significant impact on the operation of fuel injection systems. The higher compressibility modulus of vegetable oils and methyl esters may be associated with improved ignition time. Lower bulk modulus causes ignition delay [19]. It has been stated in the literature that the density, velocity and isoentropic bulk moduli of unsaturated methyl esters are higher than saturated methyl esters. These findings were confirmed by Tat et al. [20]. The compressibility bulk module modifies the behavior of fuels containing saturated fatty acids,

bringing them closer to the ignition time similar to diesel fuels. In addition, density, velocity and isoentropic bulk modulus also depend on pressure changes between 20 °C and 40 °C. [21].

SURFACE TENSION (σ) mm^2/s

Yüzey gerilimi bir sıvının mümkün olabilecek minimum yüzey alanının elastiklik eğilim kuvveti olarak tanımlanmakta olup birimi Newton/metre (N/m) cinsinden ölçülendirilmektedir. Sıvılarda yüzey gerilimi, atomizasyonu etkileyen en temel özelliklerden biri olarak kabul edilir ve biyodizel gibi yakıtlarda da, bu durum aynıdır [22]. Surface tension is an effective factor on atomization, which is the first stage of combustion of biodiesel fuel. Therefore, surface tension plays a very important role in the combustion stages of fuel in diesel engines. [23]. Although pressure has no effect on surface tension, it is important to remember that working engine injector needles are cooled by the engine fuel during atomization. This reduces the fuel temperature and reduces the vapor lock that may occur. [24]. Figure 5 shows the variation of molecular weight (g/mol) and surface tension (mN/m) for saturated methyl and ethyl esters.
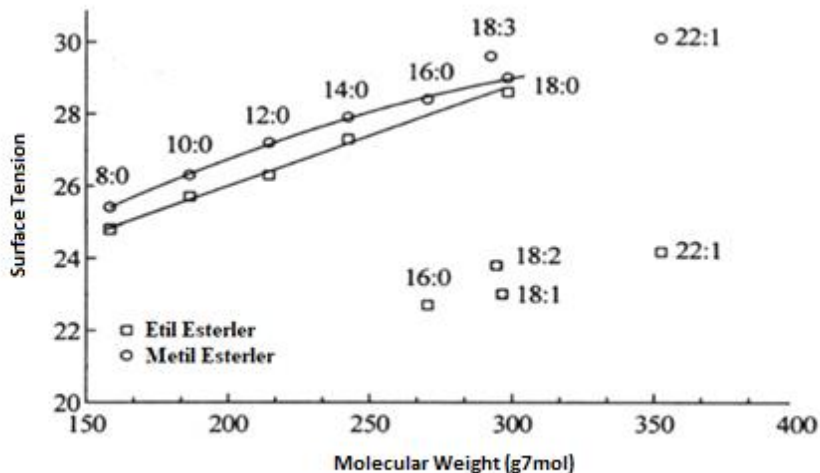
Figure 5. Surface tension variation with molecular weight of saturated methyl and ethyl esters[23].

Studies on biodiesel atomization have shown that factors such as spray tip type, leakage and fuel droplet size have an important role on the performance and emissions of the diesel engine. It was concluded that spray tip leakage increased with increasing mixture ratio in biodiesel fuel mixtures. However, this situation caused difficulties in fuel atomization due to the high surface tension of biodiesel fuels compared to diesel fuels [25]. Yuan et al. found that the reduced surface tension of pure methyl esters did not contribute to increased NOX emissions [26]. However, the surface tension increases with the unsaturation of methyl esters; In other words, it has been observed that increased viscosity and high surface tension in biodiesel fuels affect fuel atomization. This is mainly due to the increase in droplet sizes and Weber number as a result of high surface tension [27]. The increase in droplet size directly increases the leakage of the spray tip. It should be noted that droplet size,

distribution, and Sauter mean diameter are greatly affected by surface tension. This was confirmed in a study conducted with diesel engines by Lee et al. In the study, it was observed that the surface tension was also high when high biodiesel mixture ratios were combined with high injection pressure. It has been proven that as the surface area increases, atomization weakens and NOx emissions increase [28].

KINEMATIC VISCOSITY (ν)

Viscosity is defined as the fluid's resistance to flow. It is an important value in fuel supply and injection systems of diesel engines. It determines the characteristic feature of biodiesel. High viscosity causes low efficient atomization of the fuel, poor combustion, clogging of the injectors, carbon accumulation in the piston rings and deterioration of the lubricating oil. It is not desired that the viscosity value of biodiesel is high. As the chain length of hydrocarbons increases, viscosity increases, and as the number of double bonds increases, viscosity decreases [29]. Therefore, the transesterification method is used to reduce viscosity.

It has been observed that although biodiesel fuels have low spraying properties, their kinematic viscosity is higher compared to diesel fuels. Considering that these factors are related to large droplet size, it has been observed that they delay the ignition of the fuel [30]. Studies have confirmed that decreasing kinematic viscosity due to decreasing injected fuel mass reduces NOX emissions. Research has shown that increasing droplet diameter causes poor combustion and therefore increased NOX emissions. With incomplete atomization and increasing droplet diameter, physical mixing time also increases [31]. Figure 6 shows the change of kinematic viscosity with temperature.
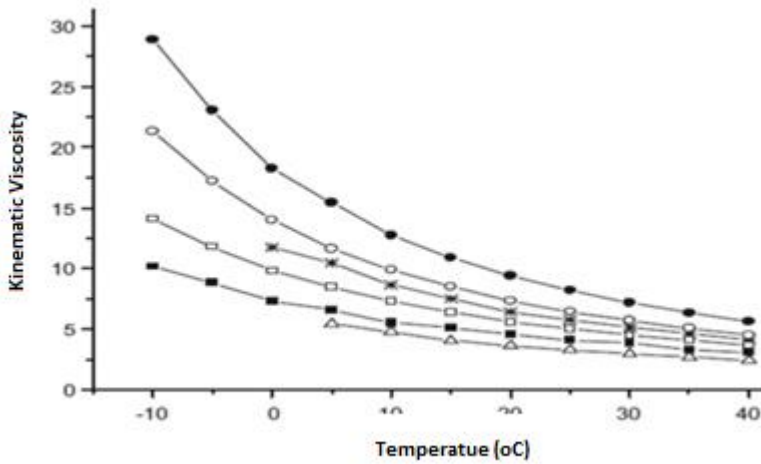
Figure 6. Change of kinematic viscosity with temperature [32].

Another factor affecting kinematic viscosity is the ratio between the injected mass volume and the leakage length. The increase in the leakage length causes slow mixing of air and fuel near the spray tip, resulting in the formation of NOX emissions [33]. The injection volume fraction and speed of biodiesel fuels are lower due to the high viscosity resistance within the injector passage [34]. As the amount of biodiesel fuel increases, the spray tip speed also increases, but the spray volume decreases [35,36].

DENSITY(ρ)

The density of vegetable oils generally varies depending on the type of oil. Although the density of oils is between 880-920 kg/m3 at 15°C, it affects fuel consumption and combustion heat. As the hydrocarbon chain lengthens, the density decreases, and as the number of double bonds increases, the density increases [29]. Density is defined as the mass of a substance per unit volume and is an important parameter

for biodiesel to provide sufficient fuel for injection systems, pumps and injectors for proper combustion to occur [37]. In other words, density is the main factor affecting the volume and mass of fuel injected into a system [38,39]. Another important issue is how density affects biodiesel performance and emission characteristics. It was concluded that there is a 10-12% reduction in NOx emissions in low density biodiesel fuels. Figure 7 shows the change in density of different soy-based biodiesel samples with temperature [37]. With high biodiesel density, injection time increases and NOX emissions and combustion chamber temperature increase due to more fuel being injected [40].
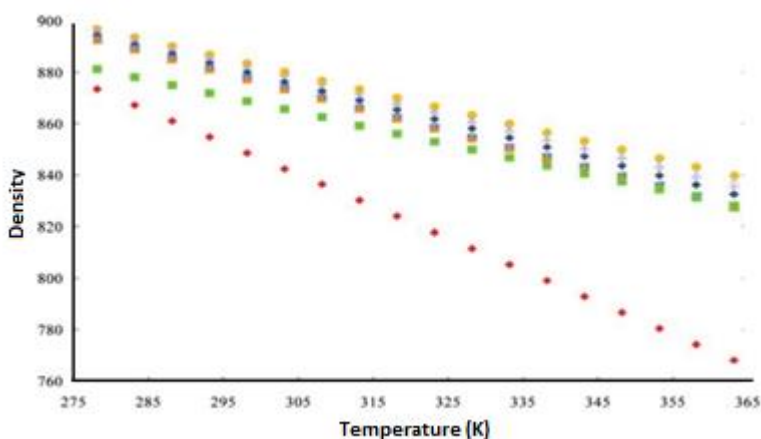

Figure 7. Change in density of different soy-based biodiesel samples with temperature [37]

Another issue related to biodiesel density is the delay in ignition. In other words, a shorter injection time results in better combustion. This situation has made it urgently necessary to produce an electronic diesel fuel injection system that calculates fuel according to density. It seems

that with any change in biodiesel density, the injected fuel volume will automatically be affected, thus NOX emissions will also be affected [41].

RESULTS AND DISCUSSIONS

Like other fuels, the combustion, performance and emission characteristics of biodiesel are directly affected by physicochemical properties. Many fuel properties, such as cetane number and calorific values, are directly related to the density of the fuel. Fuel density affects the atomization efficiency of the fuel and thus its combustion characteristics. Density is a key in compression ignition engines because of the fuel metering system in diesel engines, which is a volume-based system. Additionally, this density affects engine output depending on the mass of fuel injected. Kinematic viscosity is another key feature that affects the operating conditions of injection systems in biodiesel fuels. Because it is important to control high viscosity in cold weather conditions. Additionally, it has been observed that viscosity affects the lubrication and cooling capacity of the fuel in fuel injector pumps. For the reasons mentioned above, it should be checked that the physicochemical properties of biodiesel are within the specified standard values.

REFERENCES

[1]   G. Uguz, Inhibitory effect of thyme oil as an antioxidant for waste cooking oil biodiesel crystallization, Energy Environ. (2021) 958305. https://doi.org/10.1177/0958305X211061346.

[2]   G. Uğuz, A.E. Atabani, M.N. Mohammed, S. Shobana, S. Uğuz, G. Kumar, A.H. Al-Muhtaseb, Fuel stability of biodiesel from waste cooking oil: A comparative evaluation with various antioxidants using FT-IR and DSC techniques, Biocatal. Agric. Biotechnol. 21 (2019). https://doi.org/10.1016/j.bcab.2019.101283.

[3]   R.R. Al-Samaraae, A.E. Atabani, G. Uguz, G. Kumar, O. Arpa, A. Ayanoglu, M.N. Mohammed, H. Farouk, Perspective of safflower (Carthamus tinctorius) as a potential biodiesel feedstock in Turkey: characterization, engine performance and emissions analyses of butanol–biodiesel–diesel blends, Biofuels. 11 (2020). https://doi.org/10.1080/17597269.2017.1398956.

[4]   K. Bencheikh, A.E. Atabani, S. Shobana, M.N. Mohammed, G. Uğuz, O. Arpa, G. Kumar, A. Ayanoğlu, A. Bokhari, Fuels properties, characterizations and engine and emission performance analyses of ternary waste cooking oil biodiesel–diesel–propanol blends, Sustain. Energy Technol. Assessments. 35 (2019) 321–334. https://doi.org/10.1016/j.seta.2019.08.007.

[5]   A.E. Atabani, M. Mekaoussi, G. Uguz, O. Arpa, A. Ayanoglu, S. Shobana, Evaluation, characterization, and engine performance of complementary fuel blends of butanol–biodiesel–diesel from Aleurites moluccanus as potential alternative fuels for CI engines,

Energy Environ. (2018). https://doi.org/10.1177/0958305X18790953.

[6] M.N. Mohammed, A.E. Atabani, G. Uguz, C.-H. Lay, G. Kumar, R.R. Al-Samaraae, Characterization of Hemp (Cannabis sativa L.) Biodiesel Blends with Euro Diesel, Butanol and Diethyl Ether Using FT-IR, UV–Vis, TGA and DSC Techniques, Waste and Biomass Valorization. 11 (2020). https://doi.org/10.1007/s12649-018-0340-8.

[7] G. Uğuz, Antioxidant effect of clove oil on biodiesel produced from waste cooking oil, Biomass Convers. Biorefinery. (2021). https://doi.org/10.1007/s13399-021-01679-4.

[8] Biyodizel Sanayi Derneği, Biyodizel Endüstri Raporu 1, 2019. http://www.biyodizel.org.tr/tr/stat/genel-bakis.

[9] G. Uğuz, A. Ayanoglu, Chemical characterization of waste tire pyrolysis products, Int. Adv. Res. Eng. J. 5 (2021) 163–170. https://doi.org/10.35860/iarej.856112.

[10] G. Uğuz, A. Ayanoğlu, Characterization of Waste Tire Pyrolysis Products by GC , ICP-MS , TGA and DSC Atık Lastik Piroliz Ürünlerinin GC , ICP -MS , TGA ve DSC tarafından karakterizasyon, 10 (2021) 930–942.

[11] A.E. Atabani, S. Shobana, M.N. Mohammed, G. Uğuz, G. Kumar, S. Arvindnarayan, M. Aslam, A.H. Al-Muhtaseb, Integrated valorization of waste cooking oil and spent coffee grounds for biodiesel production: Blending with higher alcohols, FT–IR, TGA, DSC and NMR characterizations, Fuel. 244 (2019). https://doi.org/10.1016/j.fuel.2019.01.169.

[12] A. Boulal, A.E. Atabani, M.N. Mohammed, M. Khelafi, G. Uguz,

S. Shobana, A. Bokhari, G. Kumar, Integrated valorization of Moringa oleifera and waste Phoenix dactylifera L. dates as potential feedstocks for biofuels production from Algerian Sahara: An experimental perspective, Biocatal. Agric. Biotechnol. 20 (2019). https://doi.org/10.1016/j.bcab.2019.101234.

[13]   L.L. Nani Guarieiro, A.L. Nani Guarieiro, Vehicle Emissions: What Will Change with Use of Biofuel?, in: Biofuels - Econ. Environ. Sustain., 2013. https://doi.org/10.5772/52513.

[14]   J. Krahl, G. Knothe, A. Munack, Y. Ruschel, O. Schröder, E. Hallier, G. Westphal, J. Bünger, Comparison of exhaust emissions and their mutagenicity from the combustion of biodiesel, vegetable oil, gas-to-liquid and petrodiesel fuels, Fuel. 88 (2009) 1064–1069. https://doi.org/10.1016/j.fuel.2008.11.015.

[15]   K. Velmurugan, A.P. Sathiyagnanam, Effect of biodiesel fuel properties and formation of NOx emissions: a review, Int. J. Ambient Energy. 38 (2017) 644–651. https://doi.org/10.1080/01430750.2016.1155486.

[16]   H. Liu, M. Werst, S. Strank, J. Osara, R. Hebner, Es2010-90037 Combustion Emissions Modeling and Testing of Conventional, in: 2010: pp. 1–10.

[17]   S. Maroa, F. Inambao, Influence of Exhaust Gas Recirculation and Emission Characteristics of a Diesel Engine Using Pyrolyzed Waste Plastic Biodiesel and Blends, Int. J. Appl. Eng. Res. 13 (2018) 8321–8335. http://www.ripublication.com.

[18]   M. Lapuerta, J.R. Agudelo, M. Prorok, A.L. Boehman, Bulk modulus of compressibility of diesel/biodiesel/HVO blends, Energy and Fuels. 26 (2012) 1336–1343.

https://doi.org/10.1021/ef201608g.

[19]   K. Yamane, A. Ueta, Y. Shimamoto, Influence of physical and chemical properties of biodiesel fuels on injection, combustin and exhaust emission characteristics in a direct injection compression ignition engine, Int. J. Engine Res. 2 (2001) 249–261. https://doi.org/10.1243/1468087011545460.

[20]   Mustafa Ertunc Tat, Jon H. Van Gerpen, Physical Properties and Composition Detection of Biodiesel-diesel Fuel Blends, 0300 (2013). https://doi.org/10.13031/2013.9772.

[21]   M.E. Tat, J.H. Van Gerpen, P.S. Wang, Fuel property effects on injection timing, ignition timing and oxides of nitrogen emissions from biodiesel-fueled engines, ASAE Annu. Int. Meet. 2004. (2004) 6715–6732. https://doi.org/10.13031/2013.23621.

[22]   J.P. Szczap, I.C. Jacobs, Atomization and Spray-Drying Processes, in: Microencapsul. Food Ind. (Second Ed., 2023: pp. 59–71.

[23]   C.A.W. Allen, K.C. Watts, R.G. Ackman, Predicting the surface tension of biodiesel fuels from their fatty acid composition, JAOCS, J. Am. Oil Chem. Soc. 76 (1999) 317–323. https://doi.org/10.1007/s11746-999-0238-5.

[24]   J.P.O. Bruce E. Poling, John M. Prausnitz, The Properties of Gases and Liquids, 2000. https://doi.org/10.1063/1.3060771.

[25]   C.S. Lee, S.W. Park, An experimental and numerical study on fuel atomization characteristics of high-pressure diesel injection sprays, Fuel. 81 (2002) 2417–2423. https://doi.org/10.1016/S0016-2361(02)00158-8.

[26]   W. Yuan, A.C. Hansen, M.E. Tat, J.H. Van Gerpen, Z. Tan, Spray,

ignition, and combustion modeling of biodiesel fuels for investigating NOx emissions, 48 (2005) 933–939.

[27] Rao, P, Experimental investigations on the influence of properties of Calophyllum inophyllum biodiesel on performance, combustion, and emission characteristics of a DI diesel engine, World Acad Sci. Eng. Technol. 75 (2011) 855–868. https://doi.org/10.1080/01430750.2015.1023838.

[28] C.S. Lee, S.W. Park, S. Il Kwon, An experimental study on the atomization and combustion characteristics of biodiesel-blended fuels, Energy and Fuels. 19 (2005) 2201–2208. https://doi.org/10.1021/ef050026h.

[29] J. Van Gerpen, B. Shanks, R. Pruszko, D. Clements, G. Knothe, Biodiesel production technology, Natl. Renew. Energy Lab. 1617 (2004) 80401–83393.

[30] S.K. Hoekman, A. Broch, C. Robbins, E. Ceniceros, M. Natarajan, Review of biodiesel composition, properties, and specifications, Renew. Sustain. Energy Rev. 16 (2012) 143–169.

[31] A. Gopinath, S. Puhan, G. Nagarajan, Effect of biodiesel structural configuration on its ignition quality, Int. J. Energy Environ. 1 (2010) 2076–2909. www.IJEE.IEEFoundation.org.

[32] G. Knothe, K.R. Steidley, Kinematic viscosity of biodiesel components (fatty acid alkyl esters) and related compounds at low temperatures, Fuel. 86 (2007) 2560–2567. https://doi.org/10.1016/j.fuel.2007.02.006.

[33] X. Lu, J. Ma, L. Ji, Z. Huang, Simultaneous reduction of NOx emission and smoke opacity of biodiesel-fueled engines by port injection of ethanol, Fuel. 87 (2008) 1289–1296.

https://doi.org/10.1016/j.fuel.2007.07.006.

[34]   P. Boggavarapu, R. V. Ravikrishna, A review on atomization and sprays of biofuels for IC engine applications, Int. J. Spray Combust. Dyn. 5 (2013) 85–121. https://doi.org/10.1260/1756-8277.5.2.85.

[35]   B. Kegl, M. Kegl, S. Pehan, Optimization of a fuel injection system for diesel and biodiesel usage, Energy and Fuels. 22 (2008) 1046–1054. https://doi.org/10.1021/ef700657g.

[36]   H.K. Suh, H.G. Roh, C.S. Lee, Spray and combustion characteristics of biodiesel/diesel blended fuel in a direct injection common-rail diesel engine, J. Eng. Gas Turbines Power. 130 (2008) 0328071–0328079. https://doi.org/10.1115/1.2835354.

[37]   M.J. Pratas, S. V.D. Freitas, M.B. Oliveira, S.C. Monteiro, Á.S. Lima, J.A.P. Coutinho, Biodiesel density: Experimental measurements and prediction models, Energy and Fuels. 25 (2011) 2333–2340. https://doi.org/10.1021/ef2002124.

[38]   S. Baroutian, M.K. Aroua, A.A.A. Raman, N.M.N. Sulaiman, Density of palm oil-based methyl ester, J. Chem. Eng. Data. 53 (2008) 877–880. https://doi.org/10.1021/je700682d.

[39]   F. Boudy, P. Seers, Impact of physical properties of biodiesel on the injection process in a common-rail direct injection system, Energy Convers. Manag. 50 (2009) 2905–2912. https://doi.org/10.1016/j.enconman.2009.07.005.

[40]   S.M. Palash, M.A. Kalam, H.H. Masjuki, M.I. Arbab, B.M. Masum, A. Sanjid, Impacts of NOx reducing antioxidant additive on performance and emissions of a multi-cylinder diesel engine fueled with Jatropha biodiesel blends, Energy Convers. Manag.

77 (2014) 577–585. https://doi.org/https://doi.org/10.1016/j.enconman.2013.10.016.

[41] E. Alptekin, M. Canakci, Determination of the density and the viscosities of biodiesel-diesel fuel blends, Renew. Energy. 33 (2008) 2623–2630. https://doi.org/10.1016/j.renene.2008.02.020.